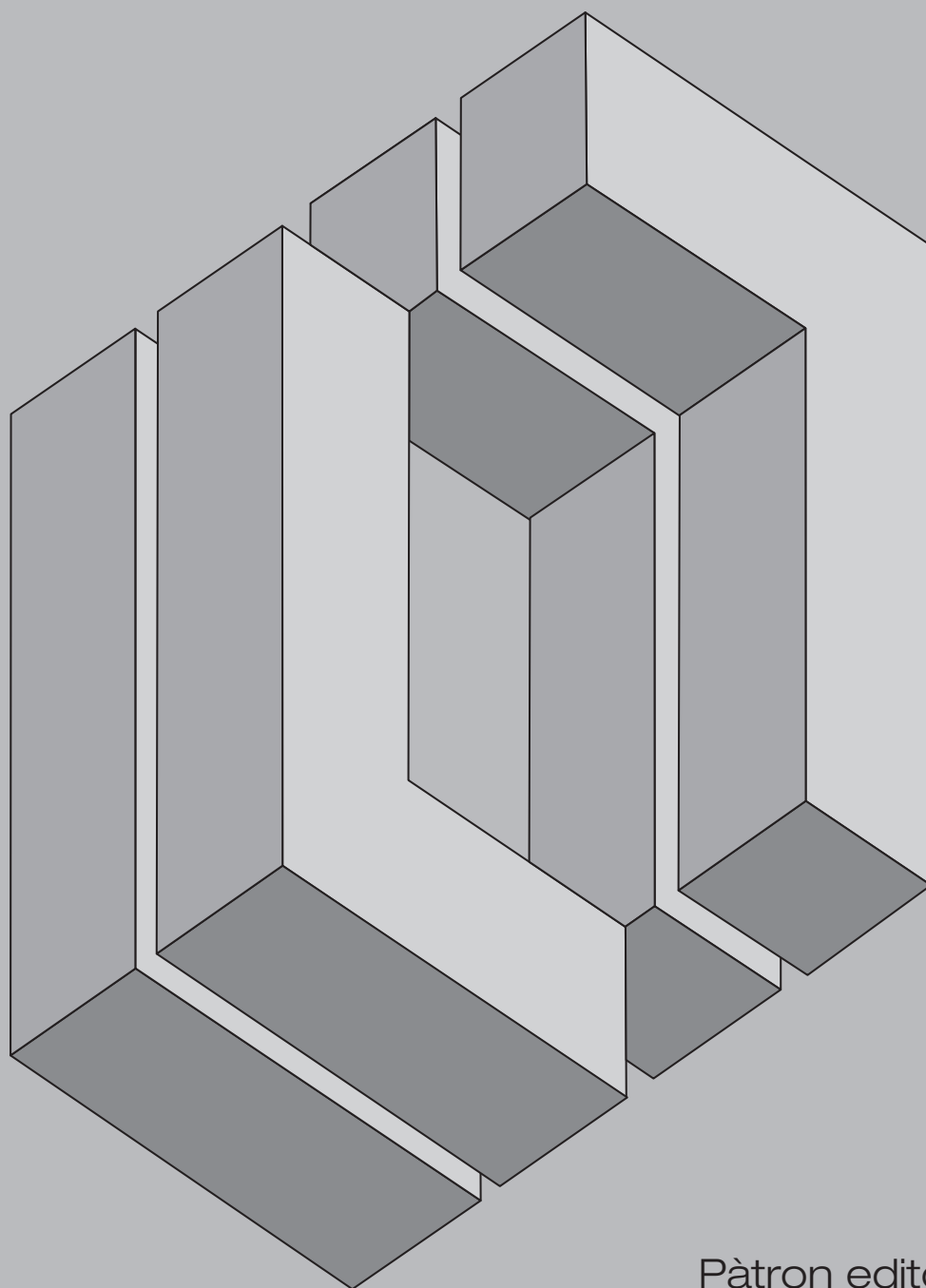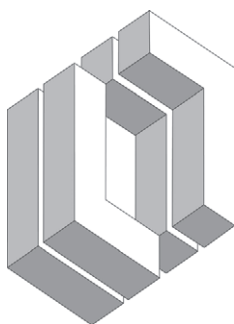1-2 2016

ingegneria sismica

International Journal of Earthquake Engineering
Trimestrale tecnico-scientifico

ingegneria sismica
International Journal of Earthquake Engineering

Editors:
Rosario Montuori, Dep. Civil Engineering, University of Salerno, Italy
Francesco Fabbrocino, Dept. of Engineering, Pegaso University, Naples, Italy

Sommario/Contents

TO READERS AND AUTHORS

We are pleased to announce that *Ingegneria Sismica* is covered by Compendex, one of Elsevier products. Compendex will index papers and possibly extract data from the full text. Coverage increases dissemination of authors' work: the benefits are high visibility to a global audience. Since 1970, Compendex has been the engineering database of choice for researchers, students, faculty and engineering professionals around the world.

AI LETTORI ED AGLI AUTORI

Siamo lieti di comunicare che *Ingegneria Sismica* fa parte del database di Compendex, uno dei prodotti di Elsevier. Questo comporta l'indicizzazione degli articoli pubblicati e la eventuale citazione di dati estratti dal testo. Verrà così fortemente accresciuta la visibilità internazionale degli autori e degli argomenti trattati. Compendex costituisce, fin dal 1970 un importante database per ricercatori, operatori accademici, studenti e professionisti di tutto il mondo.

Dear Readers,

this special issue comprises selected papers presented at the XXV edition of "Italian Steel Days" held in Salerno on October 1–2, 2015. This conference represents the place where Italian researchers present their results and development activities in the field of Steel Structures. Common papers' emphasis is about the structural performance under seismic conditions. Due to the number of selected papers, in addition to the current issue, a second one is in preparation. The Guest Editors, Rosario Montuori and Francesco Fabbrocino, wishes to thank Dr. Gianmario Benzoni for this opportunity and for his assistance.

Cari lettori,

Questo numero speciale è costituito da una selezione di lavori presentati alla XXV edizione delle "Giornate Italiane della Costruzione in Acciaio" tenutasi a Salerno il 1–2 ottobre 2015. Questa conferenza rappresenta il luogo dove i ricercatori italiani presentano gli sviluppi e i risultati delle loro attività di ricerca nel campo delle strutture metalliche. Il presente numero è stato realizzato mediante una selezione degli articoli presentati al convegno riguardanti problemi di sismica. Visto il numero dei lavori selezionati, nei prossimi mesi sarà pubblicato un altro numero speciale. Gli Editori, Rosario Montuori e Francesco Fabbrocino, desiderano ringraziare il Prof. Gianmario Benzoni per l'opportunità ricevuta e per la sua assistenza per la realizzazione di questo numero speciale.

SIMPLIFIED NUMERICAL MODELING OF ELEVATED SILOS FOR NONLINEAR DYNAMIC ANALYSIS

Carlo Andrea Castiglioni, Alper Kanyilmaz*

Department of Architecture, Built environment and Construction

SUMMARY: *Silos are industrial facilities used for storing a huge range of different materials. They should be designed to resist several loading conditions, and their seismic behaviour strongly depends on the geometrical and mechanical behaviour of their supporting frame, and the nonlinear behaviour of the content (e.g. friction, content-silo wall interaction). Nonlinear dynamic simulation of such systems can be very time-consuming, and most of the time unfeasible. This study compares a finite element model made of bricks elements and a simpler model with distributed masses on the silo walls. While simplified models were not suitable to simulate local behaviour of the silo wall, they reasonably predicted the global response of the elevated silo system. Yet, the accuracy strongly depended on the rigidity of the supporting structure, and this should be investigated carefully during the calibration phase.*

KEYWORDS: *Elevated silos, nonlinear dynamic analysis, silo content and wall interaction*

1. INTRODUCTION

In the last decades, industrial facilities were damaged by many natural events, among which the seismic events are the most significant. Indeed many plants are located in territories in which seismic risk is not negligible, such as Italy. Furthermore, most of these plants have been designed and built before the latest updates of the seismic design codes took place, and most of them are prone to earthquakes. Therefore the seismic performance of the existing plants should be validated by means of accurate numerical analysis, taking into account of structure's nonlinear behaviour and realistic ground motion data.

Stored materials have generally a very complex behaviour, characterized by stress or strain dependence, plasticity, dilatancy, and possible anisotropy. In order to take into account all of these features, sophisticated mathematical modelling is needed. Also the mechanical interaction between the walls and the material is significantly nonlinear. Besides, it has been observed that shell deformability can strongly influence wall pressures [Haroun and Housner, 1981]. To have a good description of storage material behaviour and its effects on the silo wall, approximated numerical models have been developed by several researchers.

The first notable numerical studies have been performed by Mahmoud and Abdel-Sayed [Mahmoud and Abdel-Sayed, 1981]. They developed a finite element approach in order to assess the lateral pressure on the silo wall in the static case. Their method took into account the interaction between bulk solids and the silo's wall by using one-dimensional joint elements, whose normal and tangential stiffness had to be initially assumed and modified

*Corresponding author: Alper Kanyilmaz, Department of Architecture, Built environment and Construction Engineering, Politecnico di Milano, Milano, Italy,
Email: alper.kanyilmaz@polimi.it

through an interactive procedure. Haussler and Eibl [Haussler and Eibl, 1984] focused their attention on stress field in plane strain silos during static and dynamic phases for rigid shells only. They described the storage material by means of an elastic-plastic constitutive law of cohesionless material with a viscous part. Their results were in accordance with experimental results for the static case. Askari and Elwi [Askari and Elwi, 1988] modelled the storage material as a no-tension Drucker-Prager elasto-plastic material. Their method was able to predict the incipient flow pressure on hopper-bin wall. Rombach [Rombach, 1991] summarized the finite element numerical modelling approaches developed by several European researchers.

Many researchers have used elastic-plastic models and yield criteria such as Mohr-Coulomb, Tresca and Drucker-Prager. Material laws have been modified for cohesive bulk solids and for dynamic calculations. Almost all these studies aimed to define the pressure on the silo wall during the discharge phase. However, very little attention has been given to the evaluation of seismic actions.

In this article, a comparison between two modelling approaches has been presented:

i) Complex approach, taking into account the granular material content of silo, and its interaction with silo wall

ii) Simplified approach, where the silo content is simulated with static pressures and lumped-distributed masses.

2. NUMERICAL MODELLING

Nonlinear dynamic simulation of the cyclic behaviour of bracing members has been the subject of investigation by several researchers. Some researchers developed advanced open-source numerical models capable of simulating the flexural rigidity of bracing connections, low-cycle fatigue and local buckling phenomena [Pillai, 1974; Chen et. al., 2013]. These models can estimate the hysteretic behaviour of bracings to a high degree of speed and accuracy, although their modelling is not straight forward. On the other hand, simpler bracing models have been also in use, and proved to be efficient to simulate nonlinear dynamic behaviour of steel bracings [Longo et. al., 2009; Giugliano et.al., 2010].

In this study, all the frame elements have been simulated through a fibre-based nonlinear model with distributed plasticity, which has been confirmed as a reliable approach to perform nonlinear dynamic analysis for steel frame analysis by Kanyilmaz et al. [Kanyilmaz, 2015; Kanyilmaz et al., 2015]. As a benchmark, an elevated silo supported on a braced steel frame has been considered (Figure 1 and Figure 2).

The numerical model has been developed using Straus7 software [Straus7, 2005]. Both material and geometrical nonlinearities have been taken into account. Geometrical and mechanical properties of the silo system are shown in Table 1.

In the complex model (DPconn), stored material has been modelled by three dimensional brick elements in which the Dracker-Prager soil constitutive law has been incorporated. Material properties have been decided by means of a sensitivity analysis [Andreola, 2014]. Final values are reported in Table 2. The interaction between the stored material and the silo wall, has been provided by means of connection elements. After the sensitivity analysis, translational stiffness has been defined as 4.1e+5 KN/m in x and y directions, 1e+6 KN/m in z direction. Considerations about friction coefficient of the wall were also carried out in order to assess the value of these parameters.

6

Table 1. *Geometrical and mechanical properties of silo system*

Wall thickness	Radius	Total height	Cylinder height	Hopper height	Hopper half apex angle
5 mm	3380 mm	19184 mm	11870 mm	5333 mm	32.5°
Steel grade	**Modulus of elasticity**	**Shear Modulus**	**Poisson's ratio**		
S275	210000 MPa	81000 MPa	0.3		
Unit weight	**Angle of repose**	**Angle of internal friction**	**Lateral pressure ratio**	**Wall friction coefficient**	**Hopper friction coefficient**
600 kg/m³	34°	27°	0.58	0.41	0.35
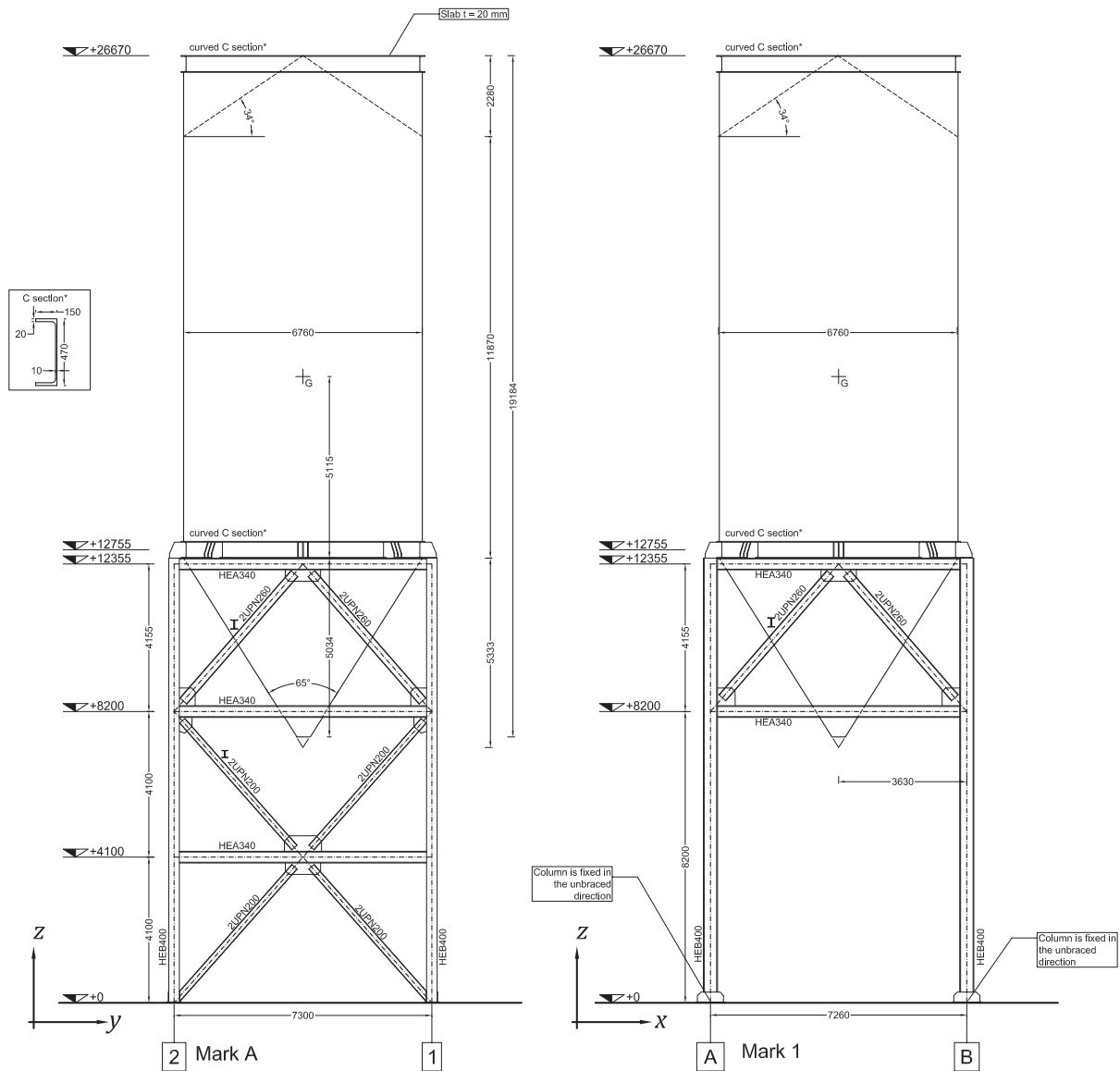
Figure 1. *Cross sections of the benchmark silo*
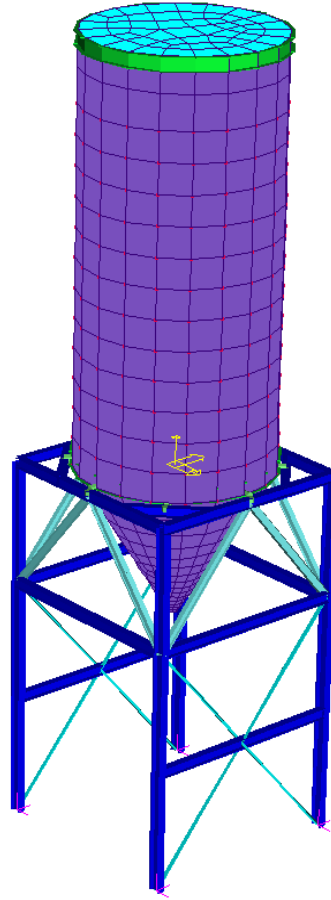
Figure 2. *3D numerical model of the benchmark silo*

Table 2. *Parameters for Drucker-Prager granular silo content*

Modulus	Poisson's ration	Bulk density	Condition
25 MPa	0.3	600 kg/m3	Drained
Drained cohesion	**Friction angle**	**Horiz. Stress ration**	**Void ratio**
0.005 MPa	27°	0.527	0.6

In the distributed mass model, the presence of stored material is simply modelled by applying additional non-structural masses on the silo wall. Two models are shown in Figure 3.

As first step, natural frequency analysis has been performed to have a first comparison between different modelling approaches.The structure presents a very dominant translational mode in x-direction (≈99%) and a dominant mode in y-direction too (≈78-85%). There are many modes with low mass participation, and particularly they are coupled modes between the shell and its content. These modes are not clearly separated in x- or y-direction. Table 3 reports results of modal analysis. It can be observed that results of simplified (distributed mass) model and complex (DPconn) model are almost identical. Nonlinear static analysis (*NLS*) has been performed in order to study the behaviour of the models under vertical loading (filling). The deformed shape under static load is used as initial condition for time history analysis. In the distributed mass model, in order to simulate the static effects of the bulk material on the silo wall, the static distribution of pressure has been applied as recommended by Eurocodes [UNI-EN 1991-4, 2006].
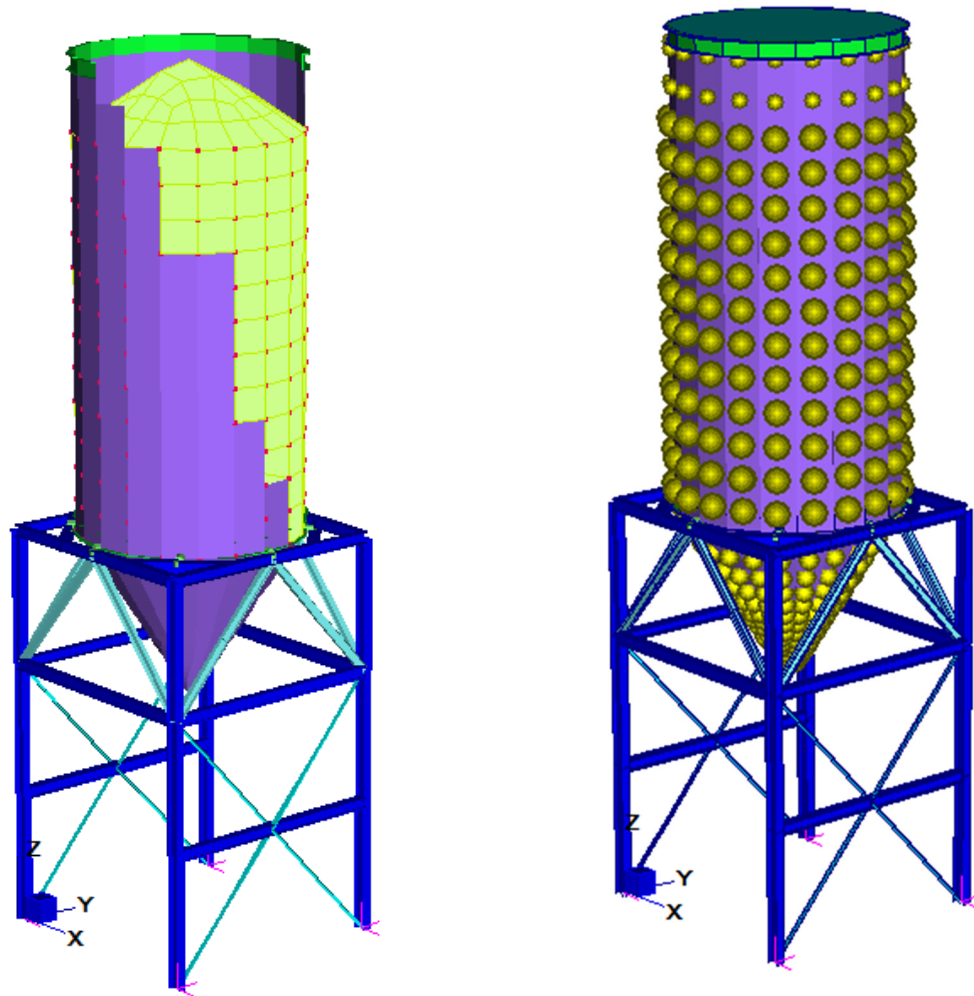
a. Drucker-Prager model with connection beams   b. Distributed mass model;

Figure 3. *Two different numerical modelling approaches*

Mass of stored material has been computed as 310.3 tons, and the total mass is 356.3 tons. In the nonlinear static analysis, a good agreement has been achieved for the expected and computed values of total vertical reaction forces. Comparison of radial displacement of the vertical wall under filling load is shown in Figure 4 for two angular coordinates ($\vartheta=0°$ and $\vartheta=45°$).

Table 3. *Results of modal analysis*

x-direction		1st global mode x-dir.		
	Mode num.	T	Participant mass	
Distributed Mass Model	1	1.51 s	98.86 %	
DPconn model	1	1.49 s	99.04 %	

y-direction	1st global mode y-dir.			2nd global mode y-dir.		
	Mode num.	T	Participant mass	Mode num.	T	Participant mass
Distributed Mass Model	2	0.72 s	77.75 %	20	0.25 s	12.48 %
DPconn model	2	0.68 s	84.43 %	6	0.25 s	14.39 %
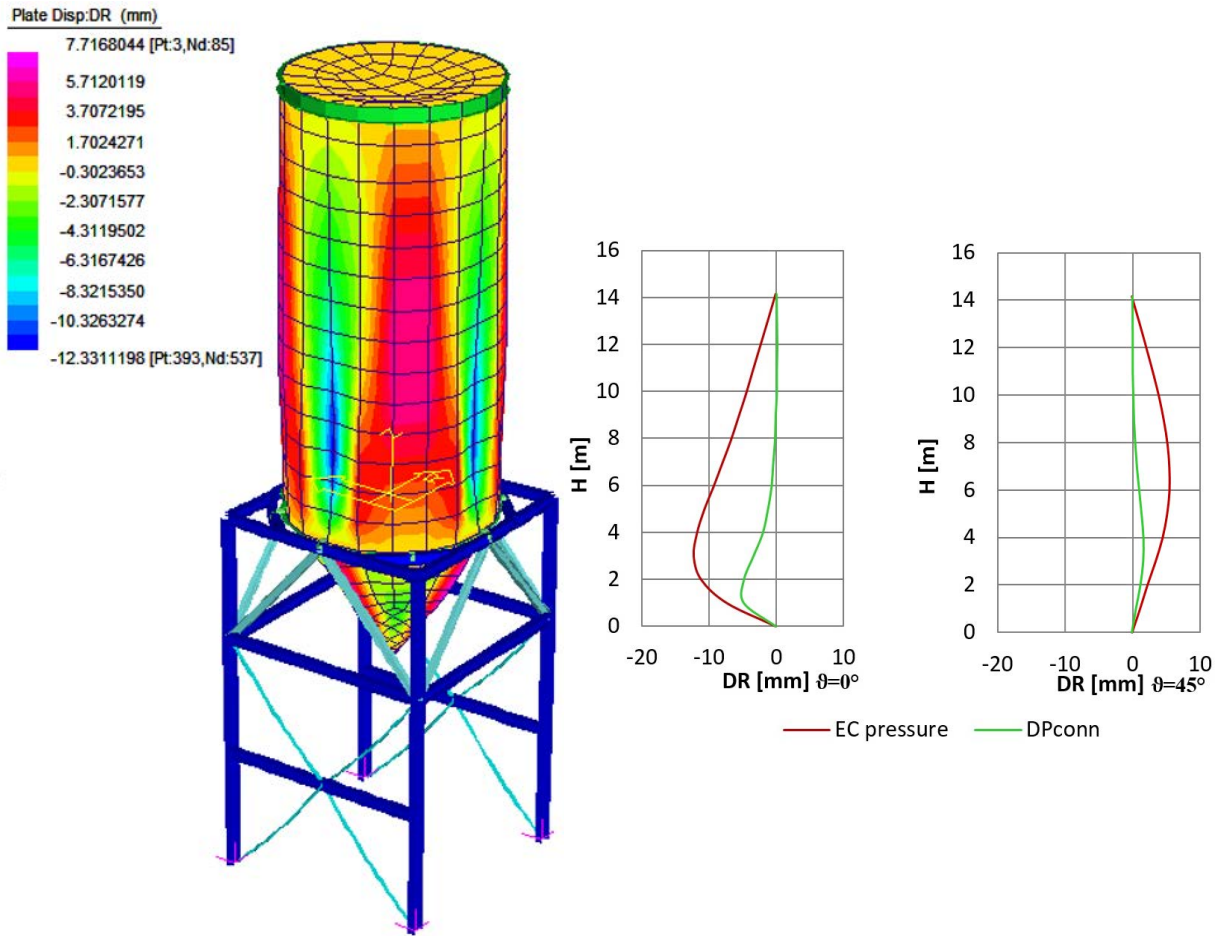
Figure 4. *Comparison of radial displacement of the vertical wall under filling load: Left graph: ϑ=0° ; Right graph: ϑ=45°*

Taking into account the supporting frame there are not significant differences between the two models. On the contrary, the presence of the brick element inside the shell, leads to a marked change in the response of the wall. Indeed, its stiffness is increased by the content.

As a last step, the performance of two modelling approaches has been compared by means of nonlinear transient dynamic analysis. First 9 seconds *El Centro-1940* ground motion recording has been taken as reference for the seismic excitation (Figure 5).
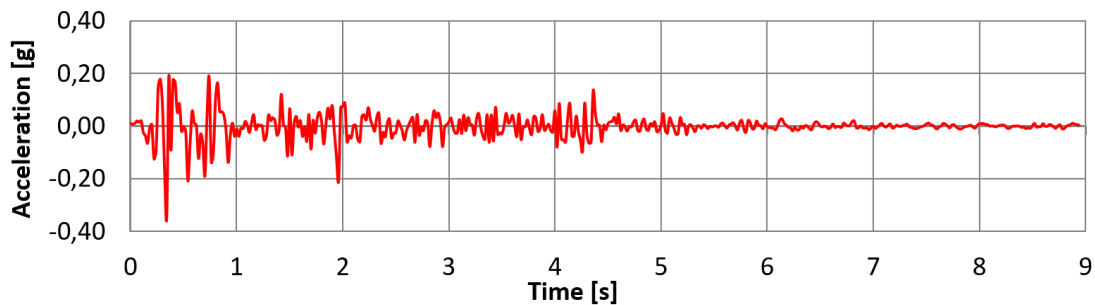
Figure 5. *El Centro-1940 Ground motion record*
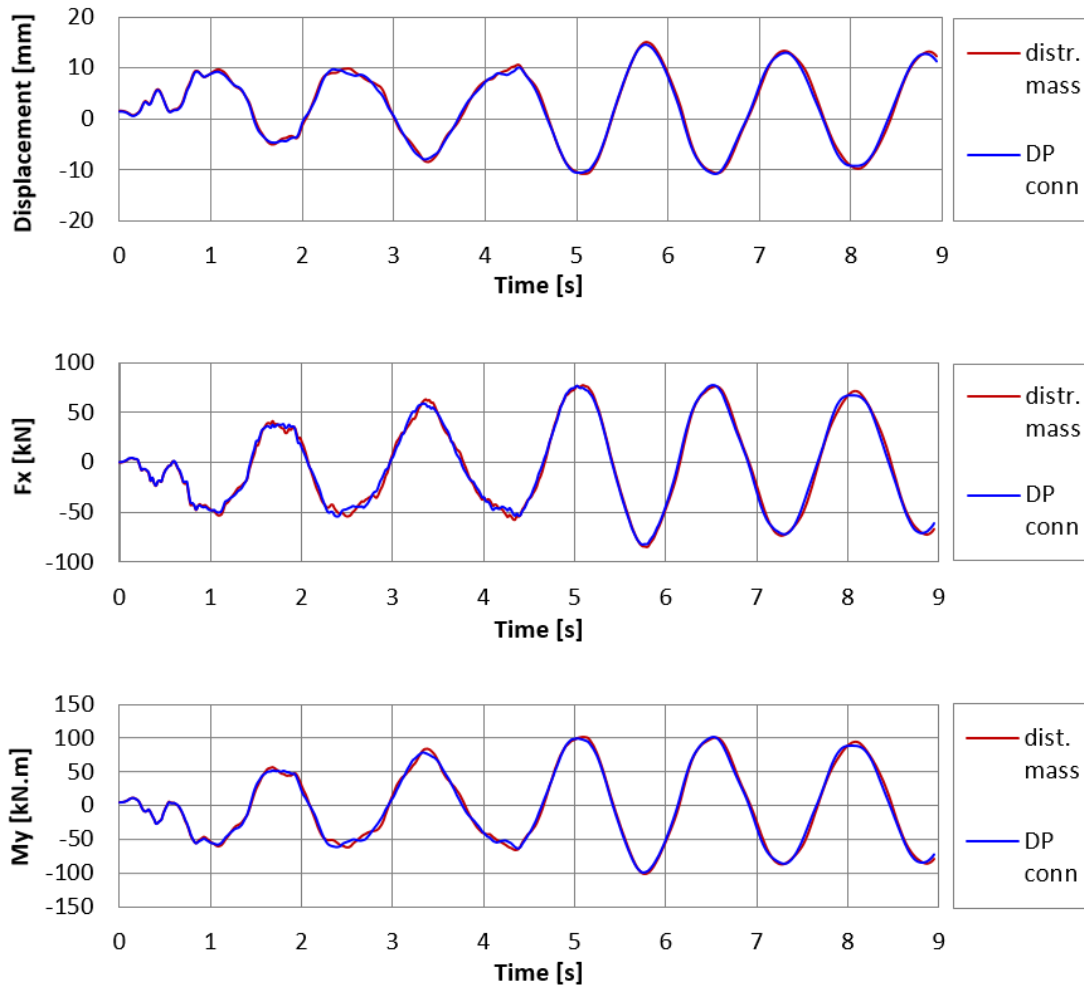
Figure 6. *Global response parameters in x-direction*

The deformed shape of the structure, obtained by *nonlinear static analysis under vertical loading* has been used as initial static condition for dynamic analysis, both for distributed mass model and Drucker-Prager model with connection beam (DPconn).

Seismic actions in x and y directions have been applied separately. Figure 6 and Figure 7 show comparisons between two models in terms of total base shear, moment (in case of non-braced direction) and axial (in case of braced direction) reaction at the base of the columns, and the horizontal displacement of the top node of the supporting structure, in x and y directions.

These parameters have been chosen as they are the most interesting parameters to describe the structure's global response. It is evident that modelling approach does not significantly affect the seismic behaviour of the supporting structure. In more flexible plane (x direction) the difference is much smaller than in the more rigid plane (y direction). On the other hand, significant differences between two models in terms of behaviour of the silo wall are presented in Figure 8.

Although both models can get a global description of the shell behaviour, catching its main features, local deformations result significantly different.
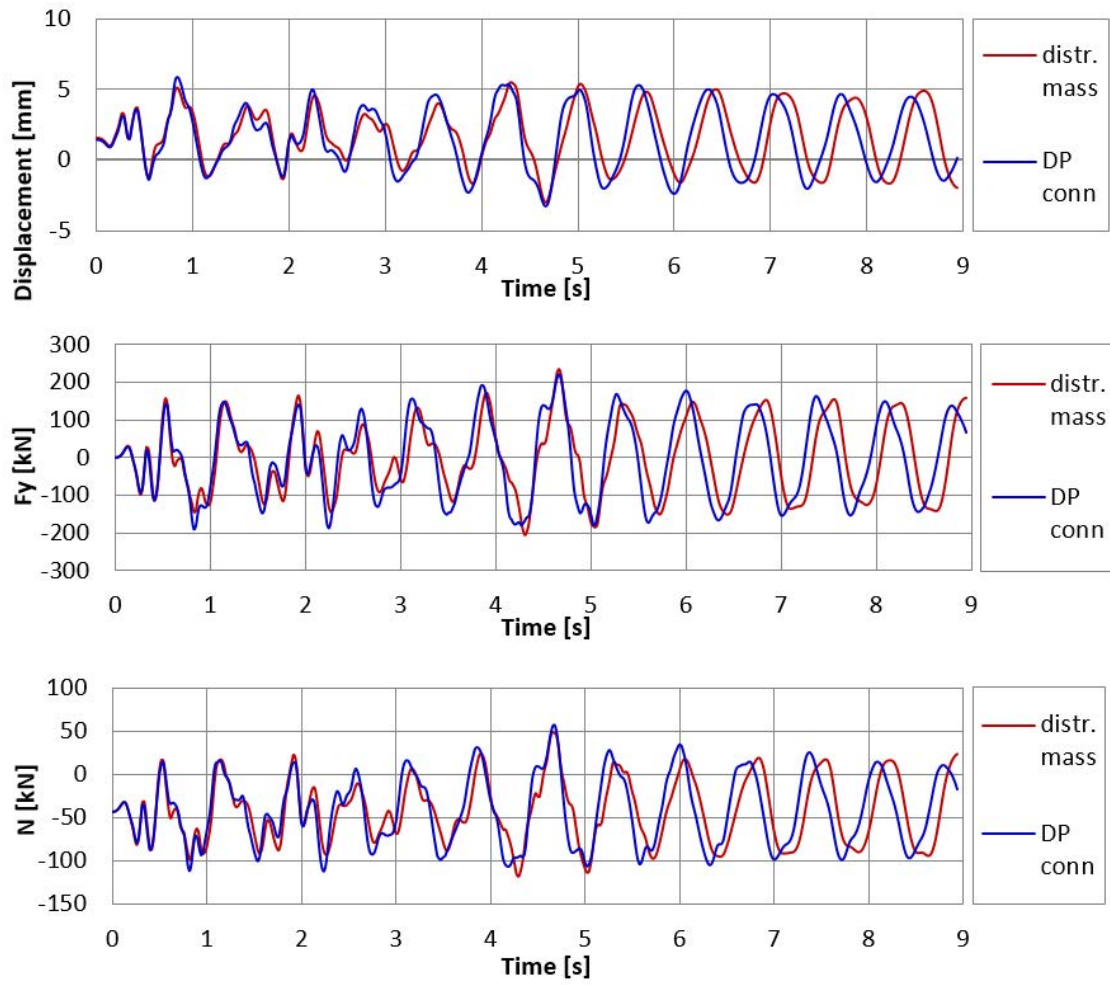
Figure 7. *Global response parameters in y-direction*
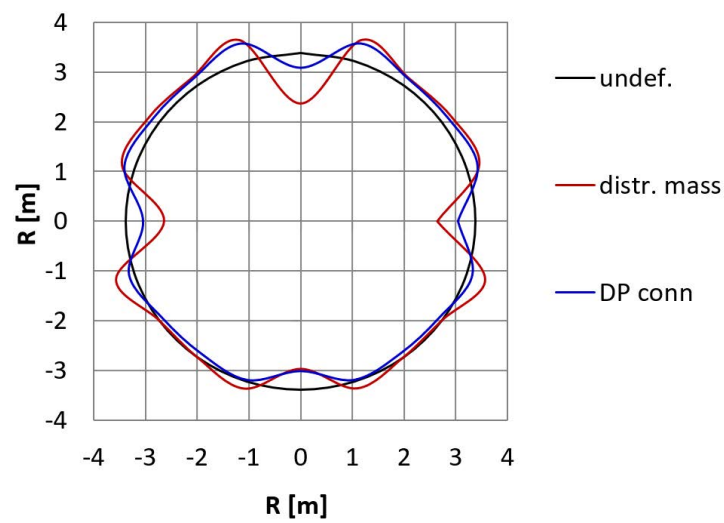
Figure 8. *Deformed cross section of the silo at h=5.935m from transition, at the PGA instant (disp. X100)*

a. Force-disp in x direction   b. Force-disp in y direction
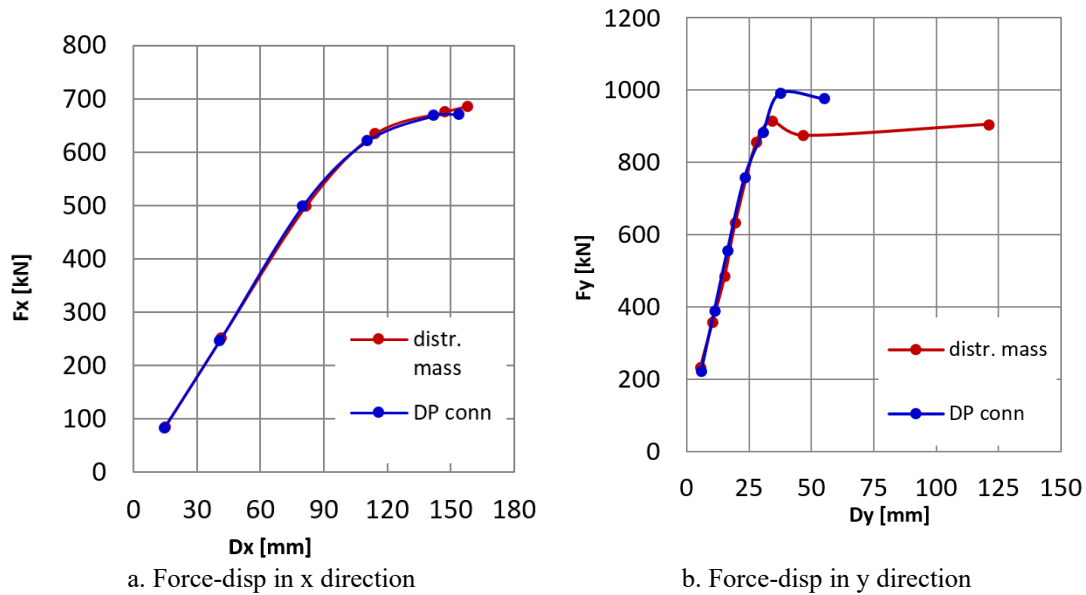
Figure 9. *Global force-displacement behaviour of the elevated silo with scaled accelerograms*

In order to observe the global resistance and ductility of the silo-system, nonlinear dynamic analysis has been performed with the accelerograms scaled in an increasing manner, based on the reference El Centro ground motion. Global force-deformation behaviour of the system can be observed in Figure 9. Also in this case, simplified model provides satisfactory results in more flexible (x-direction). The difference in the y-direction (braced) arises from the inelastic deformations taking place in the silo wall elements, due to increased rigidity of the supporting structure.

3. CONCLUSIONS

In this study, comparisons are shown between a complex modelling approach using three dimensional soil type brick elements, and a simplified approach in which ensiled material has been simulated by means of distributed masses placed on the silo wall. Comparisons have been made in terms of the results of natural frequency analysis, nonlinear static and dynamic analysis, and incremental dynamic analysis. It can be generally stated that global response of the structure can be simulated reasonably well by means of the simplified modelling approach, although it could not simulate the local behaviour of the silo wall with suitable accuracy. The complex model's behaviour is mainly led by the mass of the content, and the global response parameters obtained from the two models are similar. It should be noted that the accuracy is strongly affected by the rigidity of the supporting structure, and this should be investigated carefully during the calibration phase. This study has been realized within the project RFSR-CT-2013-00019 PROINDUSTRY.

4. REFERENCES

Andreola, N. [2014], Master Thesis, Politecnico di Milano

Askari, A. H., Elwi, A. E. [1988] "Numerical prediciton of hopper-bin pressures," Journal of Mechanical Engineering, ASCE 114(2): 342-352.

Chen, L., Tirca, L. [2013], "Simulating the Seismic Response of Concentrically Braced Frames Using Physical Theory Brace Models", Open Journal of Civil Engineering, 3, 69-81

Giugliano, M.T., Longo, A., Montuori, R., Piluso, V. [2010], "Plastic design of CB-frames with reduced section solution for bracing members", Journal of Constructional Steel Research 66 (5), pp. 611-621

Haroun M. A., Housner G. W. [1981], "Seismic design of liquid storage tanks," Journal of Technical Councils, ASCE, vol. 107, pp. 191-207.

Haussler, U., Eibl J. [1984] "Numerical investigation on discharging silos," Journal of Mechanical Engineering, ASCE 110(6): 957-971.

Kanyilmaz, A. [2015] "Inelastic Cyclic numerical analysis of steel struts using distributed plasticity approach," COMPDYN 2015 - 5th ECCOMAS 3663-3674.

Kanyilmaz, A., Castiglioni, C.A., Degee, H., Martin, P.-O. [2015] "A preliminary assessment of slenderness and overstrength homogeneity criteria used in the design of concentrically braced steel frames in moderate seismicity," COMPDYN 2015 - 5th ECCOMAS 3599-3609.

Longo, A., Montuori, R., Piluso, V. [2009], "Seismic reliability of chevron braced frames with innovative concept of bracing members", Advanced Steel Construction 5 (4), pp. 367-389

Mahmoud, A., Abdel-Sayed, G. [1981] "Loading on shallow cylindrical flexible grain bins," Journal of Powder & Bulk Solids Technology 5(3): 12-19.

Pillai, S. [1974], "Beam-Columns of Hollow Structural Sections", Canadian Journal of Civil Engineering, Vol. 1, No. 2, pp. 194-301

Rombach, G. A. [1991] "Schuttguteinwirkungen auf Silozellen," in Dissertation, University of Karlsruhe.

Straus7-Software, Theoretical Manual [2005]

UNI-EN 1991-4 [2006], Actions on structures - Part 4: Silos and tanks

MODELLAZIONE NUMERICA SEMPLIFICATA DEI SILI ELEVATI PER ANALISI DINAMICHE NONLINEARI

Carlo Andrea Castiglioni, Alper Kanyilmaz*

Department of Architecture, Built environment and Construction

SOMMARIO: *I sili sono componenti fondamentali all'interno degli impianti industriali,. Essi sono utilizzati per contenere una grande varietà di materiali solidi, particellari o liquidi, come grani, materie prime, e prodotti chimici. Si ha l'esigenza di approfondire le conoscenze legate al comportamento delle strutture di stoccaggio sotto l'azione sismica, affinché queste possano essere recepite dai riferimenti normativi e la progettazione possa essere ottimizzata. Dall'altro lato, si ha anche la necessità di avere a disposizione strumenti pratici ed immediati, che supportino la progettazione senza doverla ulteriormente appesantire. Nel presente lavoro, vengono valutate due diverse modellazioni, a partire da quelle più complesse, in cui anche il contenuto è modellato da appositi elementi finiti tridimensionali, a quelle in cui la presenza del materiale è invece simulata da distribuzioni di masse e pressioni. I modelli a elementi finiti sono stati implementati attraverso l'utilizzo del software commerciale Straus7.*

---

*Corresponding author: Alper Kanyilmaz, Department of Architecture, Built environment and Construction Engineering, Politecnico di Milano, Milano, Italy,
Email: alper.kanyilmaz@polimi.it

FULL AND PERFORATED METAL PLATE SHEAR WALLS AS BRACING SYSTEMS FOR SEISMIC UPGRADING OF EXISTING RC BUILDINGS

Antonio Formisano*, Luca Lombardi, Federico M. Mazzolani

Department of Structures for Engineering and Architecture, University of Naples "Federico II"

SUMMARY: *Metal Plate Shear Walls (MPSWs) represent an effective, practical and economical system for the seismic protection of existing RC framed buildings. They consist of one or more metallic thin plates, bolted or welded to a stiff steel frame, which are installed in the bays of RC framed structures. A case study of an existing RC residential 5-storey building, designed between the '60s and '70s of the last century and retrofitted with MPSWs, has been examined in this paper. The retrofitting design of the existing structure has been carried out by using four different MPSWs, namely three common full panels made of steel, low yield steel and aluminium and one innovative perforated steel plates. Finally, the used retrofitting solutions have been compared each to other in terms of performance and economic parameters, allowing to select the best intervention.*

KEYWORDS: *Metal Plate Shear Walls, seismic retrofitting, existing RC buildings, perforated plates, non-linear analyses*

1. INTRODUCTION

Steel Plate Shear Walls (SPSWs) represent an effective passive control system, characterized by both high initial stiffness and strength and a very stable hysteretic response up to large deformations, which can be used as a valid alternative to the classical concentrically braced frames [Longo *et al.* 2008a; 2008b] or eccentrically braced frames [Montuori *et al.,* 2014a; 2014b].

SPSWs are very effective in limiting the inter-storey drifts of framed buildings, also reducing the structure weight, as well the seismic forces, in comparison to RC shear walls. In addition, by using shop-welded or bolted connection types, the erection process can be ease, allowing a considerable reduction of construction costs. Application examples of such devices, having either bracing or dissipative functions, in new steel buildings are detected in Asia and America 0. However, SPSWs may be particularly profitable for seismic retrofitting of existing RC buildings, designed for gravity loads only, since their use confers to the existing structures a considerable performance increase. So, their use could protect existing structures from seismic damage, avoiding the failures occurred during recent Italian earthquakes [Formisano *et al.*, 2010; Formisano, 2012; Indirli *et al.*, 2013]. The beneficial contribution offered by shear panels is guaranteed by the development of a diagonal tensile bands mechanism (called *tension-field*), which is more effective as greater is the plate area involved

---

*Corresponding author: Antonio Formisano, Department of Structures for Engineering and Architecture, University of Naples "Federico II"
Email: antoform@unina.it

in the deformation process 0. In particular, when traditional full systems, arranged as simple steel panels without stiffeners, are employed, the optimal behaviour is guaranteed with plates having width/height ratios between 0.8 and 2.5 0.

Some studies have shown that when full SPSWs are used as bracing devices of framed buildings, they may compromise the capacity design criterion application, since excessive design forces are transferred to the surrounding frame members, thus increasing their size and costs 0. The scarce availability on the market of Low Yield Steel (LYS), usually used to limit the forces transmitted by the plates on the boundary steel frame [De Matteis et al., 2005; Formisano et al., 2006a], suggests the employment of aluminium alloys [Formisano et al., 2006b; De Matteis et al., 2012] and perforated steel plates 0 2007], which have the benefit of experiencing excursions in the plastic range already for low stress levels [Brando and De Matteis, 2014].

The behaviour of perforated SPSWs is similar to the behaviour of "dog-bone" connections in the case of steel moment resisting frames [Montuori, 2014; Piluso *et al.*, 2014], or to the role of a brace with reduced section in the case of concentrically braced frames [Giugliano *et al.*, 2010, Longo *et al.*, 2010]. A recent study performed by Authors has shown the suitability of such panels for seismic-resistant applications through the setup of an easy design tool for their application [Formisano *et al.*, 2015].

In this paper, the additional research on the comparison among two full LowLow-Yield (LY)(LY) (steel and aluminium) MPSWs and two perforated SPSWs for seismic upgrading of an existing RC framed structures has been done. To this purpose, the experimental test results conducted in Bagnoli (Naples) [Formisano *et al.,* 2010; De Matteis *et al.*, 2009] have been numerically calibrated on the basis of the finite element software SeismoStruct. With this software, the shear wall model has been implemented with the equivalent tensile diagonal one proposed by Thorburn et al. 0. The excellent experimental-to-numerical correspondence of results, validating the proposed model, has allowed the application of such devices for seismic reinforcing of an existing residential 5-storey RC building in Torre del Greco (Naples). Following the same design approach reported in 0, push-over analyses on the retrofitted structure with full LYMPSWs and differently-perforated SPSWs have been performed. Finally, the structural and economic differences among these solutions have been exposed and critically discussed.

2. SETUP OF A FEM MODEL

The choice of an appropriate and easily implementable FEM model to simulate the behaviour of MPSWs is a crucial importance task to understand the way they improve the performances of buildings hosting them. In order to carry out a parametric analysis on the application of both full and perforated MPSWs within existing RC framed structures, the FEM software SeismoStruct [Seismosoft, 2014] has been used. This software can predict the behaviour of three-dimensional framed structures under static and dynamic loads by taking into account both geometric and mechanical non-linearities.

For monotonic analyses, metal shear panels can be simply schematized by a single equivalent tensile diagonal having a cross-section area A_d calculated according to an elastic strain energy formulation as follows:

$$A_d = \frac{t\ b\ sin^2 2\alpha}{2\ sin\beta\ sin2\beta} \qquad (1)$$

where t and b are the plate thickness and width, respectively, whereas α and β are the tension-field and diagonal angles of the steel plate measured from the vertical direction, respectively. An alternative more refined modelling technique is the strip model one, which schematise the plate as a series of elastic trusses. In this model the tension-field angle α is given by:

$$tan^4\alpha = \frac{1 + \dfrac{t\,b}{2\,A_c}}{1 + t\,d\left(\dfrac{1}{A_b} + \dfrac{d^3}{360\,I_c\,b}\right)} \qquad (2)$$

where A_c and I_c are the cross-section area and the second moment of area of the surrounding columns, respectively, A_b is the beam cross-section area and d is the panel height 0. The Canadian code 0 provides the following minimum second moment of area I_c of columns adjoining SPSWs to prevent their excessive deformation, leading to premature buckling, under the pulling action of the plates:

$$I_c \geq \frac{0.00307\,t\,d^4}{b} \qquad (3)$$

Any contribution offered from the plate buckled in compression can be neglected. In this condition, for width/height ratios between 0.8 and 2.5, the inclination of the generated tension-field can be directly assumed to be 45°.

When the equivalent diagonal system is subjected to an initial shear load V, a horizontal displacement δ_r is detected at the top (see Figure 1). By simple analytical steps, the elongation ΔL_d and tensile force N in the equivalent diagonal with length L_d and Young modulus E_d can be evaluated from Eqs. (4) and (5).

$$\Delta L_d = \delta_r sin\beta \qquad (4)$$

$$N = E_d A_d\,\Delta L_d / L_d = V/sin\beta \qquad (5)$$

According to Sabouri-Ghomi et al. 0, the behaviour of thin plates in a pinned joint frame is schematized through an elastic-perfectly plastic bilinear behaviour, where both the shear strength F_{py} and initial stiffness K_{pw} of the panel can be evaluated as follows:

$$F_{py} = \frac{C_{m1}}{2}\,\sigma_{ty}\,b\,t\,sin2\vartheta \qquad (6)$$

$$K_{pw} = \frac{\dfrac{C_{m1}}{2}\,\sigma_{ty}\,sin2\vartheta}{\dfrac{2\,C_{m2}\,\sigma_{ty}}{E\,sin2\vartheta}}\frac{b\,t}{d} \qquad (7)$$

In Eqs. (6) and (7), E and G are the normal and shear elasticity moduli of the metal plate, σ_{ty} is the tension-field stress in the plate yielding condition, ϑ is the tension-field angle, measured from the vertical direction, and C_{m1} and C_{m2} are modification factors, taking into account beam-to-column connections, plate-to-frame connections and the effect of both flexural behaviour and stiffness of boundary elements. Such modification factors have the limitations $0.8 < C_{m1} < 1.0$ and $1.0 < C_{m2} < 1.7$, but the Authors recognized that these

values will need further refinement as more test results will become available in the next future.
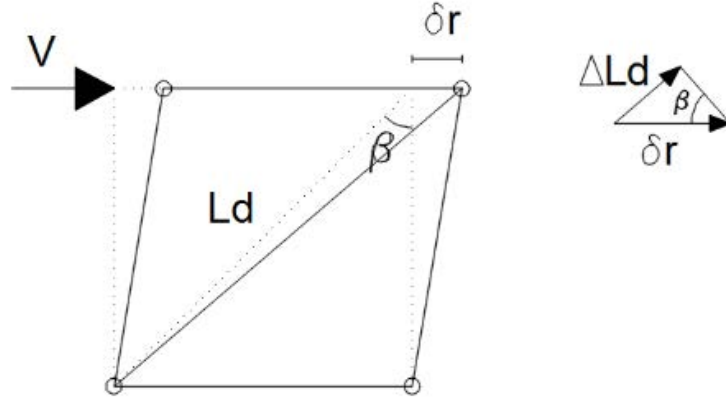
Figure 1. *Scheme of the equivalent tensile diagonal system*

Currently, a more careful estimation of these values has been obtained from the calibration of experimental tests carried out by Formisano et al. [2015], who proposed a useful analytical tool for their appraisal.

The predicted behaviour of the panel can be implemented by assigning to the equivalent diagonal a fictitious material with yielding strength $\sigma_{y,d}$ and normal elasticity modulus E_d evaluated through the Eqs. (8) and (9), respectively:

$$\sigma_{y,d} = \frac{F_{wy}}{A_d \, sin\beta} \tag{8}$$

$$E_d = \frac{K_w \, L_d}{A_d \, sin^2\beta} \tag{9}$$

In order to setup a valuable FEM model in SeismoStruct, the behaviour of the bare RC structure of Bagnoli 0 has been calibrated considering the above data. RC beams and columns have been modelled by *infrmFB* elements, while the floor has been characterized by a series of *elfrm* beams having the same stiffness and weight of the real floor. A 3D view of the modelled sub-structure is illustrated in Figure 2.
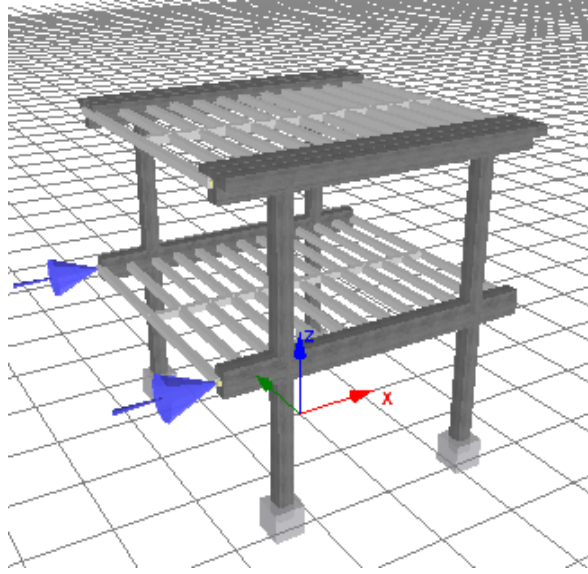
Figure 2. *Numerical model of the Bagnoli sub-structure setup with the SeismoStruct software*

Table 1. *Experimental-to-numerical comparison of vibration periods for the Bagnoli sub-structure*

	Vibration mode					
Period (s)	1	2	3	4	5	6
Experimental	0.625	0.556	0.455	0.208	0.186	0.147
Numerical	0.639	0.505	0.428	0.201	0.191	0.152

A reduced Young modulus E_c of RC beams and columns has been adopted for taking into account the degradation effect associated to the weather. In particular, $0.5E_c$ and $0.4E_c$ have been adopted for beams and columns, respectively. Degradation zones extended at lengths of 35 cm and 65 cm for beams and columns, respectively. The experimental-to-numerical modal comparison achieved with these assumptions is shown in Table 1. Subsequently, $0.3E_c$ and a reduced strength have been assumed for the column edges to consider the damages caused by the experimental pull-out test previously carried out in the transversal direction of the same structure upgraded with shape memory alloy bracings, as described in [Mazzolani, 2008].

In Figure 3, both the experimental curve and the final numerical one, the latter based on the real RC bare structure stiffness considering the previously reduction coefficients, are shown.

Once the initial structure behaviour has been calibrated, the steel frame hosting MPSWs has been modelled in SeismoStruct with elfrm elements to remain in the elastic range under the forces applied by the shear plates. The steel frame hinges have been modelled by link elements with translational stiffness infinitely greater than rotational one. Finally, the shear wall-to-RC beam connections have been modelled by means of rigid links.

The used MPSWs have been divided into six panel fields, having dimensions of 600x400 mm and being separated each to other by horizontal stiffeners, which have been numerically modelled by equivalent diagonals, as previously described (see Figure 4).

The equivalent tensile diagonal has been modelled by a *truss* element with elastic-plastic material, starting from the shear strength F_{wy} and initial stiffness K_w of the wall estimated as follows:

$$F_{wy} = \frac{C_{m1}}{2} \sigma_{ty} \, b \, t \, sin2\vartheta \tag{10}$$

$$K_w = \frac{\frac{C_{m1}}{2} \sigma_{ty} \, sin2\vartheta \, b \, t}{\frac{2 \, C_p \, \sigma_{ty}}{E \, sin2\vartheta} \, d} \tag{11}$$

where C_{m1} and C_p are modification factors, taking into account both the plate behaviour and the wall flexural effect, that should be properly calibrated [Formisano and Sahoo, 2015].

The calibration of the wall model in SeismoStruct has been conducted by deriving the force-displacement curve of the only-walls contribution. Knowing the force-displacement curve of the retrofitted structure and the initial structure one, calibrated and further pushed up to the same ultimate displacement, the only-walls contribution can be derived. By adopting the values of 1.0 and 5.4 for C_{m1} and C_p, respectively, the experimental curve appears to be well simulated by the numerical one (see Figure 5). The same comparison could be also done for the aluminium solution [De Matteis et al., 2008b; Formisano et al., 2006d], but, with the damages occurred after the test on steel panels and not repaired, a further calibration will be due.
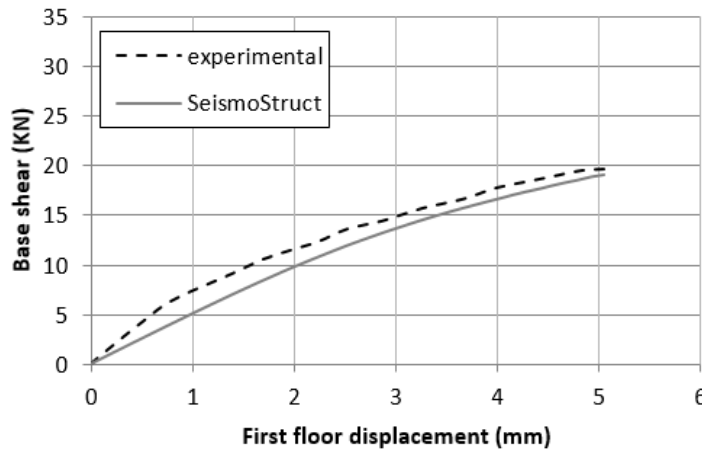
Figure 3. *Comparison between the experimental curve and the numerical one for the RC initial structure*

a)   b)
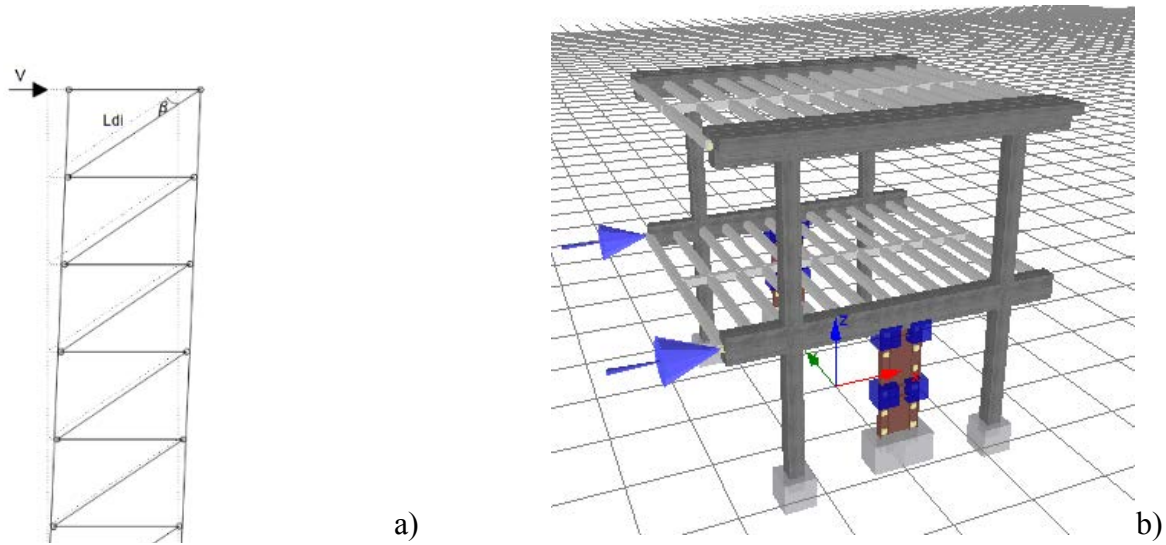
Figure 4. *Calculation scheme of the MPSW (a) and SeismoStruct numerical model of the retrofitted sub-structure (b)*
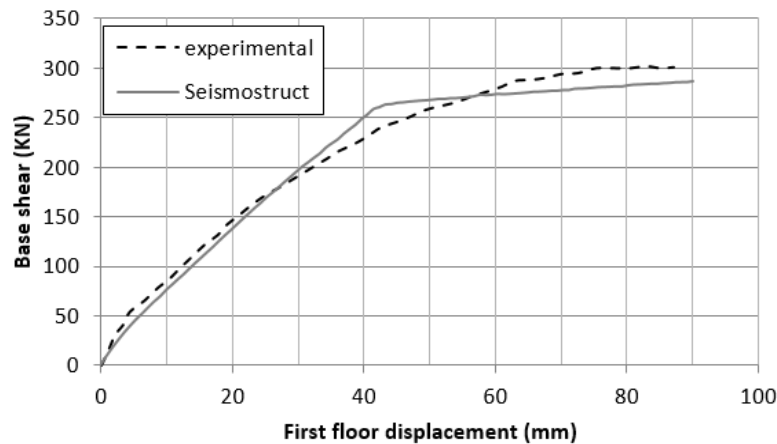
Figure 5. *Comparison between the experimental curve and the calibrated numerical one for the structure retrofitted with SPSWs.*

3. THE CASE STUDY

The benefits arising from the use of perforated steel panels instead of traditional full ones are already known [Purba and Bruneau, 2007]. However, few studies on existing RC buildings retrofitted with such devices are available. Therefore, in this paper, an existing building has been retrofitted with either traditional or perforated panels aiming at showing the different advantages deriving from their use. The case study is a residential multi-storey RC building in Torre del Greco (district of Naples, Italy), representative of the typical 1960s and 1970s constructions designed for gravity loads only. The building under investigation develops on five storeys with rectangular shape of dimensions 30x12 m (see Figure 6).

It has two bays in the transversal direction and seven bays in the longitudinal one. The ground floor, hosting commercial activities, has height of 4.0 m, while the heights of upper

floors are 3.2 m. The building total height is 16.8 m, without considering the top parapet. Seismic-resistant frames are placed in the longitudinal direction only. They are connected each to other in the transversal direction from both the slab and the edge beams only. The staircase is located in the building central position and it is made of 30x60 cm knee beams. Floors are made of RC - hollow tiles mixed slabs having depth of 28 cm and 24 cm at the intermediate levels and the top one, respectively.
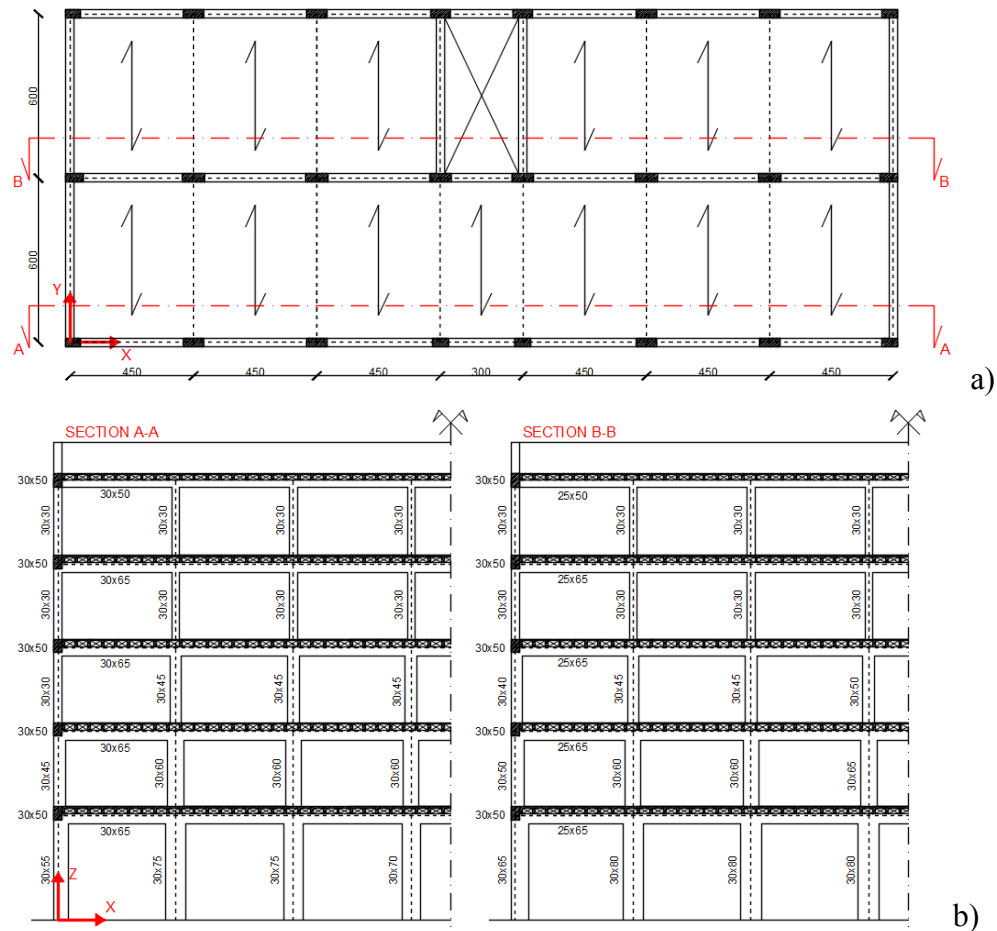
Figure 6. *Existing building under investigation: typical plan layout (a) and vertical sections (b)*
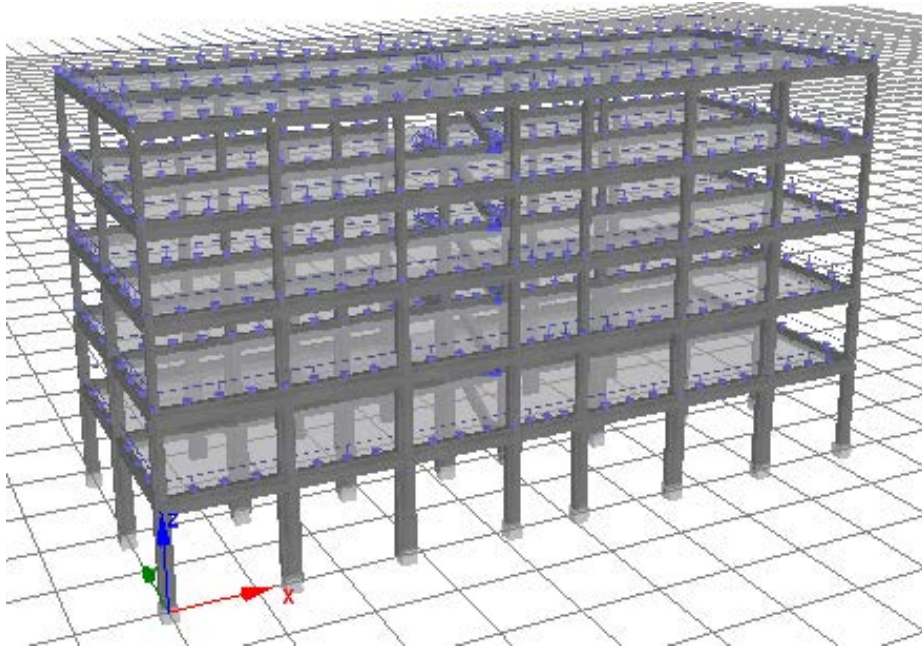
Figure 7. *Numerical model of the investigated existing 5-storey building*

In absence of specific documentation on carpentry, the elements sizes have been detected from in-situ inspections, whereas the reinforcement details have been deduced from an appropriate simulated design 0. According to the materials used at that construction time, $R_{cm}180$ concrete and Aq50 Italian steel (f_{ym} = 270 MPa and f_{um} = 550 MPa) have been considered. In order to take into account the presence of a cracking state of the structural members, according to [M.D. 14/01/08, 2008], a 50% reduced Young modulus has been assumed for both beams and columns.

The building is located on a soil type C having a peak ground acceleration a_gS equal to 0.28g and corresponding to a 975 years return period.

The three-dimensional view of the structure under study modelled with the SeismoStruct software is illustrated in Figure 7.
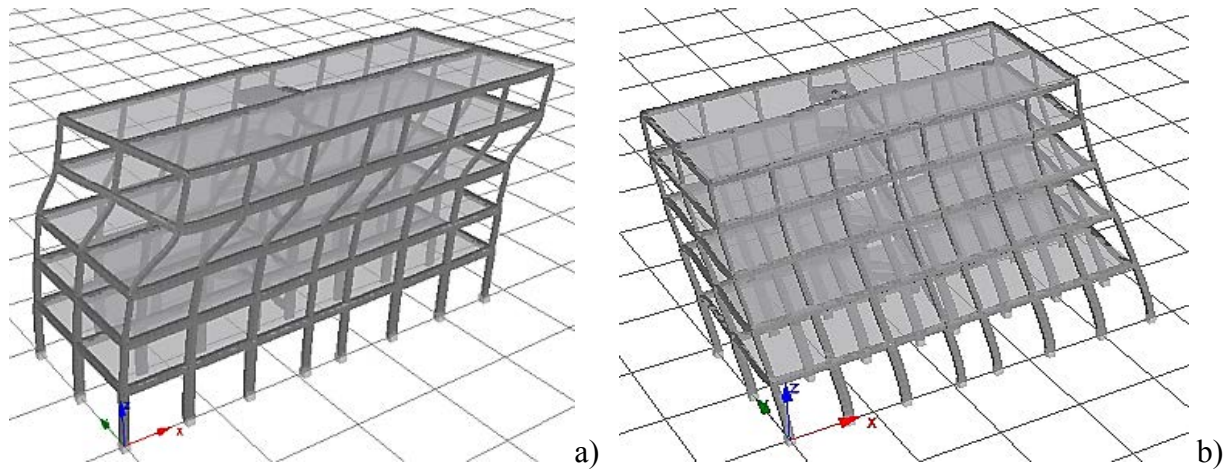
Figure 8. *Deformed shape of the building under pushover analysis in directions x (a) and y (b) (displacement amplification factor equal to 50)*

Table 2. Modal analysis results on the bare RC building

Mode	1 (U_y)	2 (R_z)	3 (U_x)
Period (s)	1.70	1.40	0.95
Participating Mass (%)	84	78	70

From the modal analysis, whose results are depicted in Table 2 and Figure 8, the building has shown a high deformability, especially in the transversal direction, due to the lack of frames. From the pushover analyses on the bare structure, it appears that in the longitudinal direction the seismic demand is particularly focused between the 3rd and 4th floor, where the variation of in elevation stiffness is very high (see Table 3). On the other hand, in the transversal direction, the failure is essentially caused by the staircase column collapse.

The seismic upgrading of the above RC building by means of full MPSWs, which provide to the structure where they are inserted a significant increase of initial stiffness, shear strength and dissipated energy, has been developed on the basis of the US procedures [ATC-40, 1996; FEMA-273, 1997]. Following a performance based design approach, which aims at increasing the overall lateral stiffness of the initial structure, the procedure involves the choice of a target spectral displacement of the retrofitted structure, $S_{d,pp}$, corresponding to a given performance level (operational, immediate occupancy, life safety or near collapse). Once the seismic hazard parameters are known, the elastic spectral acceleration $S_{ae,pp}$ is determined from the ADRS (Acceleration-Displacement Response Spectrum) format. So, the target period T_{ret} and the target stiffness K_{ret} of the retrofitted structure are calculated from Eqs. (12) and (13), respectively. In particular, in Eq. (13) the term T_{ini} is the fundamental period of the initial structure. After defining the performance points of the retrofitted structure, the stiffness contribution K_w provided by MPSWs is determined from Eq. (14), where the term K_{ini} is the initial structure stiffness.

$$T_{ret} = 2\pi \sqrt{S_{d,pp}/Sae, pp} \tag{12}$$

$$K_{ret} = K_{ini} \left(\frac{T_{ini}}{T_{ret}}\right)^2 \tag{13}$$

$$K_w = K_{ret} - K_{ini} \tag{14}$$

Considering that the retrofitted structure is able to provide at least the same damping level of the bare structure, the target shear strength of the retrofitted structure V_{ret} is obtained from Eq. (15), where V_{ini} and $S_{ai,ini}$ are the shear strength and the inelastic spectral acceleration of the initial structure, respectively, and $S_{ai,ret}$ is the retrofitted structure inelastic spectral acceleration. Finally, the contribution in terms of shear strength V_w given by MPSWs is evaluated through Eq. (16).

Table 3. *Regularity analysis of the initial structure*

Floor	Seismic Mass (t)	Relative mass variation	Direction x		Direction y	
			Lateral Stiffness (KN/m)	Lateral Stiffness variation	Lateral Stiffness (KN/m)	Lateral Stiffness variation
5	353	-25%	87877	0%	31419	-35%
4	473	0%	87760	-51%	48290	-21%
3	474	-1%	180779	-38%	60844	-14%
2	478	-4%	293620	-26%	70666	-21%
1	499	-	397521	-	89464	-

$$V_{ret} = V_{ini} \frac{S_{ai,ret}}{S_{ai,ini}} \tag{15}$$

$$V_w = V_{ret} - V_{ini} \tag{16}$$

In Figure 9, the response spectrum is plotted in the ADRS plane, considering the spectral acceleration reduction obtained with a damping equal to 20%.

Once the required stiffness and strength of the panels have been determined, their preliminary design is developed. In analogy with 0, an upgrading system with partial-bay SPSWs, arranged in one and two pairs along directions *x* and *y*, respectively, has been firstly designed (see Figure 10). The disposition of SPSWs has been dictated from both the necessity to reduce as much as possible the interruption of building activities and to respect architectural requirements.
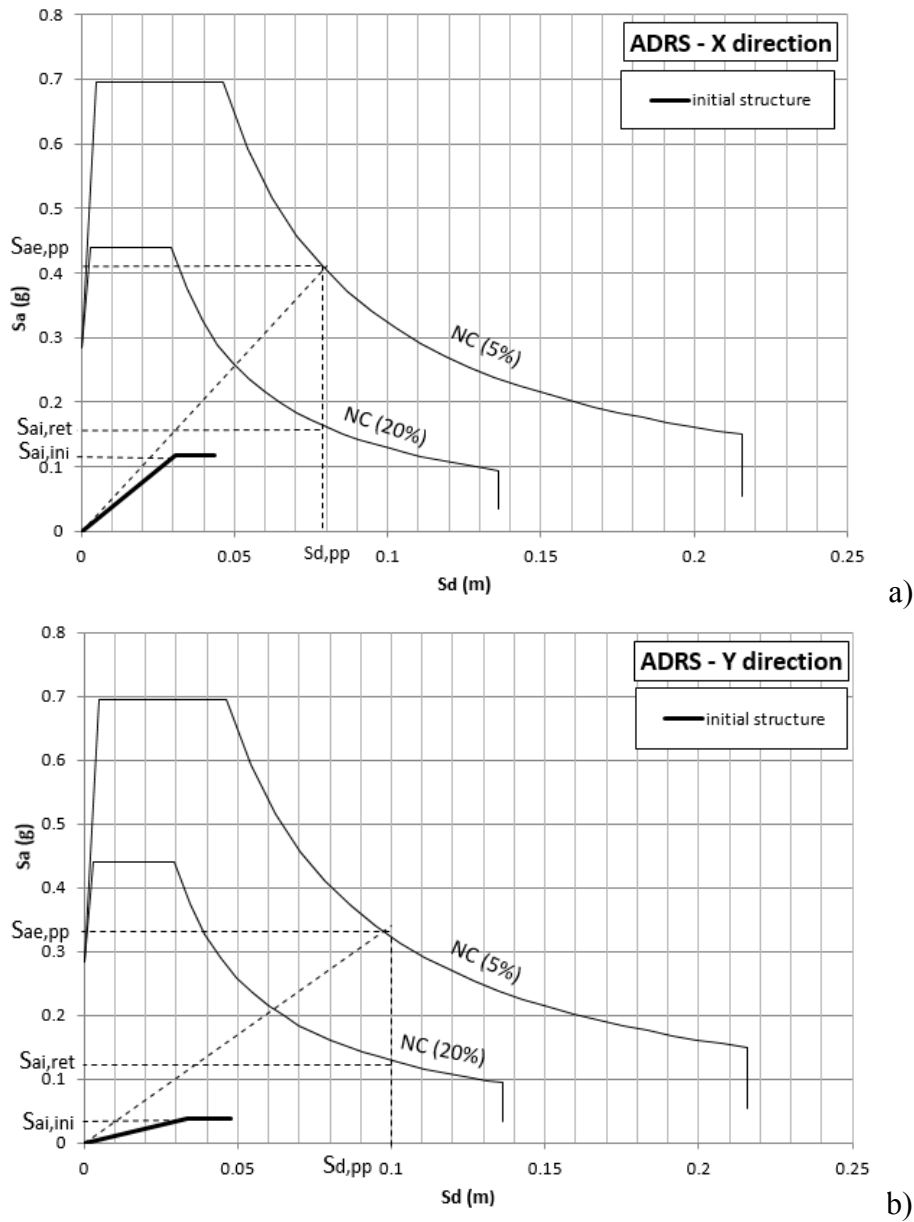
Figure 9. *Capacity curves and performance points of the initial structure in directions x (a) and y (b)*
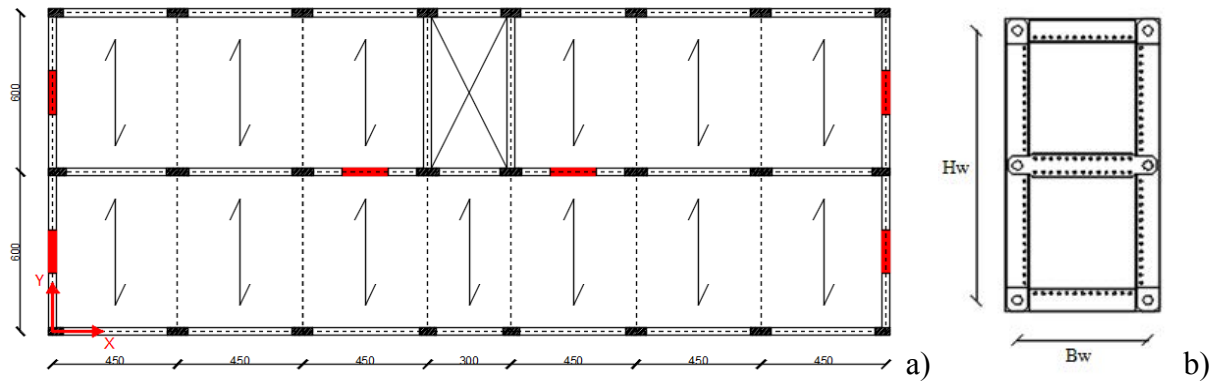
Figure 10. *Location of MPSWs (a) and details of the external frame (b)*

In order to respect the optimal panel shape ratio [Formisano et al., 2007] and considering the building inter-story height, the SPSW width B_w has been chosen equal to 1.65 m, while its depth has been divided in two equal parts by means of an intermediate steel beam placed inside the external frame. The shear walls design has been conducted initially considering the full S235 steel plates (see Tables 4 and 5).

The plate thicknesses have been firstly derived by reversing Eqs. (10) and (11) and by assuming C_{m1} and C_{m2} equal to 1.0 and 1.7 respectively, and $C_{p,x}$ and $C_{p,y}$ equal to 8.5 and 13.6 respectively. These modification factors are herein obtained by iterations in order to fit the numerical behaviour of the retrofitted structure to the design requirements both in terms of global strength and stiffness. Instead, the a priori knowledge of these values should be obtained from experimental tests on the designed shear walls.

Since the stiffness based design implies greater thicknesses than the strength based one, the values from the former design process have been considered, they being subsequently replaced by the most common commercial types. Then, the equivalent bracing behaviour is obtained through Eqs. (8) and (9) for implementation in the numerical analyses.

Table 4. *Thicknesses of full SPSWs derived from the strength design*

Floor	C_{m1}	B_p (mm)	$V_{pi,x}$ (kN)	$n_{p,x}$	$t_{p,x}$ (mm)	$V_{pi,y}$ (kN)	$n_{p,x}$	$t_{p,y}$ (mm)
5		1650	223	2	0.58	475	4	0.61
4		1650	465	2	1.20	989	4	1.27
3	1.0	1650	651	2	1.68	1383	4	1.78
2		1650	780	2	2.01	1658	4	2.14
1		1650	856	2	2.21	1818	4	2.34

Table 5. *Thicknesses of full SPSWs derived from the stiffness design*

Floor	E (MPa)	$K_{p,x}$ (KN/m)	$C_{p,x}$	$H_{p,x}$ (mm)	$t_{p,x}$ (mm)	$K_{p,y}$ (KN/m)	$C_{p,y}$	$H_{p,y}$ (mm)	$t_{p,y}$ (mm)
5				2300	1.78			2400	3.15
4				2250	1.74			2400	3.15
3	200000	14991	8.5	2250	1.74	31850	13.6	2400	3.15
2				2250	1.74			2400	3.15
1				3375	2.61			3450	4.53

Table 6. *Metallic materials considered for the shear walls design*

Material	f_y (MPa)	f_u (MPa)	ε_u	E (MPa)
Steel	235	360	35%	200000
LYS	*86	236	50%	200000
AW 1050A	*21	80	45%	70000

Assuming to guarantee the same lateral stiffness level of the full SPSWs, the study has been extended by considering full LYS (LYS-PSWs) and aluminium (AW1050A-PSW) plates, as well as perforated S235 steel ones. Table 6 shows the mechanical properties of the materials considered in the retrofit design.

Two drilling configurations have been proposed for perforated SPSWs. The first solution is characterized by plates with 36 holes having diameter of 160 mm and hole percentage ρ, that is the ratio between the holes areas A_{holes} and the panel one A_{sup}, equal to 40%, while the second solution has 36 holes having diameter of 190 mm and ρ equal to 60%. The behaviour of the perforated panels has been implemented in the FEM model by adopting a linear reduction of the modification factors in comparison to those used for full panels. The modification factor values assumed for C_{m1} and C_{m2} are equal to 0.40 and 0.70, respectively, for ρ = 40%, and to 0.20 and 0.40, respectively, for ρ = 60%.

Table 7 shows the commercial plate thicknesses used in the following analyses. Due to the different Young modulus, aluminium plates thicker than steel ones are considered in order to have comparable results among solutions in terms of the global stiffness of the retrofitted structures. The steel frame surrounding MPSWs has been designed to both possess an adequate stiffness and remain in the elastic field when the plates exhibit significant plastic strains. This outcome is achieved for full panels by both using the Eq. (3) and accomplishing the strength check of elements under the actions induced by the tension-field mechanism 0. So, the S275 steel coupled UPN profiles in Table 8 have been obtained from this design procedure applied to the examined shear walls.

Table 7. *Commercial plate thicknesses used in the numerical analyses*

Floor	Steel plates		AW1050A Plates	
	$t_{p,x}$ (mm)	$t_{p,y}$ (mm)	$t_{p,x}$ (mm)	$t_{p,y}$ (mm)
1	1.80	4.00	4.00	7.00
2	1.80	4.00	4.00	7.00
3	1.80	4.00	4.00	7.00
4	1.80	4.00	4.00	7.00
5	3.00	5.00	6.00	10.00

Table 8. *The assumed steel frame members for different MPSWs*

Floor	Full SPSWs		Perf. (40%) SPSWs & LYS-PSWs		Perf. (60%) SPSWs & AW1050A-PSW	
	Dir. X	Dir. Y	Dir. X	Dir. Y	Dir. X	Dir. Y
5	2×UPN160	2×UPN240	2×UPN120	2×UPN180	2×UPN120	2×UPN120
4	2×UPN160	2×UPN240	2×UPN120	2×UPN180	2×UPN120	2×UPN120
3	2×UPN160	2×UPN240	2×UPN120	2×UPN180	2×UPN120	2×UPN120
2	2×UPN160	2×UPN240	2×UPN120	2×UPN180	2×UPN120	2×UPN120
1	2×UPN260	2×UPN320	2×UPN160	2×UPN220	2×UPN120	2×UPN160

Table 9. *The assumed steel members for strengthening of the RC beams*

Floor	Full SPSWs	Perf. (40%) SPSWs & LYS-PSWs	Perf. (60%) SPSWs & AW1050A-PSW
	Dir. X-Y	Dir. X-Y	Dir. X-Y
5	2×UPN260	2×UPN240	2×UPN220
4	2×UPN260	2×UPN240	2×UPN220
3	2×UPN260	2×UPN240	2×UPN220
2	2×UPN260	2×UPN240	2×UPN220
1	2×UPN300	2×UPN280	2×UPN260

Moreover, in order to transfer the actions to the walls, the RC beams have been reinforced, analogously to the experimentation performed in [De Matteis et al., 2008a; Formisano et al., 2006c], by means of two S275 steel coupled UPN profiles fixed to the RC beams by means of steel bolts (see Table 9).

The analysis results on the retrofitted structures have shown that, due to the failure of existing columns, further interventions on other RC members are necessary in order to achieve the target displacement. Therefore, the retrofitting project has been completed with RC jacketing of the longitudinal perimeter columns at the 3rd and 4th floors, of the transversal perimeter columns from the 2nd to 4th floors and of the stair case columns up to the 4th floor.

Furthermore, jacketing with steel profiles has been done for members incurring brittle failure due to shear. These additional interventions on the existing members have been designed to ensure the expected performance of the structure up to the target displacement. Figure 11 shows the results obtained from the pushover analyses on the structure equipped with the mentioned interventions.

The results show that the shear strength of the structure retrofitted with full SPSWs is clearly higher than the other solutions one. As a negative consequence, the greater actions induced by the full SPSWs on the RC structure have requested the design of additional local retrofitting interventions. Also for the other solutions additional interventions on the main RC structure have been foreseen, but they have been more economic than those required by using full SPSWs. In particular, although the solutions based on plates with low yield strength metals (low yield steel and aluminium) seem to be structurally comparable with those based on perforated traditional steel plates, the differences are noticed from the economic point of view (see Table 10).

Table 10. *Economic comparison among examined solutions*

Wall Type	Plates (€)	Perimeter Steel Frame (€)	Local Interventions (€)	Total (€)
Full SPSWs	14200	36000	72000	122200
Perf. (40%) SPSWs	15100	22500	68400	106000
Perf. (60%) SPWSs	15100	17800	64100	97000
LYS-PSW	19900	22500	68400	110800
AW1050A-PSW	37100	17800	64100	119000
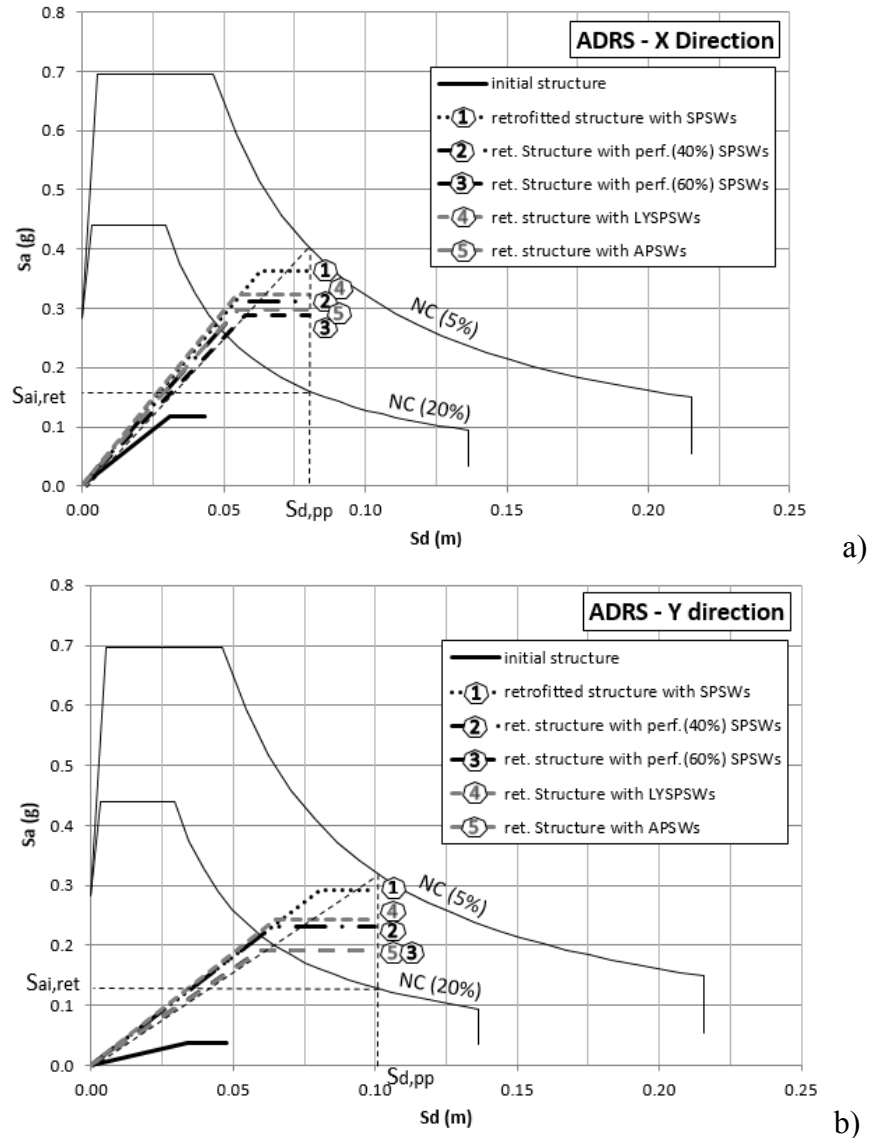
Figure 11. *Capacity curves of initial and retrofitted structures in directions x (a) and y (b)*

In fact, considering the current Italian costs of both steel elements and local reinforcing interventions, a cost saving of at least 16% and 27% has been respectively estimated for the less drilled and the more drilled perforated SPSWs with respect to the installation of full SPSWs. This confirms the benefits deriving from the use of perforated SPSWs.

4. CONCLUDING REMARKS

In this paper a study aimed to show the benefits of using perforated SPSWs for seismic protection of existing RC buildings has been carried out. The use of such systems, already known in literature for applications into new steel structures, can be particularly advantageous for retrofitting existing structures designed without seismic criteria, although the actual Eurocodes do not provide any indications.

When referred to existing RC structures, the use of traditional full SPSWs may involve the transfer of excessive stresses on the boundary members induced by the plate tension-field mechanism. Such stresses can lead to the design of massive interventions, which are very often economically inconvenient.

Starting from these premises, in the first part of the paper, the availability of recent experimental test results on a real RC building retrofitted with SPSWs has allowed both to calibrate and validate a simple FEM model developed with the SeismoStruct software.

Subsequently, the case study of an existing multi-storey RC building retrofitted with full MPSWs (traditional steel, low yield steel and aluminium plates) and perforated SPSWs, has been numerically analyzed in the static non-linear field. The main benefit deriving from the use of perforated plates is to choose *a priori* the shear strength they offer on the basis of a given drilling configuration, according to the design requirements, without changing the geometric dimensions of the walls, which sometimes represent data assigned for architectural requirements impossible to be modified. By increasing properly the drilling configuration, a significant shear strength reduction is achieved without excessively compromise both the stiffness and the ductility of the retrofitted structure. In fact, by choosing an appropriate drilling pattern, it is possible to reach large drifts without fractures around the holes, which could decrease the shear capacity. In the examined application, the analysis results have shown that perforated SPSWs with drilling percentages of 40% and 60%, provide cost savings in the retrofit design of at least 16% and 27%, respectively, compared to the cost deriving from using full plates. Although perforated SPSWs realized by common steel plates can be a viable alternative to others stiffening solutions based on more expensive (aluminium) and not available on the European market (Low Yield Steel) metals, further experimental tests are necessary for the validation of modification factor values, to be used in approved design formulas, which could extend their use on the market for seismic retrofitting interventions.

5. ACKNOWLEDGEMENTS

6. REFERENCES

Astaneh-Asl, A. [2000] "Seismic Behavior and Design of Steel Shear Walls", *Steel Technical Information and Product Services Report*, Structural Steel Educational Council, Moraga, CA.

Basler, K. [1961] "Strength of plate girders in shear", *J. Struct. Div., ASCE* 87 (7), 150-180.

Applied Technology Council (ATC)-40, [1996] "Seismic evaluation and retrofit of concrete buildings", *Report SSC 96-01*, vol. 1.

Bhowmick, A. K., Grondin, G. Y. and Driver, R. G. [2014] "Nonlinear seismic analysis of perforated steel plate shear walls", *Journal of Constructional Steel Research* 94, 103-113.

Brando, G. and De Matteis, G. [2014] "Design of low strength-high hardening metal multi-stiffened shear plates", *Engineering Structures* 60, 2-10.

Canadian Standards Association (CSA) [2001] *Limit states design of steel structures - CAN/CSA S16-01*, Willowdale, Ontario, Canada.

De Matteis, G., Brando, G., Mazzolani, F.M. [2012] "Pure aluminium: An innovative material for structural applications in seismic engineering", *Construction and Building Materials*, 26 (1), 677-686.

De Matteis, G., Formisano, A. and Mazzolani, F. M. [2008a] "RC structures strengthened by metal shear panels: experimental and numerical analysis", *Proc. of the 2008 Seismic Engineering Conference commemorating 1908 Messina and Reggio Calabria Earthquake (MERCEA'08)*, Reggio Calabria, Italy, Vol. 1, 27-34.

De Matteis, G., Formisano, A., Mazzolani F.M. and Panico, S. [2005] "Design of low-yield metal shear panels for energy dissipation", *Improvement of Buildings' Structural Quality by New Technologies - Proceedings of the Final Conference of COST Action C12*, Innsbruck, Austria, 665-675.

De Matteis, G., Formisano, A., Panico, S. and Mazzolani, F.M. [2008b] "Numerical and experimental analysis of pure aluminium shear panels with welded stiffeners", Computers & Structures 86, 545-555.

De Matteis, G., Formisano, A. and Mazzolani, F.M. [2009] "An innovative methodology for seismic retrofitting of existing RC buildings by metal shear panels", *Earthquake Eng. & Struct. Dynamics* 38, 61-78.

Federal Emergency Management Agency (FEMA)-273 [1997] *Guidelines for the seismic rehabilitation of buildings*, Washington (DC).

Formisano, A. [2012] "Seismic damage assessment of school buildings after 2012 Emilia Romagna earthquake". *Journal of Earthquake Engineering, Special Number "Emilia Romagna earthquake – May 2012"*, 2-3, 72 – 86.

Formisano, A. and Mazzolani, F.M. [2015] "On the selection by MCDM methods of the optimal system for seismic retrofitting and vertical addition of existing buildings", Computers and Structures 159, 1-13.

Formisano, A. and Sahoo, D.R. [2015] "Steel shear panels as retrofitting system of existing multi-story RC buildings: case studies", Advances in Structural Engineering, Vol.1, 1 January 2015, Pages 495-512.

Formisano, A., De Matteis G. and Mazzolani, F.M. [2010] "Numerical and experimental behaviour of a full-scale RC structure upgraded with steel and aluminium shear panels", *Computers and Structures* 88, 1348-1360.

Formisano, A., Lombardi, L. and Mazzolani, F.M. [2015] "On the use of perforated metal shear panels for seismic-resistant application", *Proc. of the 8th International Conference on Behaviour of Steel Structures in Seismic Areas (STESSA 2015)*, Shanghai, China, 409-416.

Formisano, A., Mazzolani, F.M. and De Matteis, G. [2007] "Numerical analysis of slender steel shear panels for assessing design formulas", *International Journal of Structural Stability & Dynamics* 7, 273-294.

Formisano, A., De Matteis, G., Panico, S. and Mazzolani, F.M. [2006a] "Full scale test of an existing RC frame reinforced with pure aluminium shear panels", *Proc. of the Int,Colloquium on Stability and Ductility of Steel Structures (SDSS '06)*, Lisbon, Portugal, 903-910.

Formisano, A., De Matteis, G., Panico, S. and Mazzolani, F.M. [2008]. "Seismic upgrading of existing RC buildings by slender steel shear panels: a full-scale experimental investigation", *Advanced Steel Construction* 4, 26-45.

Formisano, A., De Matteis, G., Panico, S., Calderoni, B. and Mazzolani, F.M., [2006b] "Full-scale test on existing RC frame reinforced with slender shear steel plates", Proc. of the 5th International Conference on Behaviour of Steel Structures in Seismic Areas (STESSA 2006), Yokohama, Japan, 827-834.

Formisano,, A., De Matteis, G., Panico, S., Calderoni, B. and Mazzolani, F.M. [2006c] "Full-scale experimental study on the seismic upgrading of an existing R.C. frame by means of slender steel shear panels", *Proc. of the Int. Conference in Metal Structures (ICMS '06),* Poiana Brasov, Romania, 609-617.

Formisano, A., Di Feo, P., Grippa, M.R. and Florio, G. [2010] "L'Aquila earthquake: A survey in the historical centre of Castelvecchio Subequo", *COST ACTION C26: Urban Habitat Constructions under Catastrophic Events - Proceedings of the Final Conference*, Nsples, Italy, 371-376.

Formisano, A., Mazzolani, F.M., Brando, G. and De Matteis, G. [2006d] "Numerical evaluation of the hysteretic performance of pure aluminium shear panels", *Proc. of the 5th International Conference on Behaviour of Steel Structures in Seismic Areas (STESSA 2006)*, Yokohama, Japan, 211-217.

Giugliano, M.T., Longo, A., Montuori, R. and Piluso, V. [2010] "Plastic design of CB-frames with reduced section solution for bracing members", *Journal of Constructional Steel Research* 66 (5), 611-621.

Indirli, M., Kouris, L. A. S., Formisano, A., Borg, R. P. and Mazzolani, F. M. [2013] "Seismic damage assessment of unreinforced masonry structures after the Abruzzo 2009 earthquake: the case study of the historical centres of L'Aquila and Castelvecchio Subequo", *International Journal of Architectural Heritage,* 7 (5), 536-578.

Longo, A., Montuori, R. and Piluso, V. [2008a] "Failure mode control of X-braced frames under seismic actions", *Journal of Earthquake Engineering* 12 (5), 728-759.

Longo, A., Montuori, R. and Piluso, V. [2008b] "Influence of design criteria on the seismic reliability of X-braced frames", *Journal of Earthquake Engineering* 12 (3), 406-431.

Longo, A., Montuori, R. and Piluso, V. [2009] "Seismic reliability of chevron braced frames with innovative concept of bracing members", *Advanced Steel Construction* 5 (4), 367-389.

Ministerial Decree (M.D.) 14/01/08 [2008] "Approval of new technical codes for constructions" (in Italian), *Official Gazette of the Italian Republic No. 29*.

Mistakidis, E. S., De Matteis, G. and Formisano, A. [2007] "Low yield metal shear panels as an alternative for the seismic upgrading of concrete structures", *Advances in Engineering Software* 38, 626-636.

Montuori, R. [2014] "The influence of gravity loads on the seismic design of RBS connections", *Open Construction and Building Technology Journal* 8, 248-261.

Montuori, R., Nastri, E. and Piluso, V. [2014a] "Theory of plastic mechanism control for eccentrically braced frames with inverted y-scheme", *Journal of Constructional Steel Research* 92, 122-135.

Montuori, R., Nastri, E. and Piluso, V. [2014b] "Theory of plastic mechanism control for the seismic design of braced frames equipped with friction dampers", *Mechanics Research Communications* 58, 112-123.

Mazzolani, F.M. [2008] "Innovative metal systems for seismic upgrading of RC structures", *Journal of Constructional Steel Research* 64, 882-895.

Piluso, V., Montuori, R. and Troisi, M. [2014] "Innovative structural details in MR-frames for free from damage structures", *Mechanics Research Communications,* Vol. 58, 146-156.

Purba, R. and Bruneau, M. [2007] "Design recommendations for perforated steel plate shear walls", *Technical Rep. MCEER-07-0011*, Multidisciplinary Center for Earthquake Engineering Research, State Univ. of New York, Buffalo, N.Y.

Royal Decree (R.D.) n. 2229 [1939] "Standards for the execution of concrete and reinforced concrete constructions" (in Italian).

Sabouri-Ghomi, S., Ventura, C.E. and Kharrazi, M.H.K. [2005] "Shear analysis and design of ductile steel plate walls", *Journal of Structural Engineering* 131, 878-889.

Seismosoft [2014] *SeismoStruct v7.0 – A computer program for static and dynamic nonlinear analysis of framed structures*, available from http://www.seismosoft.com.

Thorburn, L.J., Kulak, G.L. and Montgomery, C.J. [1983] "Analysis of steel plate shear walls", *Struct. Eng. Rep. No. 107*, Dept. of Civ. Eng., University of Alberta, Canada.

Timler, P.A. and Kulak, G.L. [1983] "Experimental study of steel shear walls", *Struct. Eng. Rep. No. 114*, Dept. of Civ. Eng., University of Alberta, Edmonton, Alberta, Canada.

Vian, D. and Bruneau, M. [2005] "Steel plate shear walls for seismic design and retrofit of building structures", *Technical Rep. MCEER-05-0010*, Multidisciplinary Center for Earthquake Engineering Research, State Univ. of New York, Buffalo, N.Y.

PARETI A TAGLIO METALLICHE COME SISTEMI DI CONTROVENTAMENTO PER L'ADEGUAMENTO SISMICO DI STRUTTURE ESISTENTI IN C.A.

Antonio Formisano*, Luca Lombardi, Federico M. Mazzolani

Department of Structures for Engineering and Architecture, University of Naples "Federico II"

SOMMARIO: *Le pareti a taglio metalliche rappresentano un sistema efficace, pratico ed economico per la protezione sismica di edifici esistenti in c.a.. Questi sistemi consistono in uno o più piatti sottili metallici, bullonati o saldati ad un telaio di acciaio rigido, che vengono installati all'interno delle campate della struttura intelaiata in c.a. Il comportamento del sistema è caratterizzato dallo sviluppo di bande diagonali di trazione (meccanismo di tension-field), che dipendono dalla dimensione dei piatti e dalla presenza di irrigidimenti flessionali o di aperture al loro interno. In questo articolo, è stato esaminato un caso studio di un edificio esistente in c.a. di 5 piani, progettato tra gli anni '60 e '70 dello scorso secolo, adeguato con pareti a taglio metalliche. Il progetto di adeguamento della struttura esistente è stato effettuato mediante quattro sistemi di pareti a taglio: tre pannelli a parete piena realizzati in acciaio tradizionale, acciaio a basso snervamento ed alluminio ed un pannello innovativo di tipo perforato in acciaio. Le differenti tipologie di pannelli impiegate sono state in conclusione confrontate*

_____

*Corresponding author: Antonio Formisano, Department of Structures for Engineering and Architecture, University of Naples "Federico II"
Email: antoform@unina.it

FEM SIMULATIONS OF A NEW HYSTERETIC DAMPER: THE DISSIPATIVE COLUMN

Paolo Castaldo*, Bruno Palazzo, Francesco Perri

Department of Civil Engineering, University of Salerno, Fisciano (SA), Italy

SUMMARY: *A new replaceable hysteretic damper to better control seismic building damage, consisting of two adjacent steel vertical elements connected to each other with continuous X-shaped mild/low strength steel shear links, is investigated in this study. New Dampers, called Dissipative Columns (DC), provide additional stiffness and damping to a lateral system by using a basic and minimally invasive construction element: the column. The Dissipative Column has been conceived or as a device installed within a frame either external damper to provide macro-dissipation. In fact, considering different configurations, a parametric analysis, based on FEM simulations, is developed in order to evaluate the effect of the main geometrical and structural parameters as well as provide the design capacity curves of this new damper. In particular, non-linear pushover and cyclic analyses have been carried out in ABAQUS in order to characterize the local and global behaviour of the device also considering different steel grades.*

KEYWORDS: *Replaceable hysteretic damper, dissipative column, FEM simulations, low yielding point steel, damage control, lever arm*

1. INTRODUCTION

Strong earthquakes have shown that a large percentage of buildings in the affected areas, even if properly built and designed according to the most advanced codes, suffer such severe damages [De Iuliis *et al.*, 2010] that they need to be demolished after a strong earthquake, since they would be expensive to repair. As is known, the acceptance of such level of damage due to severe earthquakes is related to the ductility-based design criteria that assume design seismic actions decreased by corresponding reduction factors. Inspired by new performance criteria, there is a growing belief that code design criteria are not sustainable for the high level of accepted damage and that common buildings should be designed with a higher performance level. At the beginning of this century, performance based engineering0 [Vision, 2000] introduced new principles with the scope to select more articulated targets better corresponding to different building roles and use, defining a variety and complex subdivision of performance objectives for seismic events with different intensities and frequencies of occurrence.
The "Direct Displacement Based Design" philosophy [Priestley, 1993] relates the specified performance level to the strain or drift limits for a specified seismic intensity. With the scope of minimizing structural damage, several frictional isolation devices [Castaldo *et al.*, 2015; Castaldo and Tubaldi, 2015; Palazzo *et al.* 2014a; Castaldo *et al.* 2016a; Castaldo *et al.* 2016b] and dampers [Symans *et al.*, 2008; Wada *et al.*, 1992], new replaceable hybrid composite or

---

*Corresponding author: Paolo Castaldo, Department of Civil Engineering, University of Salerno, Fisciano, Italy. Email: pcastaldo@unisa.it

steel or aluminium devices [Brando *et al.*, 2013; Castaldo *et al.* 2016c; De Matteis *et al.*, 2007; Formisano and Mazzolani, 2015; Formisano and Sahoo, 2015; Formisano *et al.*, 2006; Formisano *et al.*, 2010; Montuori, 2014; Pampanin, 2005; Pampanin, 2013; Palazzo *et al.*, 2014b; Palazzo *et al.*, 2015; Piluso *et al.*, 2014] have been recently proposed as well as integrated design approaches [Castaldo, 2014; Castaldo and De Iuliis, 2014] and new strategies, i.e., based on the collapse mechanism control [Longo *et al.*, 2014; Montuori and Muscati, 2015; Montuori *et al.*, 2014; Montuori *et al.*, 2015; Montuori *et al.*, 2016; Nastri, 2016; Nastri and Paciello, 2016] or energy balance [De Iuliis and Castaldo, 2012], have been developed in order to dissipate seismic input energy outside of the primary structure. Dampers should absorb a significant portion of the input energy reducing the hysteretic energy demand to the primary structural elements. Another damper employed to dissipate energy dynamic energy through stable hysteretic behavior [Kim and Seo, 2004] consists in the buckling-restrained braces (BRBs). Low Yielding Strength (LYS) steel is investigated by [Susantha *et al.*, 2004] for improving the ductility capacity of box-shaped steel bridge piers carrying out an experimental work for four specimens having different thickness and sectional configurations under cyclic loads. The test results reveal that the LYS steel portion with longitudinal stiffeners greatly improves the strength and ductility capacity of box columns and it is observed that LYS steel has a great cyclic strain-hardening characteristic. The advantage of use of LYS steel is that it can effectively use large plastic deformation in component plates and the failure of column is concentrated at the LYS steel segment and the energy dissipation occurs far beyond the yield point. The aim of this paper is to investigate a new replaceable hysteretic damper having a basic form of the art of building, minimally architecturally invasive, consisting of two or more dissipative steel columns directly connected to two floors linked to each other with X-shaped low/mild steel plates. The new element is able to add significant stiffness and damping to the structural system in order to reduce seismic response and damage in primary structural members under severe earthquakes. The Dissipative Columns (DC) element will be investigated through non-linear pushover and cyclic analyses useful to characterize the yielding properties of the damper depending on the steel grades, the characteristics of the primary structure and the expected performance as discussed by [Oviedo *et al.*, 2010].

2. THE DISSIPATIVE COLUMN: MECHANICAL PRINCIPLES

The Dissipative Column model, shown in Fig.1, can be considered as a sort of framed bi-pendulum with height equal to *H*, connected in parallel to the primary structure, able to react to the story drift Δ_D with a lateral force Q_D adding stiffness, strength and damping [Palazzo *et al.*, 2014b; Palazzo *et al.*, 2015]. The design concept of the DC element aims to obtain a lever mechanism by which a small inter-story drift provides an amplified vertical drift between the X-plate ends (Fig. 1) reacting with shear forces. The X-shaped steel plates made of mild or Low Yielding Strength steel, having length *a*, thickness *t*, width at the ends *b* and vertical distance *i*, are also used as shear links between coupled elements. Each lever arm is characterized by an eccentricity *e*, while, *r* is the rigid element representing half section of each column (Fig. 1). The top ends of the model are linked to the upper floor through slotted bolted connections to allow large vertical displacements.
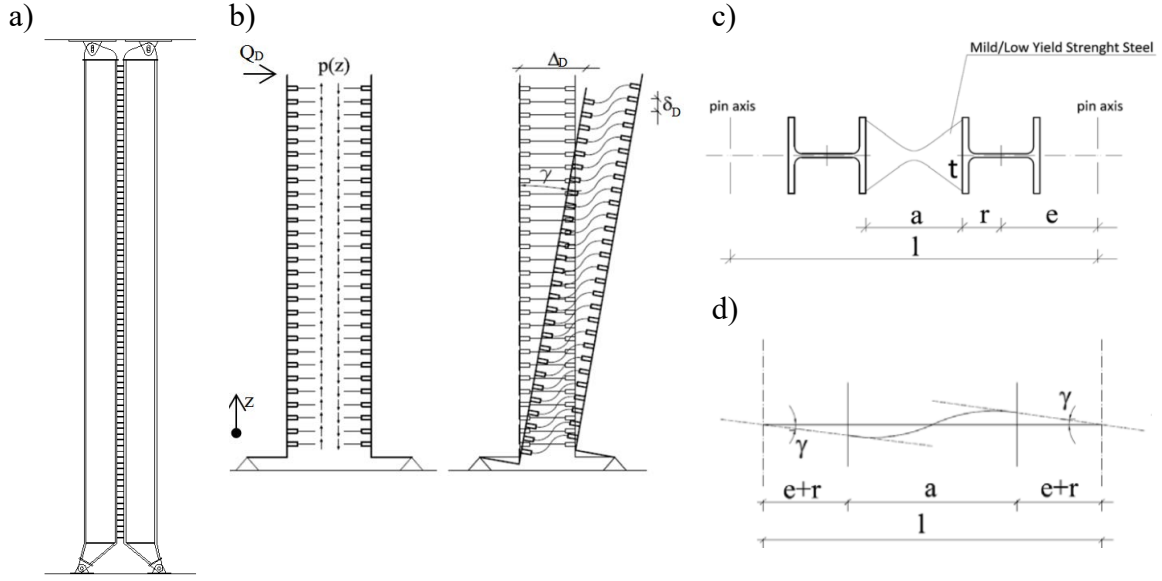
Figure 1. *Eccentric Dissipative Column (a), structural model (b) and dissipative amplified mechanism (c)-(d)*

By yielding a large volume of steel, the shear devices are able to dissipate substantial input energy during earthquakes, while also increasing damping in the entire system in order to reduce the damage in the primary system. With reference to reinforced concrete structures, the limit values of Inter-Story Drift Angle (ISDA) corresponding to different structural performance levels are suggested by Ghobarah [Ghobarah, 2004]. The great advantages of the DC, if compared with classical steel dissipative braces [Kim and Seo, 2004], are the reduced architectural invasiveness, so that it is able to be integrated in any building, the ease of installation everywhere, replacement after earthquakes and the stable behavior in cyclic reversal deformation. In fact, in [Castaldo *et al.*, 2016], an example of a r.c. building, modeled without considering specific constitutive laws [Etse *et al.*, 2016; Mroginski *et al.*, 2015; Ripani *et al.*, 2014; Vrech *et al.*, 2015], with the DC is described.

3. SIMPLIFIED MECHANICAL BEHAVIOUR OF THE DC

As extensively discussed in [Palazzo *et al.*, 2015], the vertical drift δ between the ends of a generic shear link in the elastic range, being the curvature χ constant along each half plate, is related to shear force V_d developed by each X-shaped plate, as:

$$\delta_D = 2 \int_0^{a/2} \int_0^{a/2} \chi(x)dxdx = \frac{3}{2} \frac{a^3}{Ebt^3} V_d \qquad (1)$$

where *a*, *t*, *b* are, respectively, the X-plate length, thickness, width at the ends and *E* is Young's modulus of the steel plates. The axis *x* represents the barycentric axis of a generic steel plate. Hence, the single X-plate vertical stiffness is equal to:

$$K_d = \frac{V_d}{\delta_D} = \frac{2}{3} \frac{Ebt^3}{a^3} \qquad (2)$$

In the case of small eccentricity, a simplified analysis of the DC behavior subjected to relative displacements can be easily carried out assuming that the column flexural deformation is negligible respect to the case of flexible inextensible links. An inter-story drift produces a shear

drift angle γ and vertical drifts δ_D along the X-shaped steel plate. Under such simplified assumptions, the top-base relative displacement Δ_D of a DC element with height H is related to the drift angle γ as:

$$\Delta_D = \gamma \cdot H \tag{3}$$

Therefore, each X-plate undergoes a vertical drift equal to:

$$\delta_D = (l-a)\frac{\Delta_D}{H} \tag{4}$$

where l represents pin axes distance (Fig.1). Therefore, the uniform distributed vertical load, along the vertical axis having origin in the hinge (Fig.1), due to the shear drift angle γ applies:

$$p = \frac{2}{3}\frac{Ebt^3}{a^3 i}(l-a)\frac{\Delta_D}{H} \tag{5}$$

where i represents the plates vertical distance. The term $(l-a)/2 = r$ represents a small lever arm that can be amplified using eccentricity e between the vertical axis and the supports as will be shown in the following. The axial force at the base of each column is equal to:

$$N_c = \frac{2}{3}\frac{Ebt^3}{a^3 i}(l-a)H\frac{\Delta_D}{H} \tag{6}$$

For the equilibrium, lateral force-displacement relationship is expressed as:

$$Q_D = \frac{2}{3}\frac{Ebt^3}{a^3 i}l\frac{\Delta_D}{H}(l-a) = K_D\Delta_D \tag{7}$$

where K_D represents the lateral stiffness of the Dissipative Column given by:

$$K_D = \frac{2}{3}\frac{Ebt^3}{a^3 i}\frac{l}{H}(l-a) \tag{8}$$

According to experimental tests [Aiken et al., 1993; Whittaker et al., 1989], the load-deformation curve of the X-shaped mild steel plates can be idealized as a bilinear curve with a ratio of post yielding stiffness to the initial one equal to 0.03 and available displacement ductility ratio $\mu=\delta_D/\delta_{Dy}$ varying in the range between 3 and 5 [Whittaker et al., 1991]. Since yielding strength f_y is reached almost uniformly along the device, the yielding vertical load p_y can also be expressed as:

$$p_y = \frac{2M_{d,y}}{ia} = f_y\frac{bt^2}{2ia} \tag{9}$$

while, the relative yielding displacement of each link can be written as:

$$\delta_{D,y} = \frac{V_{d,y}}{K_d} = f_y\frac{3a^2}{4Et} \tag{10}$$

Therefore, the lateral yield strength of the doubly hinged DC element can be evaluated as:

$$Q_{D,y} = f_y\frac{blt^2}{2ia} \tag{11}$$

and the yielding displacement applies:

$$\Delta_{D,y} = \frac{3}{4}\frac{f_y}{E}\frac{a^2 H}{t(l-a)} \tag{12}$$

Moreover, in presence of a significant eccentricity the column flexural deformation should not be neglected, therefore, as extensively described in [Palazzo et al., 2015], the top-base relative displacement Δ_D and lateral force of the DC element can respectively be expressed as:

$$\Delta_D = \gamma \cdot H + Q_D \left(\frac{eH^3}{3EI_c l} + \frac{e^2 H^2}{2EI_e l} \right) \quad (13)$$

$$Q_D = \frac{N_c l}{H} = \frac{\frac{2}{3} \frac{Ebt^3}{a^3 i} \gamma(l-a)H \frac{l}{H}}{1 - \left[\frac{2}{3} \frac{Ebt^3}{a^3 i} \frac{l}{H} \left(2\frac{H^2}{l} \frac{e^3}{3EI_e} + \frac{H^2}{l} \frac{e^2}{EI_e} r + \frac{e}{l} \frac{H^3}{3EI_c} r \right) \right]} \quad (14)$$

4. NON LINEAR ANALYSIS OF THE X-SHAPE STEEL PLATES

Non-linear analyses in ABAQUS [ABAQUS, 2010a; ABAQUS, 2010b] are performed in order to characterize the non-linear behavior of the X-shape steel plates. In Table 1, the geometric and mechanical properties are reported with reference to two different steel grades: S235 [CEN, 2007] and LYP [Saeki *et al.*, 1998; Susantha *et al.*, 2004].

Table 1. *Geometrical and structural properties of the X-shaped steel plates*

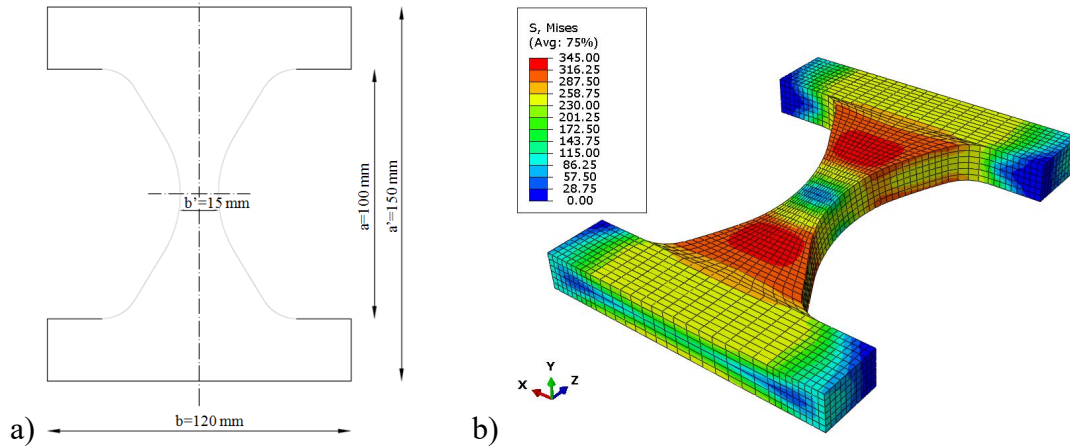| Plate Length *a* (mm)	Plate Thickness *t* (mm)	Plate Width *b* (mm)	Plate Yield Stress *f_y* (N/mm²)
150	15	120	132
150	15	120	235

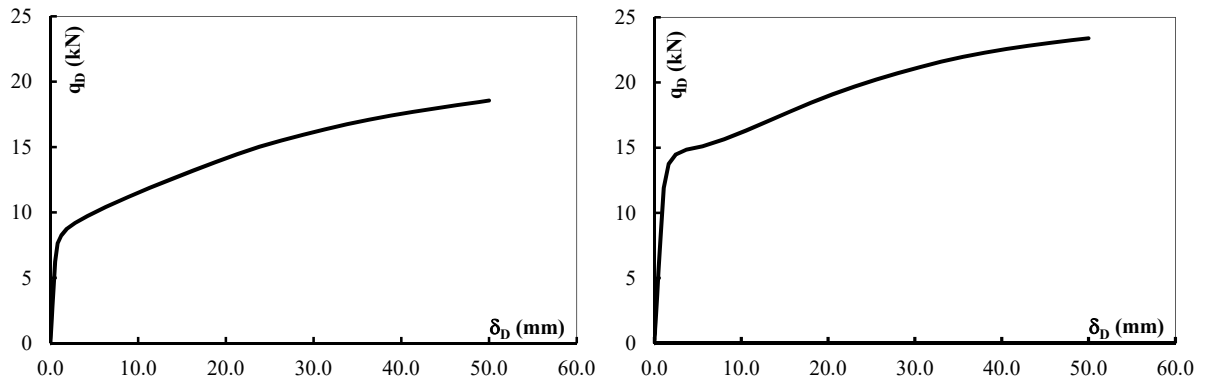Figure 2. *Geometric shape (a) and deformed shape (b) of a X-shaped steel plate*

Figure 3. *Pushover curves of the X plates: (a) LYP [Susantha et al., 2004; Saeki et al., 1998]; (b) S235 [CEN, 2007]*

Fig. 2 shows the geometric shape as well as the deformed shape of the steel plates. A FE model has been defined in ABAQUS [ABAQUS, 2010a; ABAQUS, 2010b] with means of 3D elements with nonlinear stress-strain behaviour. The geometric model proposed by [Tena-Colunga, 1997] has been adopted for the X-shape steel plates. The displacement-controlled pushover analyses of the X plates have been performed until to reach 50 mm in terms of relative displacement and the corresponding curves related to the two different steel grades are plotted in Fig. 3.

4.1 Cyclic analysis and fatigue life curves

In order to obtain the fatigue life curves of the X-shape steel plates, a database of several experimental data developed by [Chang-Hwan *et al.*, 2014; Chang-Hwan *et al.*, 2015; Latour and Rizzano, 2012; Teruna *et al.*, 2015] has been previously defined. The experimental data, related to the different configurations of steel plates and hysteretic devices with different steel grades, are shown in Fig. 4, demonstrating that the data of the different typologies of the devices can be fitted through different linear regressions in the logarithmic scale having the same slope. The dashed line, illustrated in Fig. 4, represents both the average linear regression of all data tests as well as a good fitting of the data [Latour and Rizzano, 2012]. By this way, the abovementioned average regression curve has been adopted as the fatigue life curve characterizing the S235 X-shape steel plates. Regarding LYP steel plates [Saeki *et al.*, 1998; Susantha *et al.*, 2004], the damage properties have been set to be equal to the S235 [CEN, 2007] steel plates. Next, regarding both LYP [Saeki *et al.*, 1998; Susantha *et al.*, 2004] and S235 [CEN, 2007] steel, it has been possible to develop a parametric analysis for different thickness values of the steel plates and for increasing the imposed displacement δ_D. In Fig. 5, with reference to a thickness of the LYP steel [Saeki *et al.*, 1998; Susantha *et al.*, 2004] plate equal to 15 mm, the cyclic curves with imposed ultimate displacements $\delta_D = \delta_{D,u}$ equal to 12, 16, 20 and 24 mm, respectively, are shown. In Fig. 6, the fatigue life curves related to the plate thicknesses equal to 5, 10, 15 and 20 mm, respectively, are illustrated for both LYP [Saeki *et al.*, 1998; Susantha *et al.*, 2004] and S235 [CEN, 2007] steel showing that the number of cycles decreases for higher thickness values.
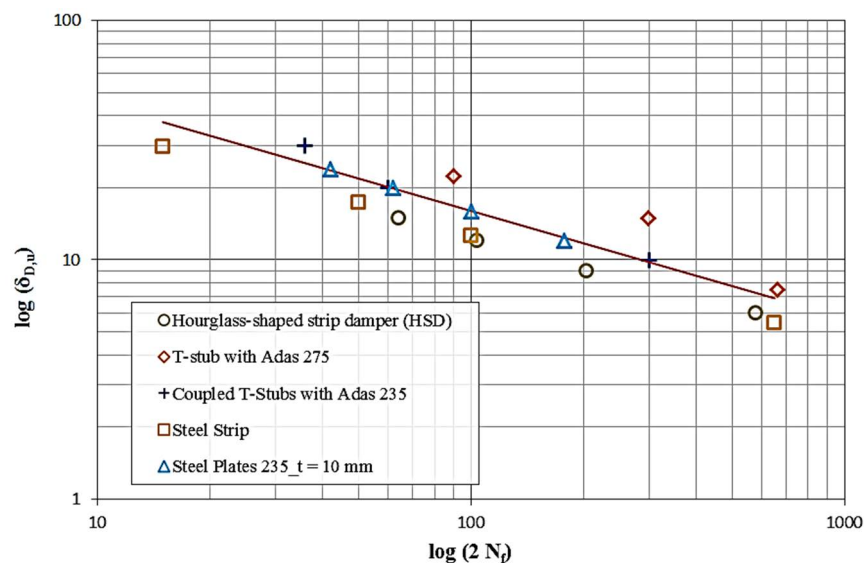
Figure 4. *Fatigue life curves points of the experimental data and the average fatigue life curve*
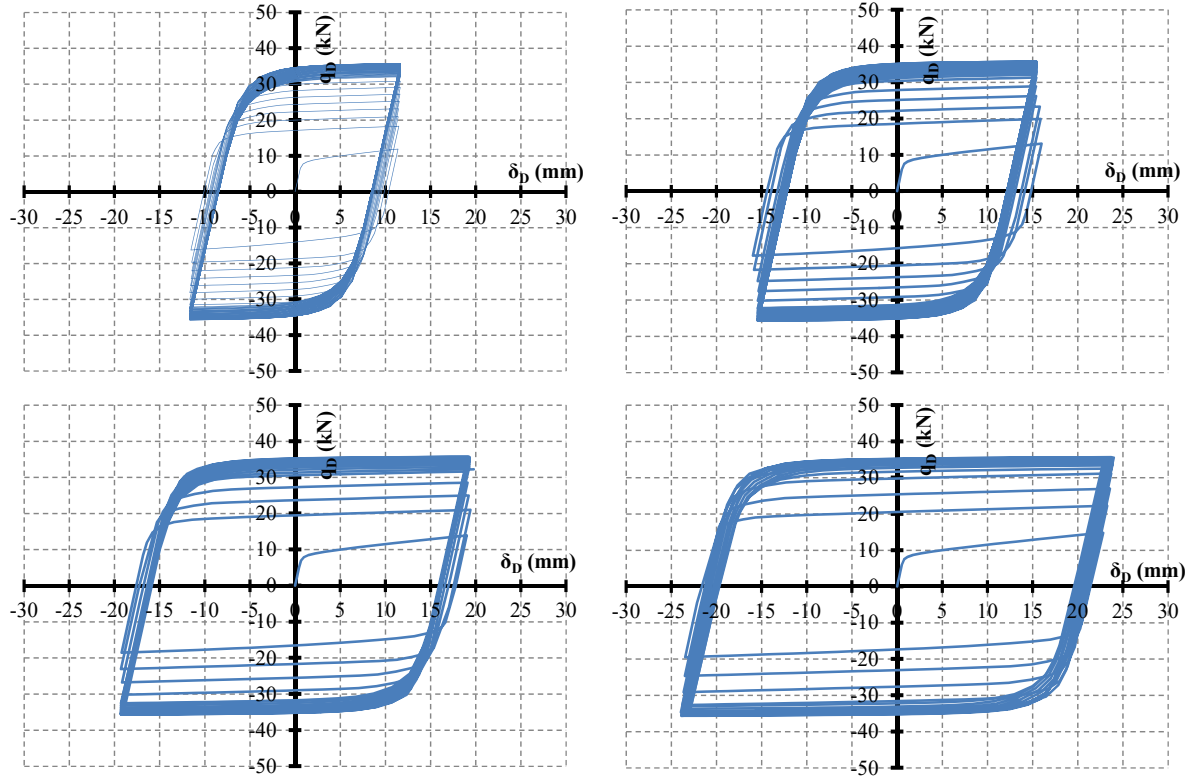
Figure 5. *Cyclic curves of the LYP steel [Saeki et al., 1998; Susantha et al., 2004] plates for increasing the imposed displacement δ_D*
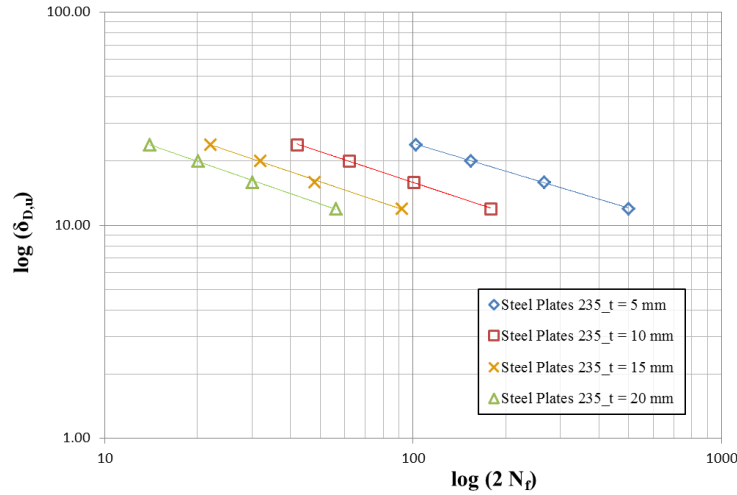
Figure 6. *Fatigue life curves of the X-shape steel plates for different thickness values*

5. NON LINEAR ANALYSIS OF THE DISSIPATIVE COLUMN

Defined the non-linear behavior of the X-shape steel plates, non-linear static and dynamic analyses of the whole Dissipative Column have been performed in ABAQUS [ABAQUS, 2010a; ABAQUS, 2010b]. In Table 2, the main geometric and mechanical properties of the DC are reported. A FE model has been also defined in ABAQUS [ABAQUS, 2010a; ABAQUS, 2010b] with means of 3D elements with nonlinear stress-strain behaviour.
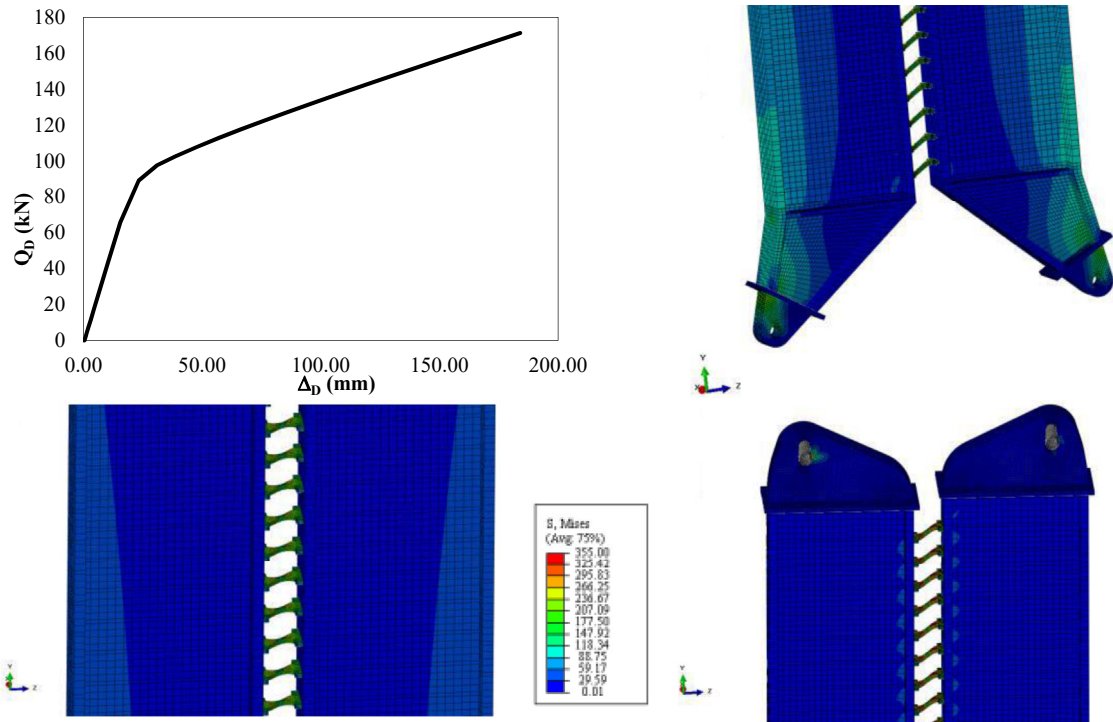
Figure 7. *Pushover curve of the DC and its deformed shape in ABAQUS [ABAQUS, 2010a; ABAQUS, 2010b]*
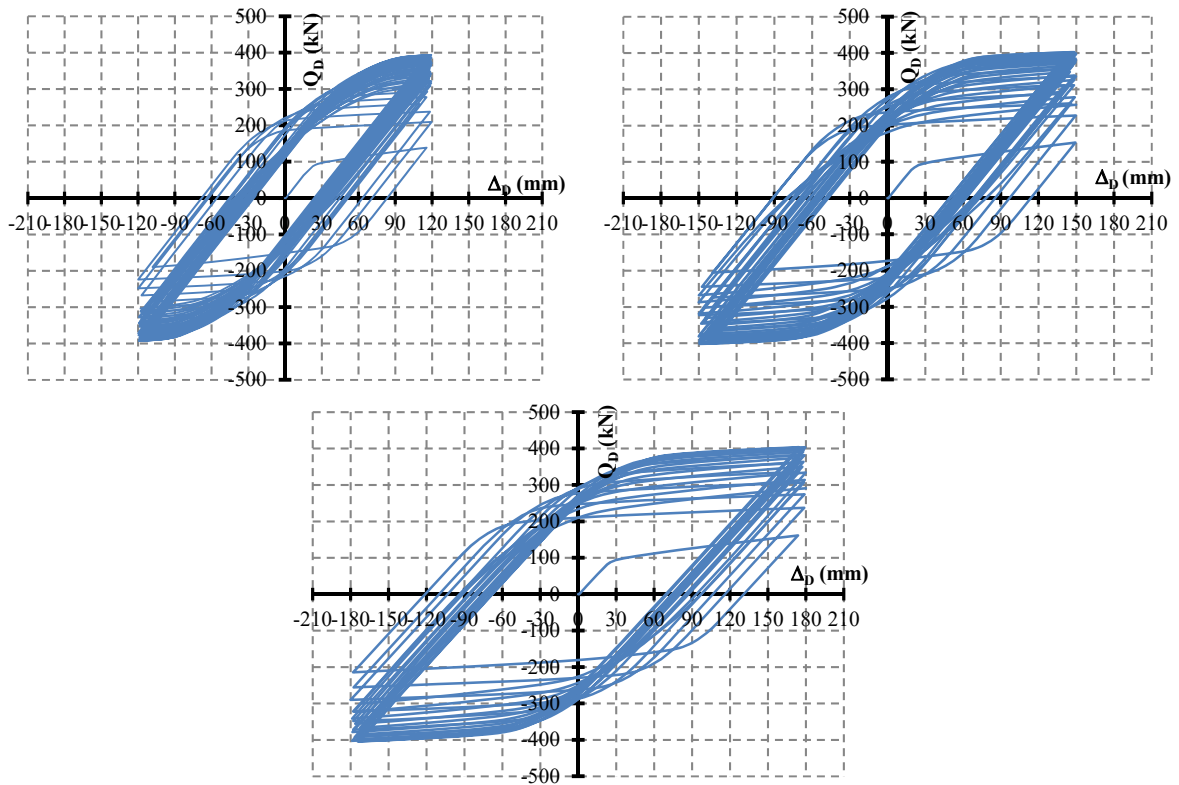
Figure 8. *Cyclic curves of the DC for increasing the imposed displacement Δ_D*
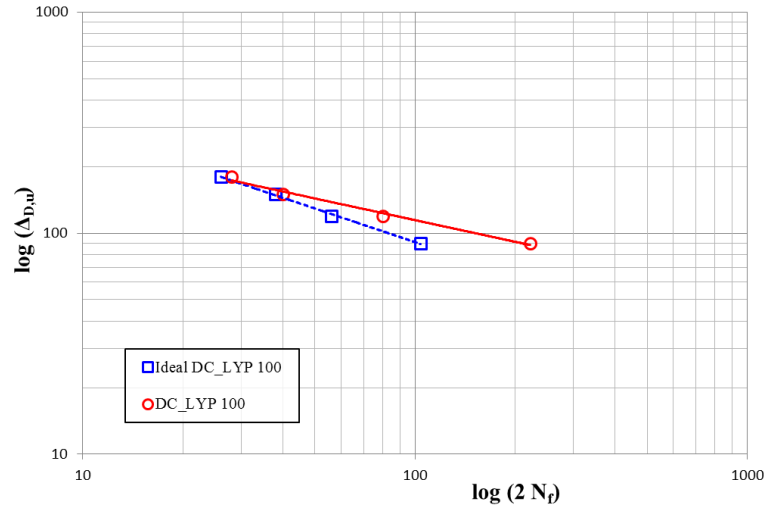
Figure 9. *Fatigue life curves of the DC*

Table 2. *Geometrical and structural properties of the Dissipative Column (DC)*

Height H (mm)	Column Distance *l* (mm)	Plate Length *a* (mm)	Plate Thickness *t* (mm)	Plate Distance *i* (mm)	Plate Width *b* (mm)	Plate Yield Stress f_y (N/mm²)	Eccentricity *e* (mm)	Column Profile
11500	1650	150	15	125	120	132	400	ISE700

Fig. 7 shows the geometric shape as well as the deformed shape of the DC. The displacement-controlled pushover analyses of the DC has been carried out until to reach 200 mm in terms of relative displacement as plotted in Fig. 7, showing a yielding point at about 20 mm (0.17%). The cyclic curves with an imposed ultimate displacement $\Delta_D=\Delta_{D,u}$ equal to 120, 150 and 180 mm, respectively, are shown in Fig. 8. In Fig. 9, the fatigue life curve of the DC is illustrated showing a good agreement with the ideal fatigue life curve of the DC supposed to be characterized by a rigid deformed shape as described in section 3. For low displacements $\Delta_{D,u}$, the fatigue life curve demonstrates a higher number of cycles respect to the ideal case due to a lower energy rate dissipated by the steel plated located at the base of the DC.

6. CONCLUSIONS

A new replaceable hysteretic steel damper, defined ad Dissipative Column (DC), to control seismic building damage consisting of two adjacent steel columns connected to each other with continuous mild/low strength steel X-shape plates, has been proposed and investigated. The behavior of the proposed DC element has been investigated at linear and non-linear ranges, developing several parametric analyses in order to evaluate the hysteretic performances. Numerical tests of the DC elements showed that the eccentricity acts as a mechanical lever arm in order to amplify energy dissipation increasing plate vertical drift producing easier yielding conditions in hysteretic dampers. In any case, lateral stiffness increases for greater values of the X-shape plate thickness and for lower values of their distance, and for greater eccentricities between bearings and column axes. For greater values of the device thickness, the yielding displacement decreases as well as for lower values of link steel strength. The number of DC elements should be designed for the buildings where they are installed. The DC elements can

be considered as new low-yield, ductile replaceable and minimally invasive dampers easy to install to new as well as to existing buildings, providing significant additional stiffness, strength and damping to a structural system potentially capable to reduce building seismic response and damage in primary structural members under severe earthquakes.

7. REFERENCES

ABAQUS [2010a] "User's Manual: Volume III: Materials".

ABAQUS [2010b] "User's Manual: Volume IV: Elements".

Aiken, I., Nims, D., Whittaker, A., Kelly, J., [1993] "Testing of passive energy dissipation systems," Earthq. Spectra Earthq. Eng. Res. Inst. Calif. 9, 335–370.

Brando, G., D'Agostino, F., De Matteis, G. [2013] "Experimental tests of a new hysteretic damper made of buckling inhibited shear panels," Mat. and Str./Materiaux et Const. 46 (12), 2121-2133.

Castaldo, P., [2014] Integrated Seismic Design of Structure and Control Systems. Springer International Publishing: New York,. DOI 10.1007/978-3-319-02615-2.

Castaldo, P., Amendola, G. & Palazzo, B. [2016a]. Seismic reliability-based design of structures isolated by FPS. ECCOMAS Congress2016, Crete Island, Greece, 5–10 June 2016.

Castaldo P., De Iuliis M. [2014]. Optimal integrated seismic design of structural and viscoelastic bracing-damper systems, Earthquake Engineering and Structural Dynamics 43(12), 1809–1827, DOI: 10.1002/eqe.2425.

Castaldo P., Palazzo B., Della Vecchia P. [2015] "Seismic reliability of base-isolated structures with friction pendulum bearings," Engineering Structures 95:80-93.

Castaldo P., Palazzo B., Della Vecchia P. [2016b] "Life-cycle cost and seismic reliability analysis of 3d systems equipped with FPS for different isolation degrees," Engineering Structures, *http://dx.doi.org/10.1016/j.engstruct.2016.06.056.*

Castaldo, P., Palazzo, B., Perri, F., Marino, I., Faraco, M.M. [2016c]. Seismic retrofit of existing buildings through the dissipative columns. ECCOMAS Congress2016, Crete Island, Greece, 5–10 June 2016.

Castaldo P., Tubaldi E. [2015] "Influence of FPS bearing properties on the seismic performance of base-isolated structures," Earthquake Engineering and Structural Dynamics 44(15):2817–2836.

CEN-European Committee for Standardization [2007] Eurocode 3 Part 1: General Rules and Rules for Buildings, Brussels, Belgium.

Chang-Hwan, L., Seung-Ki, W., Young K., J., Dong-Won, L., Sang-Dae K. [2014] "Modified Fatigue Model for Hourglass-Shaped Steel Strip Damper Subjected to Cyclic Loadings," J. Struct. Eng., 04014206-1-12.

Chang-Hwan, L., Young K. Ju, Jeong-Ki, M., Seung-Hee L., Sang-Dae K. [2015] "Non-uniform steel strip dampers subjected to cyclic loadings," Engineering Structures 99, 192–204.

De Iuliis M, Castaldo P. [2012] "An energy-based approach to the seismic control of one-way asymmetrical structural systems using semi-active devices," Ingegneria Sismica - International Journal of Earthquake Engineering XXIX(4):31-42.

De Iuliis M., Castaldo P., Palazzo B. [2010] "Analisi della domanda sismica inelastica del terremoto de L'Aquila su sistemi dimensionati secondo le NTC2008," Ingegneria Sismica, Patron Editore XXVII(3):52–65.

De Matteis, G., Brando, G., Formisano, A., Panico, S., Mazzolani, F.M. [2007] "Numerical and experimental study on pure aluminum shear panels with welded stiffeners," 5th International Conference on Advances in Steel Structures, ICASS 2007, 3, 855-860.

Etse, G., Vrech, S.M., Ripani, M. [2016] Constitutive theory for Recycled Aggregate Concretes subjected to high temperature, *Construction and Building Materials* 111: 43-53.

Formisano, A., Matteis, G.D., Mazzolani, F.M. [2010] "Numerical and experimental behaviour of a full-scale RC structure upgraded with steel and aluminium shear panels," Computers and Structures 88(23-24), 1348-1360.

Formisano, A., Mazzolani, F.M. [2015] "On the selection by MCDM methods of the optimal system for seismic retrofitting and vertical addition of existing buildings," Comp. and Struct. 159, 1-13.

Formisano, A., Mazzolani, F.M., Brando, G., De Matteis, G. [2006] "Numerical evaluation of the hysteretic performance of pure aluminium shear panels," Proceedings of the 5th International Conference on Behaviour of Steel Structures in Seismic Areas - Stessa 2006, 211-217.

Formisano, A., Sahoo, D.R. [2015] "Steel shear panels as retrofitting system of existing multi-story RC buildings: Case studies," Advances in Structural Engineering: Mechanics, I, 495-512.

Ghobarah, A. [2004] "On Drift Limits Associated with Different Damage Levels," In Proceedings of the International Workshop on Performance-Based Seismic Design, Department of Civil Engineering, McMaster University, Bled, Slovenia, 28 June–1 July.

Kim, J.; Seo, Y. [2004] "Seismic design of low-rise steel frames with buckling-restrained Braces," Eng. Struct. 26, 543–551.

Latour, M., Rizzano, G. [2012] "Experimental Behavior and Mechanical Modeling of Dissipative T-Stub Connections," J. Struct. Eng. 138:170-182.

Longo, A., Montuori, R., Nastri, E., Piluso, V. [2014] "On the use of HSS in seismic-resistant structures," Journal of Constructional Steel Research 103:1-12.

Montuori, R. [2014] "The influence of gravity loads on the seismic design of RBS connections," Open Construction and Building Technology Journal 8:248-261.

Montuori, R., Muscati, R. [2015] "Plastic design of seismic resistant reinforced concrete frame," Earthquake and Structures 8(1), 205-224.

Montuori, R., Nastri, E., Piluso, V. [2014] "Theory of plastic mechanism control for the seismic design of braced frames equipped with friction dampers," Mechanics Research Communicat. 58:112-123.

Montuori, R., Nastri, E., Piluso, V. [2015] "Advances in theory of plastic mechanism control: Closed form solution for MR-Frames," Earth. Engineering and Structural Dynamics 44(7):1035-1054.

Montuori, R., Nastri, E., Piluso, V., Troisi, M., [2016] "Influence of connection typology on seismic response of MR-Frames with and without 'set-backs'", Earthquake Engineering and Structural Dynamics, 10.1002/eqe.2768.

Mroginski, J.L., Etse, G., Ripani, M. [2015] "A non-isothermal consolidation model for gradient-based poroplasticity," *PANACM 2015 - 1st Pan-American Congress on Computational Mechanics, in conjunction with the 11th Argentine Congress on Computat. Mec.cs,* MECOM 2015, pp. 75-88.

Nastri E., Paciello A., [2016] "An Example of Energy Dissipation Optimization for Steel MRFs with Pin-Jointed Column Bases" ECCOMAS Congress 2016 VII European Congress on Computational Methods in Applied Sciences and Engineering, Crete Island, Greece, 5–10 June 2016.

Nastri E., [2016] "Eccentrically Braced Frames Designed for Energy Dissipation Optimization", ECCOMAS Congress 2016 VII European Congress on Computational Methods in Applied Sciences and Engineering, Crete Island, Greece, 5–10 June 2016.

Oviedo, A.J.A., Midorikawa, M., Asari, T. [2010] "Earthquake response of ten-story story-drift-controlled reinforced concrete frames with hysteretic dampers," Eng. Struct. 32, 1735–1746.

Palazzo B., Castaldo P., Della Vecchia P. [2014a] "Seismic reliability analysis of base-isolated structures with friction pendulum system," 2014 IEEE Workshop on Environmental, Energy and Structural Monitoring Systems Proceedings, Napoli, September 17-18.

Palazzo, B., Castaldo, P., Marino, I. [2014b] "The steel column damper: a new hysteretic device providing additional stiffness and damping," EUROSTEEL 2014, September 10-12, Naples, Italy.

Palazzo, B., Castaldo, P., Marino, I. [2015] "The Dissipative Column: A New Hysteretic Damper," Buildings 5(1), 163-178; doi:10.3390/buildings5010163.

Pampanin, S. [2005] "Emerging solutions for high seismic performance of precast-prestressed concrete buildings," J. Adv. Concr. Technol. 3, 202–222.

Pampanin, S. [2013] "Reality-check and renewed challenges in earthquake engineering: Implementing low-damage structural systems-from theory to practice," In Proceeding of the 15WCEE, Lisbon, Portugal, 24–28 September.

Piluso, V., Montuori, R., Troisi, M. [2014] "Innovative structural details in MR-frames for free from damage structures," Mechanics Research Communications 58:146-156.

Priestley, M.J.N. [1993] "Myths and fallacies in earthquake engineering-conflicts between design and reality," Bull. NZNSEE 26, 329–341.

Ripani, M., Etse, G., Vrech, S., Mroginski, J. [2014] "Thermodynamic gradient-based poroplastic theory for concrete under high temperatures," *International Journal of Plasticity*; 61: 157-177.

Saeki, E., Sugisawa, M., Yamaguchi, T., Wada, A. [1998] "Mechanical properties of low yield point steels," J. Mater. Civ. Eng. 10:143-152.

Susantha, K.A.S., Aoki, T., Kumano, T., Yamamoto, K. [2004] "Application of Low-Yield Strength Steel in Steel Bridge Piers," In Proceeding of the 13th WCEE, Vancouver, Canada, 1-6 August.

Symans, M.D., Charney, F.A., Whittaker, A.S., Constantinou, M.C., Kicher, C.A., Johnson, M.W., McNamara, R.J. [2008] "Energy dissipation system for seismic applications: Current practise and recent developments," J. Struct. Eng. 134, 3–21.

Tena-Colunga A. [1997] "Mathematical modelling of the ADAS energy dissipation device," Engineering Structures 19(10), 811-821.

Teruna R. D., Taksiah, A., M., Budiono, B. [2015] "Experimental Study of Hysteretic Steel Damper for Energy Dissipation Capacity," Advances in Civil Engineering, doi.org/10.1155/2015/631726.

Vision 2000: California Office of Emergency Services (OES) [1995] Performance Based Seismic Engineering of Buildings, Structural Engineers Association of California: Sacramento, CA, USA.

Wada, A., Watanabe, A., Connor, J., Kawai, H., Iwata, M. [1992] "Damage Tolerant Structures," In Proceeding of the Fifth US-Japan Workshop on the Improvement of Building Structural Design and Construction Procedures, ATC-15, San Diego, CA, USA, 8–10 September.

Whittaker, A., Bertero, V., Alonso, J., Thompson, C. [1989] "Earthquake Simulator Testing of Steel Plate Added Damping and Stiffness Elements," Report No. UCB/EERC-89/02; Earthquake Engineering Research Center, University of California, Berkeley, CA, USA.

Whittaker, A.S., Bertero, V.V., Thompson, C.L., Alonso, L.J. [1991] "Seismic testing of steel plate energy dissipation devices," Earthq. Spectra 7, 563–604.

Vrech, S.M., Ripani, M., Etse, G. [2015] "Localized versus diffused failure modes in concrete subjected to high temperature," PANACM 2015 - *1st Pan-American Congress on Computational Mechanics, in conjunction with the 11th Argentine Congress on Computational Mechanics*, MECOM 2015, pp. 225-236.

LA COLONNA DISSIPATIVA COME UN NUOVO DISPOSITIVO ISTERETICO

Paolo Castaldo*, Bruno Palazzo*, Francesco Perri

Department of Civil Engineering, University of Salerno, Fisciano (SA), Italy

SOMMARIO: *Un nuovo dissipatore isteretico sostituibile per migliorare le prestazioni di un edificio in caso di sisma, costituito da due elementi verticali in acciaio adiacenti collegati tra loro con continui piatti in acciaio dolce/bassa soglia di snervamento, è proposto e studiato. I nuovi dispositivi, chiamati Colonne Dissipative (DC), connessi con piatti in acciaio a forma di X, offrono maggiore rigidezza e smorzamento ad un sistema strutturale utilizzando l'elemento base e poco invasivo della costruzione: la colonna. In analogia alle pareti di taglio accoppiate, il comportamento dell'elemento proposto è teoricamente analizzato sia in campo lineare che non lineare. La Colonna Dissipativa è stata concepita o come dispositivo installato all'interno di una maglia di piano o dissipatore esterno per ottenere una macro-dissipazione. Infatti, considerando diverse configurazioni, un'analisi parametrica è sviluppata al fine sia di valutare l'effetto dei principali parametri geometrici e strutturali che di fornire le curve di capacità per la progettazione di questo nuovo dispositivo. In particolare, analisi statiche non lineari e cicliche sono state effettuate in SAP2000 che in ABAQUS per caratterizzare il comportamento locale e globale del dispositivo. La Colonna Dissipativa può essere considerata un nuovo dispositivo isteretico, facile da installare sia in edifici nuovi che esistenti al fine di garantire un'adeguata protezione sismica.*

---

*Corresponding author: Paolo Castaldo, Department of Civil Engineering, University of Salerno, Fisciano, Italy. Email: pcastaldo@unisa.it

AN ADAPTIVE CAPACITY SPECTRUM METHOD
FOR ESTIMATING SEISMIC RESPONSE
OF STEEL MOMENT-RESISTING FRAMES

Massimiliano Ferraioli*, Angelo Lavino, Alberto Mandara

Department of Civil Engineering, Design, Building and Environment

Second University of Naples, Aversa (CE)

SUMMARY: *An adaptive version of the capacity spectrum method is proposed to estimate deformation demands of steel moment-resisting frames under seismic loads. Its computational attractiveness and capability of providing satisfactory predictions of seismic demands in comparison with those obtained by other advanced nonlinear static procedures in literature are examined. Both effectiveness and accuracy of these approximated methods based on pushover analysis are verified through an extensive comparative study involving both regular and irregular steel moment-resisting frames. The results obtained by nonlinear static procedures and nonlinear dynamic time-history analysis under spectrum-compatible accelerograms are eventually compared. The proposed procedure generally gives a more accurate solution than that obtained from the other nonlinear static procedures.*

KEYWORDS: *steel moment-resisting frames, nonlinear analysis, adaptive pushover*

1. INTRODUCTION

The estimation of lateral displacement demands is of primary importance in performance-based earthquake-resistant design. In fact, both structural and non-structural damage are primarily related to lateral displacements. However, estimating seismic demands at high performance levels, such as life safety and collapse prevention, requires explicit consideration of the inelastic behaviour of the structure. To this purpose, the nonlinear response history analysis (NRHA) is the most rigorous method for the estimation of seismic demands. Nevertheless, the Nonlinear Static Procedures (NSPs) are widely used to calculate the deformation demands with satisfactory accuracy without the complex modelling and computational effort of NRHA. Some NSPs were incorporated in the new generation of seismic codes in procedures based on Capacity Spectrum Method (CSM) or Displacement Coefficient Method (DCM), such as in FEMA 273 [1997], ATC-40 [1997], FEMA 356 [2000], Eurocode 8 [2004], Italian Building Code [2008], FEMA-440 [ATC-55, 2005], ASCE/SEI 41-06 Standard [2005]. In general, applying displacement rather than force loading in pushover procedures would be the most suitable option for nonlinear static analysis of structures subjected to earthquake ground motion. However, due to the unvarying nature of the applied displacement loading vector, this approach may neglect the strong variations of the displacement pattern in post-yield failure mechanism produced, for example, by strength irregularities and soft storeys. Consequently, when an invariant load pattern is used, the force-based pushover is to be preferred to the displacement-

based pushover. However, the accuracy of these conventional force-based pushover analyses in predicting seismic demands of structures and their limitations especially for high-rise buildings remain among the most controversial topics. In fact, the traditional pushover analysis with an invariant lateral force pattern accurately estimates the seismic response of low-rise and regular buildings when the structural response is dominated by the first mode. On the contrary, significant differences were found in high-rise buildings, where the effects of the higher modes cannot be neglected. The two major limits of the conventional pushover procedures are that, owing to the invariant loading pattern, the higher mode effects are ignored and, therefore, the changes in the dynamic properties of the structures are neglected. This is mainly because inertia force distribution changes continuously under earthquake ground motion due to higher mode contribution and stiffness degradation.
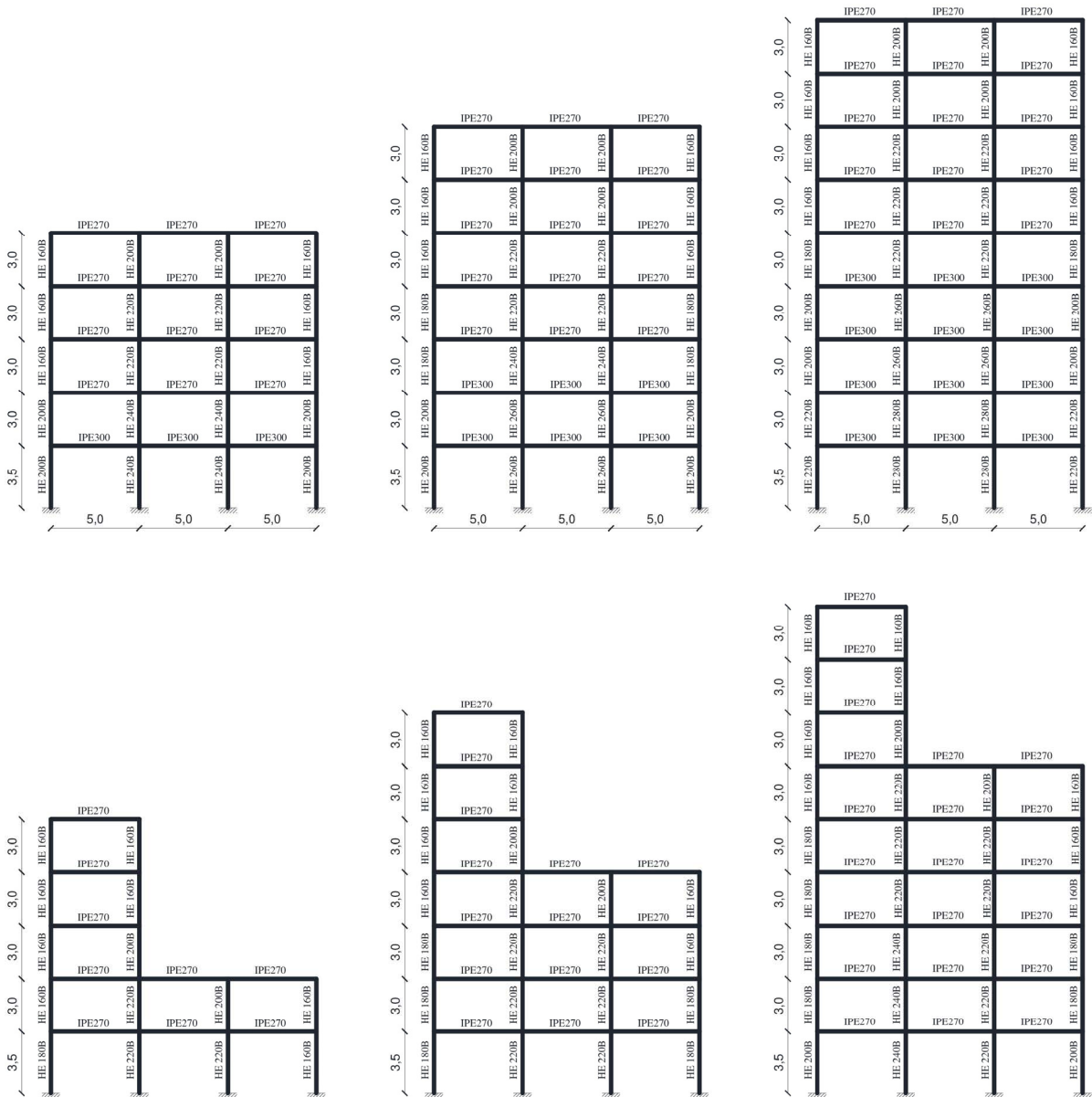

Figure 1. *Cases studies: regular and irregular moment-resisting frames*

Table 1. *Main Characteristics of accelerograms*

No.	Input	Station ID	Date	Time	Dir.	PGA (m/s²)	M_w
1	Friuli	ST20	06/05/1976	20:00	NS	3.499	6.5
2	Montenegro	ST64	15/04/1979	06:11	EW	2.199	6.9
3	Campano Lucano	ST93	23/11/1980	18:34	NS	1.363	6.9
4	Izmit	ST575	17/08/1999	00:01	NS	1.576	7.6
5	South Iceland	ST108	17/06/2000	15:40	NS	1.238	6.0
6	Olfus	ST101	29/05/2008	15:45	EW	0.439	6.3
7	LomaPrieta	ST47379	18/10/1989	00:04	NS	4.029	6.9

In order to overcome these drawbacks, some researchers proposed invariant loading patterns taking into account the higher mode effects [Chopra et al., 2002- 2004], [Fajfar et al., 2005], [Jianmeng et al., 2008], [Poursha et al., 2009], [Reyes et al., 2011], [Kreslin et al., 2012]. Other researchers developed adaptive pushover procedures accounting for higher mode effects and progressive damage accumulation [Gupta et al., 2000], [Antoniou et al., 2004], [Kalkan et al., 2006], [Pinho et al., 2008], [Ferraioli et al., 2008], in order to overcome the most important limitations of traditional methods especially for estimating seismic demands of tall buildings. However, some of these nonlinear static procedures require very complex analyses and they fail the target of using procedures simpler than NRHA. Nevertheless, these adaptive pushover methods may represent an attractive displacement-based tool for structural assessment, fully complying with the recently introduced deformation and performance oriented trends in the field of earthquake engineering.

2. ADAPTIVE AND MULTIMODAL NONLINEAR STATIC PROCEDURES

Generally, using modal properties of the structure in nonlinear static analysis is the most accessible approach to take into account the dynamic characteristics of the system. However, the conventional nonlinear static procedures (NSPs) are based on the assumption that the structure vibrates predominantly in a single mode and that the dynamic properties of the structure remain unchanged.
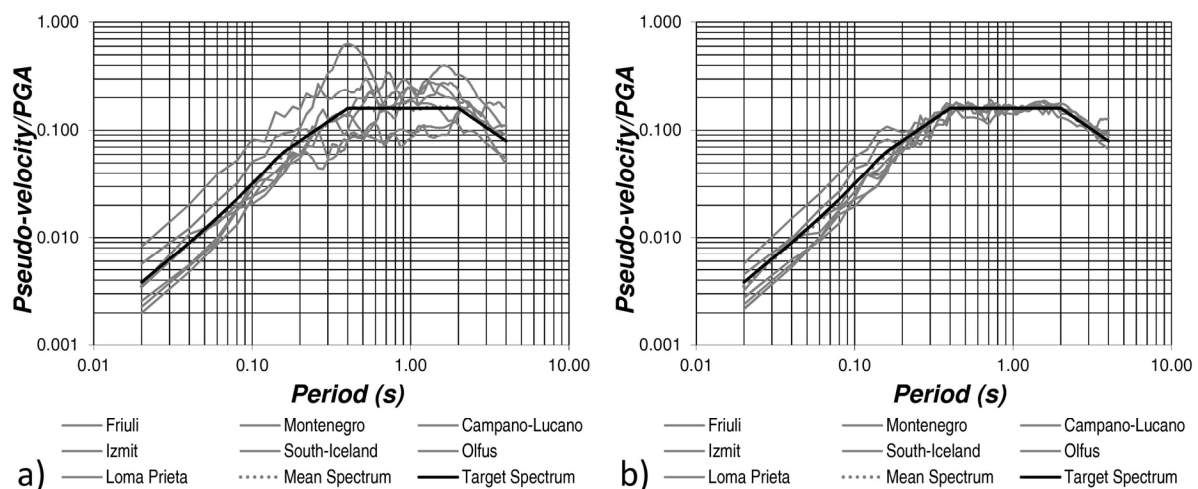
Figure 2. *Pseudo-velocity spectra: a) recorded accelerograms b) adjusted accelerograms*

The first assumption is not always fulfilled, especially in the case of high-rise buildings and/or torsionally flexible plan-asymmetric buildings [Chopra *et al.*, 2004], [Erduran *et al.*, 2008], [Kreslin *et al.*, 2012], [Ferraioli, 2010-2015].

Furthermore, the progressive changes in the modal properties due to structural yielding are generally neglected. In order to include the effects of higher modes some advanced modal pushover procedures based on the elastic modal decomposition concepts were developed in literature. Many of these procedures consider higher modes in lateral load pattern in order to take into account higher mode effects both in plan and in elevation. In particular, in the well-known modal pushover analysis (MPA) proposed by Chopra *et al.* [2004] higher mode effects are considered by analysing each mode as an equivalent single-degree-of-freedom system including nonlinear properties related to that mode. Kunnath [2004] investigated simple modal combination schemes to indirectly account for higher-mode effects. In order to take into account higher-mode effects, Poursha *et al.* [2009] proposed the consecutive modal pushover procedure that employs multi-stage and single-stage pushover analyses. The main problem of conventional nonlinear static procedures is that they are based on the assumption that the mode shape remains un-changed after the structure yields. In order to overcome this drawback in recent years some adaptive pushover methods were proposed to include the effects of higher modes and the changes in vibration characteristics due to the inelastic response. Specifically, in order to include the changes in the dynamic properties of the structure Gupta *et al.* [2000] proposed an adaptive pushover procedure based on an elastic demand spectrum. Kalkan *et al.* [2006] suggested a new pushover analysis procedure derived through adaptive modal combinations (AMC) that accounts for the effects of both higher modes and varying dynamic characteristics due to inelastic response. Antoniou *et al.* [2004] proposed an innovative displacement-based adaptive pushover (DAP) procedure, in which an incremental updating with increment of dis-placement calculated according to the spectrum scaling is applied at each analysis step. Two shortcomings of the modal combination rules can be pointed out: the first one is that the result obtained does not fulfil equilibrium; the second limitation is that signs are lost during the combination process eliminating the contribution of negative quantities and considering an "always-additive" contribution of higher modes. In addition, no solution is provided to determine the target displacement in the adaptive nonlinear static analysis. Summing up, in spite of their deep theoretical background, many of the aforementioned methods suffer from the quadratic modal combination rules, in which the change in the sign of storey components at higher modes is not considered as the sign reversals of load vectors in higher modes are neglected. Thus, the magnitudes of the applied loads in all storey levels are positive. This inappropriate always-additive inclusion of higher mode contribution through a non-weighted SRSS combination rule represents a further weakness of modal pushover procedures. Finally, no multi-run methods are able to reflect the interaction between modes in the nonlinear range.

3. PROPOSED ADAPTIVE CAPACITY SPECTRUM METHOD

In this study, a displacement-based Adaptive Capacity Spectrum Method (ACSM) based on the Inelastic Demand Response Spectra (IDRS) is proposed. At first, the displacement-based adaptive pushover (DAP) procedure proposed by Antoniou *et al.* [2004] is used to define the capacity of the structure. This results in a variation of the lateral force pattern during pushover analysis. Thus, also the equivalent Single-Degree-of-Freedom system (SDOF), which is representative of the MDOF 3D model of the building in the Capacity Spectrum Method (CSM),

changes during pushover analysis. In order to consider such effect, an adaptive version of the Capacity Spectrum Method (ACSM) is proposed. At each step of the pushover analysis, a different equivalent SDOF system is defined as a function of the actual lateral displacement pattern. In particular, the equivalent mass M_{eq} and stiffness K_{eq} of the SDOF system at the i-*th* step of the pushover analysis is expressed as a function of the j-*th* storey displacement δ_j^i and force F_j^i, as follows [Ferraioli *et al.*, 2008]:

$$M_{eq}^i = \frac{\left(\sum_{j=1}^{N} m_j \delta_j^i\right)^2}{\sum_{j=1}^{N} m_j \delta_j^{i^2}} \tag{1}$$

$$K_{eq}^i = \frac{\left(\sum_{j=1}^{N} m_j \delta_j^i\right)^2}{\sum_{j=1}^{N} m_j \delta_j^{i^2}} \sum_{j=1}^{N} F_j^i \delta_j^i \tag{2}$$

The global force-displacement capacity curve of the structure (base shear V versus top displacement δ_{TOP}) is transformed step by step in the capacity spectrum (spectral acceleration S_a versus spectral displacement S_d) in ADRS format (Acceleration-Displacement Response Spectra), as follows:

$$\Delta S_a^i = \Delta V^i \frac{\sum_{j=1}^{N} m_j \delta_j^{i^2}}{\left(\sum_{j=1}^{N} m_j \delta_j^i\right)^2} \tag{3}$$

$$\Delta S_d^i = \Delta \delta_{TOP}^i \frac{1}{\delta_N^i} \frac{\sum_{j=1}^{N} m_j \delta_j^{i^2}}{\sum_{j=1}^{N} m_j \delta_j^i} \tag{4}$$

where ΔV^i and $\Delta \delta_{TOP}^i$ are the base shear and the corresponding top displacement increments at the i-*th* step of pushover analysis, respectively, m_j is the mass of the j-*th* storey, δ_j^i is the lateral displacement of the j-*th* storey at the i-*th* step of pushover analysis and N is the number of storeys. The seismic demand is represented through Inelastic Demand Response Spectra (IDRS) that are indirectly computed by scaling the 5% damped Elastic Demand Response Spectra (EDRS) according to the R-μ-T relations available in literature for the strength reduction factor [Vidic *et al.*, 1994]. Specifically, the inelastic pseudo-acceleration S_a and displacement S_d, which are the coordinates of the IDRS in ADRS format, are characterized by the coordinates [S_{de}; S_{ae}] of the EDRS (ξ=5%) as follows:

$$S_a = \frac{S_{ae}}{R_\mu} \tag{5}$$

$$S_d = \mu \frac{S_{de}}{R_\mu} \tag{6}$$

where μ is the ductility ratio and R_μ is the ductility reduction factor defined by Vidic *et al.* [1994], as follows:

$$T^* \leq T_0 \quad R_\mu = (\mu - 1)\frac{T^*}{T_0} + 1, \tag{7}$$

$$T^* > T_0 \quad R_\mu = \mu. \tag{8}$$

In Eqs. (7) and (8) R_μ depends on the ductility μ and, therefore, on the lateral displacement of the equivalent SDOF system. Thus, some iterations are required in order to match the values of ductility obtained from the demand spectrum and the capacity diagram, respectively, within a given tolerance.
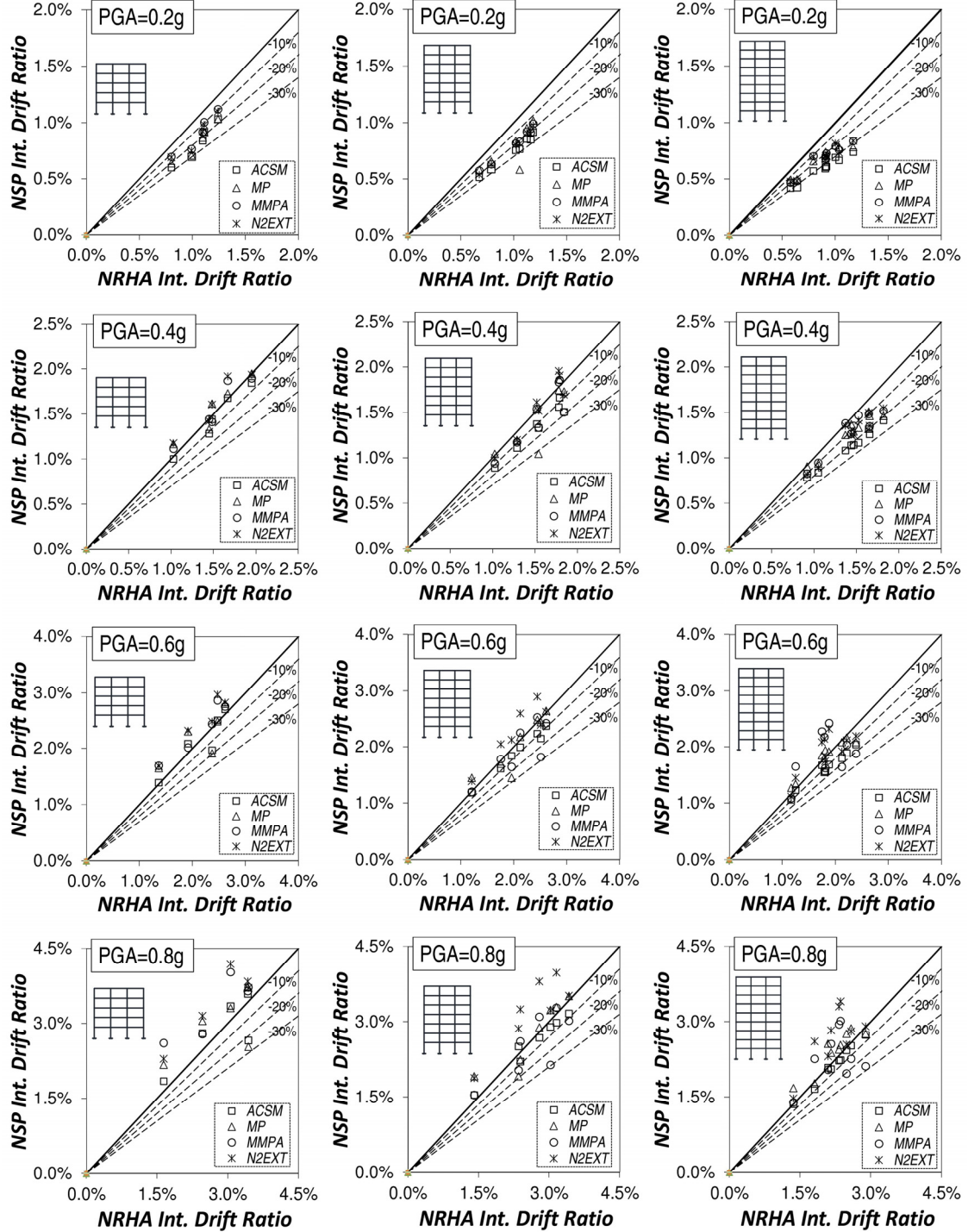
Figure 3. *Scatter plot of estimated target interstorey drift for regular frames*

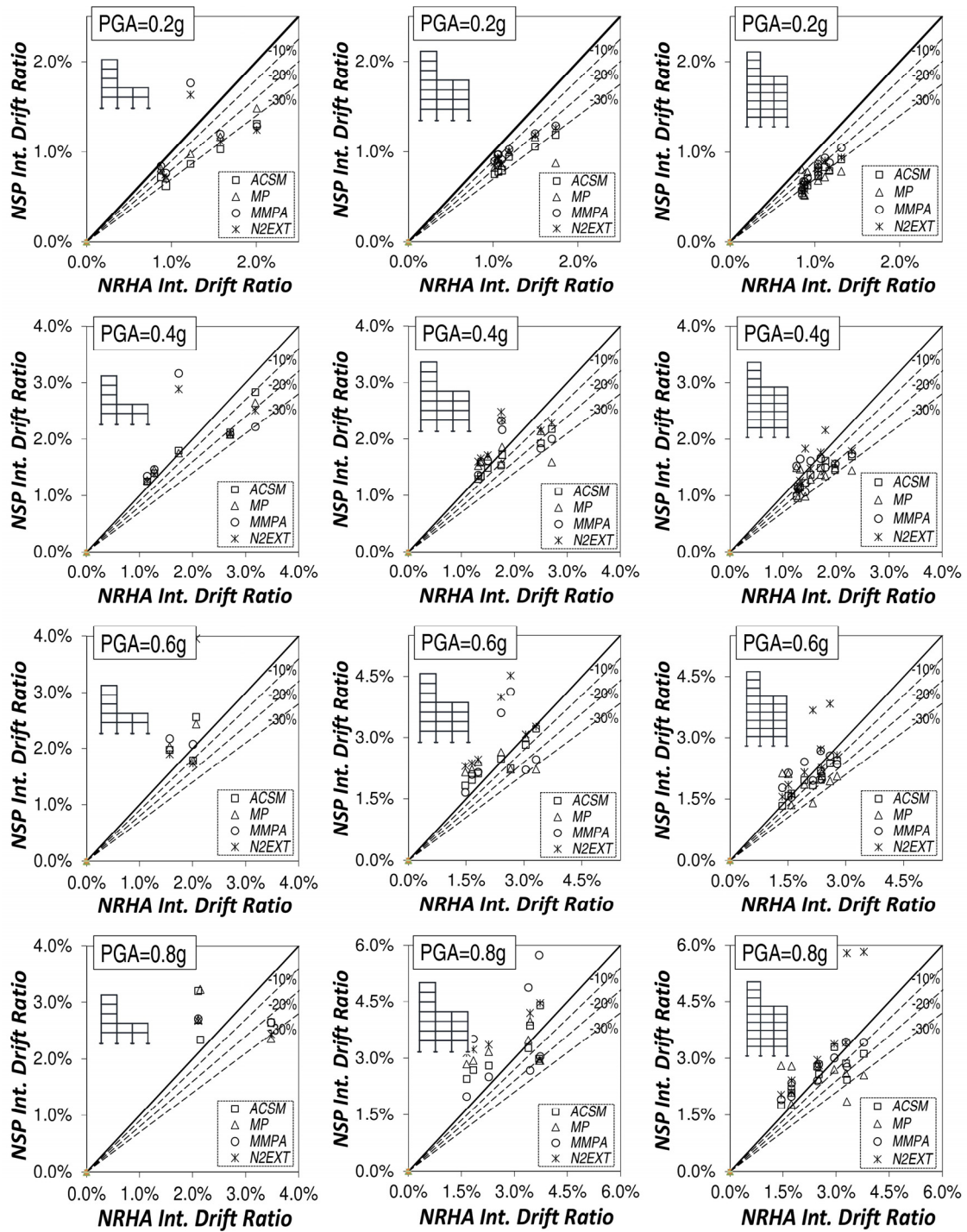Figure 4. *Scatter plot of estimated target interstorey drift for irregular frames*

4. VALIDATION AND COMPARISON WITH OTHER NSPs

A number of steel moment-resisting frames designed to meet seismic requirements of Italian Building Code [2008] have been considered in the numerical analyses (Fig. 1). The design seismic action has been defined assuming soil class A, damping ratio ξ=5%, peak ground

acceleration *PGA*=0.25g, behaviour factor *q*=6.5 for regular frames and *q*=6.5×0.80=5.2 for irregular frames. Steel members are made of S275 steel grade (*f_y*=275 MPa). The interstorey height is 3.5m for the first floor and 3.0m for the upper floors. The bay length is 5.0m. A distributed plasticity-fibre element model implemented in the SeismoStruct code [2004] has been used in nonlinear analyses. Sources of geometrical nonlinearity taken into account are both local and global. A bilinear kinematic hardening material model has been used for steel. More details about the case studies can be found in Ferraioli *et al.* [2014a, 2014b, 2014c]. The effectiveness of the proposed adaptive capacity spectrum method (ACSM) is evaluated by comparing its predictions with estimates obtained from a comprehensive set of nonlinear response history analyses (NRHA).
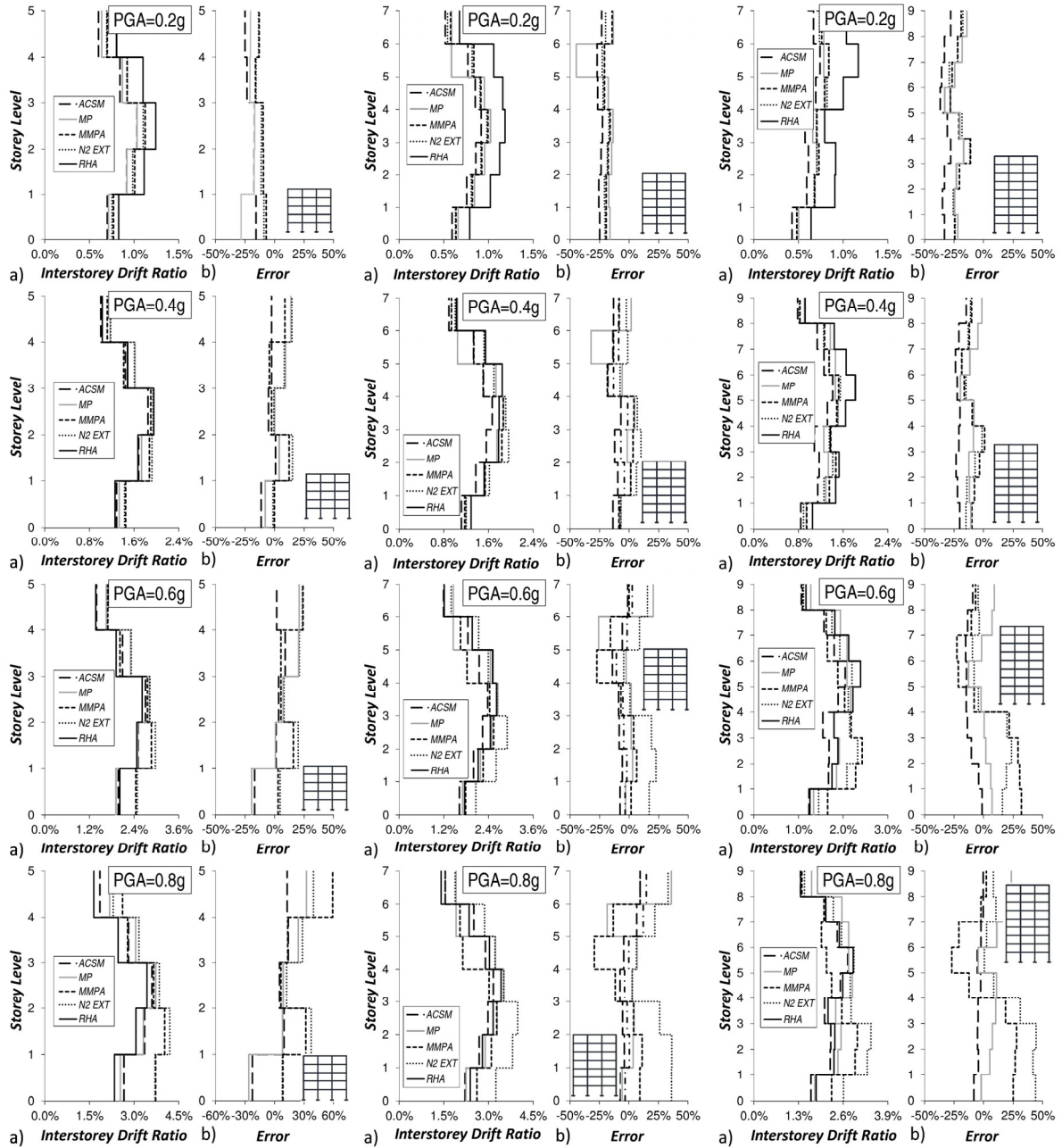

Figure 5. *a) Interstorey drift profile. b) Error profile. Regular frames*

To this aim, a set of seven input ground motions have been carefully chosen in such a way to be consistent with the selected target response spectrum (5%-damped Eurocode 8 type 1 elastic spectrum for soil class A). The SeismoMatch software [2004] has been used to enforce the spectrum-compatibility of the selected accelerograms. Table 1 shows the parameters of the ground motion records. In Fig. 2, the pseudo-velocity response spectra of both recorded and adjusted accelerograms are plotted. The accuracy of ACSM is compared with other more advanced nonlinear static procedures: 1) MP: Multi-mode Pushover analysis [Sucuoğlu *et al.*, 2011]; 2) MMPA: Modified Modal Pushover Analysis procedure assuming higher modes as elastic [Chopra *et al.*, 2004]; 3) N2-EXT: Extended N2 method considering higher mode effects both in plan and in elevation [Kreslin *et al.*, 2012]. The interstorey drift ratio of each storey (defined as the storey drift divided by the storey height) plays an important role in the amount of damage induced in the structure during earthquake ground motion. Consequently, this quantity has been used for comparing the results of Nonlinear Static Procedures (NSPs) and Nonlinear Response History Analysis (NRHA). Specifically, the mean value of the seven interstorey drifts resulted from NSPs has been compared with the mean value of the peak interstorey drifts resulted from NRHA. In Fig. 3-4, the interstorey drift ratios obtained with Nonlinear Response History Analysis (NRHA) are assumed as reference values (X-axis) and the corresponding values obtained with the Nonlinear Static Procedures (NSPs) are shown on the Y-axis. The bisector represents the cases when the NSP and the NRHA give the same results. The straight lines numbered -10%, -20% and -30% are representative of error rates (defined in subsequent Eq. (9)) equal to -10%, -20% and -30% , respectively.

$$Error(\%) = 100 \times \frac{\overline{\Delta}_{j,NSP} - \overline{\Delta}_{j,NRHA}}{\overline{\Delta}_{j,NRHA}} . \tag{9}$$

In Eq. (9) $\overline{\Delta}_{j,NRHA}$ is the mean value of the seven peak interstorey drifts in the j-*th* storey resulting from NRHA, $\overline{\Delta}_{j,NSP}$ is the mean value of the seven interstorey drifts in the j-*th* storey resulting from NSP. The scatter plot of Figs. 3-4 evaluates the coherence between NSP and NRHA. When all the points representing the pairs of values are clustered around the bisector, both methods tend to give the same results. On the contrary, when some values lie below the straight lines numbered -10%, it means that the error of the mean interstorey drift coming from the NSP with respect to the mean interstorey drift of the NRHA is greater than 10%. Finally, it is to be observed that the points over the bisector are situations where the value estimated from NSP procedure is greater than the corresponding value from NRHA. In these cases, the NSP gives conservatives estimates of the nonlinear dynamic response. Figs. 3-4 show that all the procedures tend to underestimate the interstorey drift demand for *PGA*=0.20g and underestimation is even greater than 30%. For *PGA*=0.20g, all framed structures respond elastically, and the differences between NSP and NRHA are not dependent on the inelasticity in the structure, but entirely arise due to the difference in the analysis method. For values of *PGA* ranging from 0.40g to 0.80g the amount of inelasticity in the structure increases, and the accuracy depends on the NSP used to compute the seismic demand. Specifically, both N2-EXT and MMPA tend to overestimate the interstorey drifts when compared to NRHA. The discrepancy increases with both the number of storeys and irregularity in elevation. On the other side, the MP procedure underestimates the interstorey drift demand of irregular frames, while the proposed ACSM tends to give the most accurate solutions.
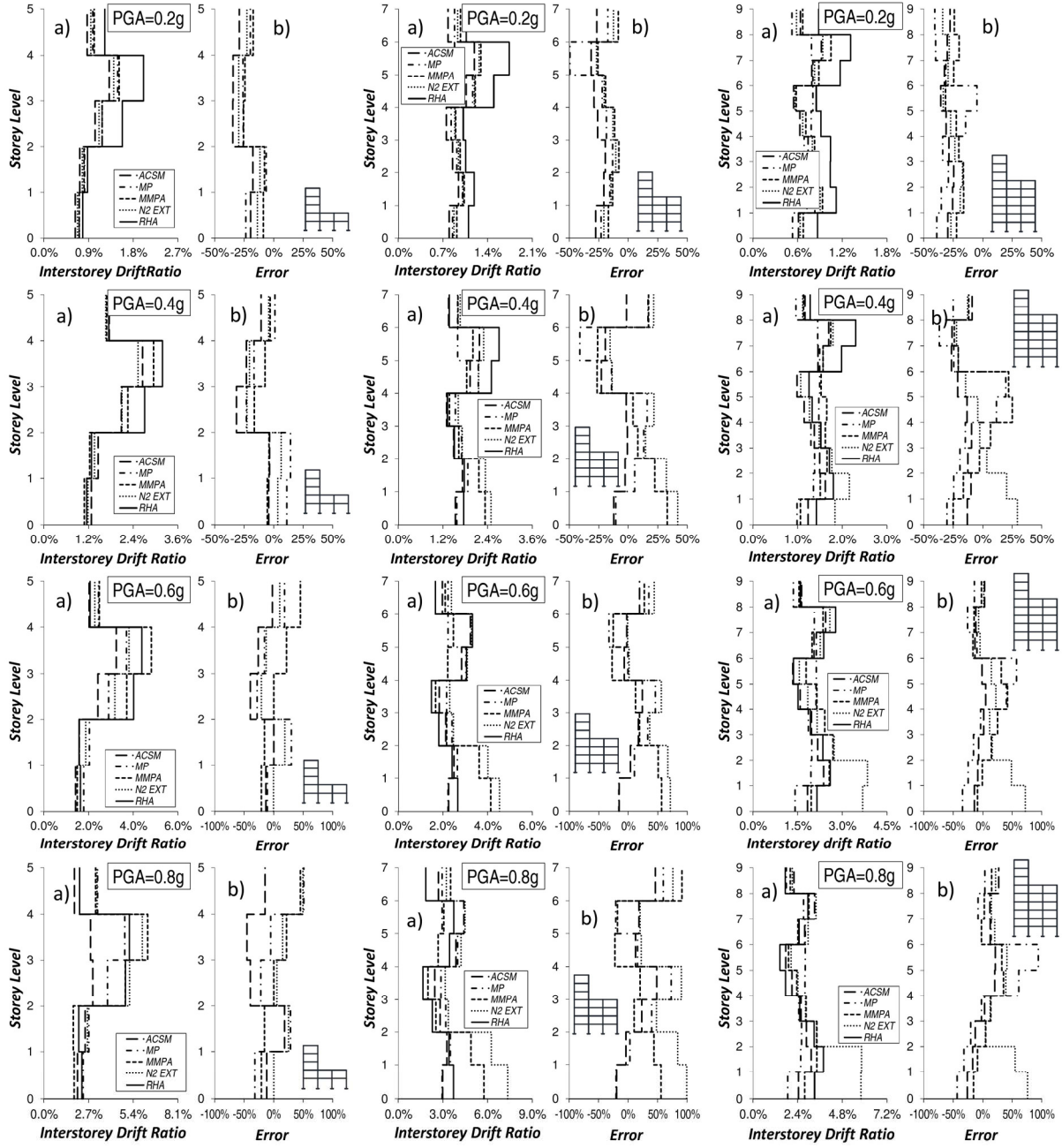
Figure 6. *a) Interstorey drift profile. b) Error profile. Irregular frames*

Practically, the pushover procedures based on invariant lateral force patterns tend to accurately estimate the seismic response of low-rise and regular frames, where the response is dominated by the first mode and the development of a collapse mechanism of the global type is possible. On the contrary, these procedures become inaccurate when applied to high-rise and irregular frames, where the higher modes effects are significant and undesired collapse mechanism typologies may be developed. In particular, high-rise frames are more prone to develop partial mechanisms involving a limited number of storeys compared to the total number. The occurrence of such storey mechanism confirms the importance of design procedures focusing on plastic mechanism control of MR-frames [Montuori *et al.*, 2012-2015] [Piluso *et al.*, 2014].

In Fig. 5 the interstorey drift and the error profiles of the regular frames are plotted. The results obtained for *PGA*=0.20g show that all procedures underestimate the interstorey drift of all storeys. Moreover, the error is slightly variable along the height. When the value of *PGA* rises to 0.40g, the differences increase both along the height and between the NSPs. For *PGA*=0.60g and even more for *PGA*=0.80g both N2-EXT and MMPA overestimate the interstorey drifts, especially in the upper and lower storeys of the taller frames. On the contrary, the proposed ACSM procedure gives errors that are lower and less variable along the height even when compared to the MP procedure. In Fig. 6 the interstorey drift profiles and the error profiles of the irregular frames are plotted. Also in this case, all procedures underestimate the interstorey drift of all storeys for *PGA*=0.20g. Greater differences, both along the height and between the NSPs, are evidenced for *PGA*=0.40g and, even more, for *PGA*=0.60g and *PGA*=0.80g. Both N2-EXT and MMPA overestimate the interstorey drift, especially in the lower storeys, also for shorter frames and for *PGA*=0.40g. In the case of irregular frames, also the MP procedure seems inaccurate since it overestimates the interstorey drifts, especially in the middle storeys for *PGA* ranging between 0.40g and 0.80g. The proposed ACSM procedure gives errors that turn to be lower and less variable along the height than other methods. In order to estimate the global accuracy of results given by the mentioned NSPs, the mean value of maximum interstorey drift obtained from NRHA is assumed as the reference value and the total error has been evaluated as follows:

$$Total\ Error(\%) = 100 \times \sqrt{\frac{1}{N}\sum_{j=1}^{N}\left(\frac{\overline{\Delta}_{j,NSP} - \overline{\Delta}_{j,NRHA}}{\overline{\Delta}_{j,NRHA}}\right)} \qquad (10)$$

In Fig. 7 the total error is plotted as a function of the peak ground acceleration. The application of both N2-EXT and MMPA procedure can potentially result in very inaccurate solutions for the high values of peak ground acceleration.
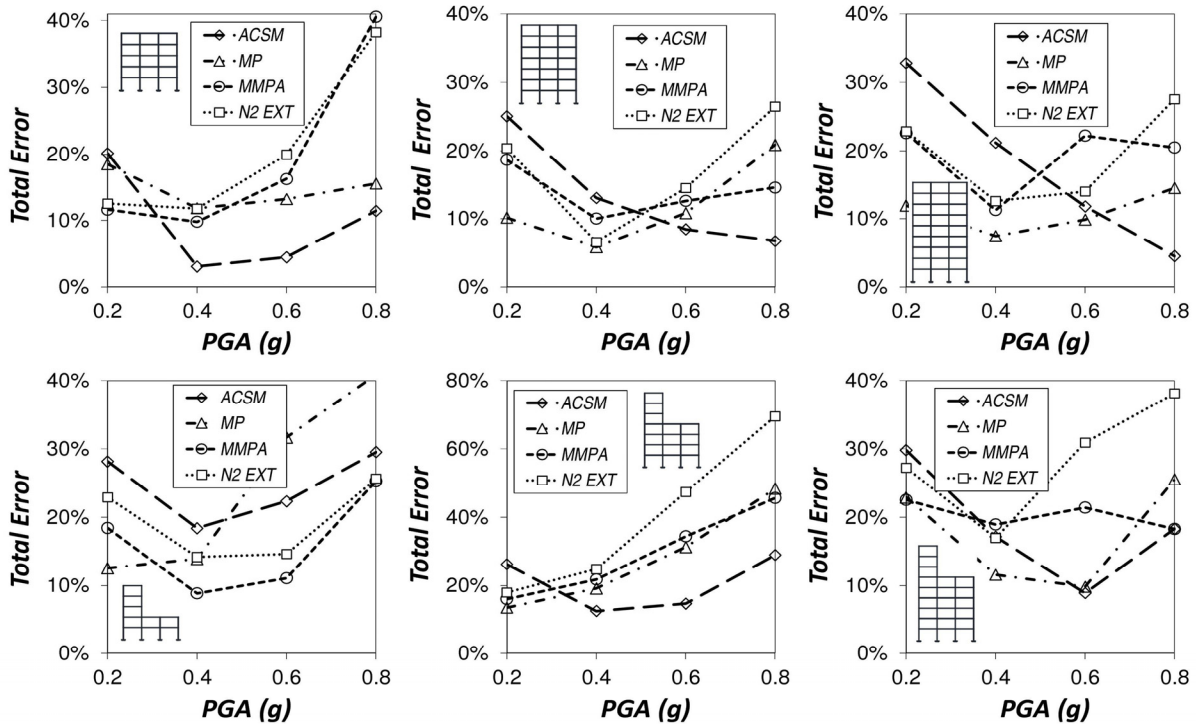

Figure 7. *Total error as a function of the peak ground acceleration*

This conclusion is true for both regular and irregular frames. On the other side, the results of MP procedure may become very inaccurate when the peak ground acceleration and the irregularity in elevation increase. On the contrary, the proposed Adaptive Capacity Spectrum Method give the most accurate solutions for both regular and irregular frames, especially for high values of peak ground acceleration.

5. CONCLUSIONS

An adaptive capacity spectrum method for estimating seismic demands of steel moment-resisting frames was presented in this paper. The proposed procedure takes into account the frequency content of response spectra, the higher mode effects, the progressive changes in the modal properties due to structural yielding and the interaction between modes in the inelastic range. The accuracy and efficiency of the proposed approach was validated by comparing its results with estimates obtained from the nonlinear response history analysis. The results were eventually compared with those provided by other methods suggested in literature. The accuracy of nonlinear static procedures based on invariant load patterns proved to be insufficient at the lower storey levels, and this discrepancy increases with both the number of storeys and the irregularity in elevation. The multimodal pushover methods accounting for higher mode effects along the elevation provide a more accurate estimation of seismic demands, but they become very inaccurate when the peak ground acceleration and the irregularity in elevation increase. The proposed Adaptive Capacity Spectrum Method generally gives a more accurate solution for both regular and irregular frames, especially for the high values of peak ground acceleration. Moreover, the estimated errors are lower and less variable along the height than other methods suggested in literature.

6. ACKNOWLEDGEMENTS

7. REFERENCES

Antoniou, S. and Pinho, R. [2004] "Development and verification of a displacement-based adaptive pushover procedure", *Journal of Earthquake Engineering* 8(5), 643-661.

ASCE [2005] *Seismic Rehabilitation of existing buildings*, ASCE/SEI 7-05, Published by the American Society of Civil Engineers.

ATC [1997] *Seismic Evaluation and Retrofit of Concrete Buildings*, Report No. ATC-40, Applied Technology Council, Redwood City, CA.

CEN [2004] *Eurocode 8: Design of structures for earthquake resistance, Part 1: general rules, seismic actions and rules for buildings*, EN1998-1, European Committee for Standardization.

Chopra, A.K. and Goel, R.K. [2002] "A modal pushover analysis procedure for estimating seismic demands for buildings", *Earthquake Engineering and Structural Dynamics* 31(3), 561–582.

Chopra, A.K., Goel, R.K. and Chintanapakdee, C. [2004] "Evaluation of a Modified MPA Procedure Assuming Higher Modes as Elastic to Estimate Seismic Demands", *Earthquake Spectra* 20(3), 757-778.

Erduran, E. [2008] "Assessment of current nonlinear static procedures on the estimation of torsional effects in low-rise frame buildings", *Engineering Structures* 30, 2548–2558.

Fajfar, P., Marušić, D. and Perus, I. [2005] "Torsional effects in the pushover-based seismic analysis of buildings", *Journal of Earthquake Engineering* 9(6), 831-854.

FEMA [1997] *NEHRP guidelines for the seismic rehabilitation of buildings*, Report FEMA-273 (Guidelines) and Report FEMA-274 (Commentary), Washington (DC).

FEMA [2000] *Prestandard and Commentary for the Seismic Rehabilitation of Buildings*, FEMA 356, prepared by the American Society of Civil Engineers for the Federal Emergency Management Agency. Washington, D.C, 2000.

FEMA [2005] *Improvement of nonlinear static seismic analysis procedures*, prepared by the Applied Technology Council (ATC-55 Project), FEMA 440, published by the Federal Emergency Management Agency, Washington.

Ferraioli, M., Lavino, A., Avossa, A.M. and Mandara, A. [2008] "Displacement-based seismic assessment of steel moment resisting frame structures", *Proc. of the 14th World Conference on Earthquake Engineering*, Beijing, China.

Ferraioli, M. [2010] "Inelastic torsional response of an asymmetric-plan hospital building in Italy", *Proc. of the Final Conference COST ACTION C26: Urban Habitat Constructions under Catastrophic Events*, Naples, Italy, 365-370.

Ferraioli, M., Lavino, A. and Mandara, A. [2014a] "Behaviour factor of code-designed steel moment-resisting frames", *International Journal of Steel Structures* 14(2), 1-12.

Ferraioli, M., Avossa, A.M., Lavino, A. and Mandara, A. [2014b] "Accuracy of Advanced Methods for Nonlinear Static Analysis of Steel Moment-Resisting Frames", *The Open Construction and Building Technology Journal* 8, 310-323.

Ferraioli, M., Avossa, A.M. and Mandara, A. [2014c] "Assessment of Progressive Collapse Capacity of Earthquake-Resistant Steel Moment Frames Using Pushdown Analysis", *The Open Construction and Building Technology Journal* 8, 324-336.

Ferraioli, M. [2015] "Case study of seismic performance assessment of irregular RC buildings: hospital structure of Avezzano (L'Aquila, Italy)", *Earthquake Engineering and Engineering Vibration* 14, 141-156.

Gupta, B. and Kunnath, S.K. [2000] "Adaptive spectra-based pushover procedure for seismic evaluation of structures", *Earthquake Spectra* 162, 367–391.

Jianmeng, M., Changhai, Z. and Lili, X. [2008] "An improved modal pushover analysis procedure for estimating seismic demands of structures", *Earthquake Engineering & Engineering Vibration* 7, 25-31.

Kalkan, E. and Kunnath, S.K. [2006] "Adaptive modal combination procedure for nonlinear static analysis of building structures", *Journal of Structural Engineering* 132(11), 1721–31.

Kreslin, M. and Fajfar, P. [2012] "The extended N2 method considering higher mode effects in both plan and elevation", *Bulletin of Earthquake Engineering* 10, 695–715.

Kunnath, S.K. [2004] "Identification of modal combination for nonlinear static analysis of building structures", *Computer-Aided Civil and Infrastructure Engineering* 19, 246–59.

Ministry of Infrastructure and Transport [2008] *Italian Building Code*, Ministerial decree of Jan 14th, 2008, Official gazette 29, Rome (in Italian).

Montuori, R., Nastri, E. and Piluso, V. [2015] "Advances in theory of plastic mechanism control: Closed form solution for MR-Frames", *Earthquake Engineering and Structural Dynamics* 44(7), 1035–1054.

Montuori, R., Troisi, M. and Piluso, V. [2012] "Theory of plastic mechanism control of seismic-resistant MR-frames with set-backs", *Open Construction and Building Technology Journal* 6, 404-413.

Piluso, V., Montuori, R. and Troisi, M. [2014] "Innovative structural details in MR-frames for free from damage structures", *Mechanics Research Communications* 58, 146-156.

Pinho, R. and Casarotti C. [2008] "Using the Adaptive Capacity Spectrum Method for Seismic Assessment of Irregular Frames", *Proc. of the 5th European Workshop on the Seismic Behaviour of Irregular and Complex Structures*, Catania, Italy.

Poursha, M., Khoshnoudiana, F. and Moghadam, A.S. [2009] "A consecutive modal pushover procedure for estimating the seismic demands of tall buildings", *Engineering Structures* 31, 591-599.

Reyes, J.C. and Chopra, A. [2011] "Three-dimensional modal pushover analysis of buildings subjected to two components of ground motion, including its evaluation for tall buildings", *Earthquake Engineering and Structural Dynamics* 40, 789–806.

SeismoSoft [2014] *SeismoStruct: A computer program for static and dynamic analysis for framed structures*, [Online] Available from URL: www.seismosoft.com.

SeismoSoft [2014] *SeismoMatch*, [Online] Available from URL: www.seismosoft.com.

Sucuoğlu, H. and Günay, M.S., [2011] "Generalized force vectors for multi-mode pushover analysis", *Earthquake Engineering and Structural Dynamics* 40, 55–74.

Vidic, T., Fajfar, P. and Fischinger, M. [1994] "Consistent inelastic design spectra: strength and displacement", *Earthquake Engineering and Structural Dynamics* 23, 502-521.

UNA VERSIONE ADATTIVA DEL METODO DELLO SPETTRO DI CAPACITÀ PER LA VALUTAZIONE DELLA RISPOSTA SISMICA DI TELAI SISMORESISTENTI IN ACCIAIO

Massimiliano Ferraioli*, Angelo Lavino, Alberto Mandara

Department of Civil Engineering, Design, Building and Environment
Second University of Naples, Aversa (CE)

SOMMARIO: *É stata proposta una variante adattiva del metodo dello spettro di capacità per la valutazione della risposta inelastica di telai sismoresistenti in acciaio soggetti ad azioni di tipo sismico. Sono stati esaminati i suoi vantaggi computazionali e la sua capacità di fornire previsioni accurate dell'effet-tiva risposta sismica in rapporto a quelle ottenute impiegando altre procedure statiche non lineari disponibili in letteratura. L'efficacia e l'accuratezza dei metodi approssimati basati sull'analisi di pushover è stata verificata attraverso un'estesa indagine parametrica condotta su telai sismoresi-stenti in acciaio sia regolari, sia irregolari. I risultati ottenuti sono stati confrontati con quelli ottenuti dall'analisi dinamica non lineare condotta utilizzando segnali accelerometrici spettrocompatibili.*

---

*Corresponding author: Massimiliano Ferraioli, Department of Civil Engineering, Design, Building and Environment, Second University of Naples, Aversa (CE), Italy.
Email: massimiliano.ferraioli@gmail.com

SEISMIC APPLICATION OF PENTAMODE LATTICES

Francesco Fabbrocino[1], Ada Amendola[2], Gianmario Benzoni[3], Fernando Fraternali[2]

[1] Department of Engineering, Pegaso University, Napoli, Italy
[2] Department of Civil Engineering, University of Salerno, Fisciano (SA), Italy
[3] Department of Structural Engineering, University of California San Diego, CA, USA

SUMMARY: *The category of "extremal materials" has been introduced in the literature to define materials that simultaneously show very soft and very stiff deformation modes (unimode, bimode, trimode, quadramode and pentamode materials, depending on the number of soft modes). This definition applies to a special class of mechanical metamaterials – composite materials, structural foams, cellular materials, etc. – which feature special mechanical properties. Pentamode materials have been proposed for transformation acoustics and elasto-mechanical cloak, but their potential in different engineering fields is still only partially explored. We here present novel versions of pentamode materials: artificial structural crystals showing shear moduli markedly smaller than the bulk modulus. Novel pentamode lattices with tensegrity architecture are designed, through the insertion of actuated struts and/or prestressed cables within basic pentamode lattices. Such systems are proposed as tunable seismic base-isolation devices, profiting from their low and adjustable shear moduli, which can be easily adapted to the dynamic properties of the structure to be isolated.*

KEYWORDS: *Metamaterials, Periodic Lattices, Pentamode Materials, Seismic Isolation*

1. INTRODUCTION

The nascent, rapidly growing field of mechanical and acoustic metamaterials is attracting increased attention from many research sectors, due to the great technological potential of un-conventional materials with properties mainly derived by their geometrical structure, rather than their chemical composition (refer, e.g., to review papers [Lu *et al*., 2009], [Maldovan, 2013]). Mechanical and acoustic metamaterials exhibit a variety of unusual behaviors that are not found in natural materials. These may include: exceptional strength- and stiffness-to-weight ratios; excellent strain recov-erability; very soft and/or very stiff deformation modes; auxetic behavior; phononic band-gaps; sound control ability; negative effective mass density; negative effective stiffness; negative effective refraction index; superlens behavior; and/or localized confined waves, to name some examples (cf. [Lu *et al*., 2009], [Maldovan, 2013], [Milton and Cherkaev, 1995], [Daraio *et al*., 2010], [Fraternali, *et al*., 2012], [Meza *et al*., 2014], [Zheng *et al*., 2014], [Schittny *et al*., 2013], [Kadic *et al*., 2012], [Bückmann *et al*., 2014], [Norris, 2014], [Amendola *et al*., 2014], [Fraternali *et al*., 2015], [Fraternali *et al*., 2014] and references therein). The category of "extremal materials" has been introduced in [Milton and Cherkaev, 1995] to define materials that simultaneously show very soft and very stiff defor-mation modes (unimode, bimode, trimode, quadramode and pentamode materials, depending on the number

---
*Corresponding author: Fernando Fraternali, Department of Civil Engineering, University of Salerno, Fisciano, Italy.
Email: f.fraternali@unisa.it

of soft modes). This definition applies to a special class of mechanical metamaterials – composite materials, structural foams, cellular materials, etc. – which feature special mechanical properties. Rapid prototyping techniques for the manufacture of materials with near-pentamode behavior have been recently presented in [Schittny *et al.,* 2013] (macroscale) and [Kadic *et al.,* 2012] (microscale). Pentamode materials have been proposed for transformation acoustics and elasto-mechanical cloak (refer, e.g., to the recent paper [Bückmann *et al.,* 2014] and the references therein), but their potential in different engineering fields is still only partially explored. The present study with the use of pentamode lattices as tunable seismic isolation devices, making profit from the control of the soft modes of such materials through the tuning of the bending moduli of members and junctions [Schittny *et al.*, 2013], [Kadic *et al.*, 2012], [Bückmann *et al.*, 2014], [Norris, 2014]. An illustrative numerical example shows a practical implementation of a pentamode lattice as a base isolation device, establishing a comparison of the elastic moduli and the force-displacement response of such a system with those exhibited by a conventional rubber bearing.
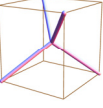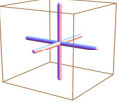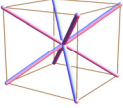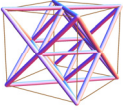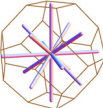
2. ELASTIC MODULI OF LATTICE MATERIALS

A recent study by [Norris, 2014] presents a discrete-to-continuum approach to the elastic moduli of different periodic structures, including pentamode, simple cubic, BCC, FCC octet truss and tetrakaidecahedral lattices. We hereafter summarize the main results of such a study, with reference to the unit cell of a d-dimensional lattice that is composed of a number Z of elastic members (rods) and occupies a volume V. With reference to the unit cells examined in [Norris, 2014], it is easily shown that the elastic stiffness tensor that characterize the lattice response at the mesoscopic scale shows cubic symmetry with independent stiffness coefficients C_{11}, C_{12} and C_{44} (Voigt notation). Let us introduce the following notations:

$$M_i = \int_0^{R_i} \frac{dx}{E_i A_i}, \; N_i = \int_0^{R_i} \frac{x^2 dx}{E_i I_i} \tag{1}$$

for the axial and bending compliances of the lattice members, where x is an axial coordinate with origin at the junction of the rods; while R_i, E_i, A_i and I_i respectively indicate the reference length, the Young modulus of the material, the cross-sectional area and the moment of inertia of the cross-section of i-th rod, assuming polar-symmetry of such a cross-section ($i = 1, ..., Z$). By discarding the member forces induced by the node compliances, we obtain the results presented in Table 1, where $K = (C_{11} + 2C_{12})/3$ denotes the bulk modulus of the lattice; $G = \mu_1 = C_{44}$ denotes the shear modulus; and we set: $\mu_2 = (C_{11} - C_{12})/2$. All the lattices examined in Table 1, with exception to the case $Z = 14$ (*tetrakaidecahedral lattice*), are characterized by members with equal values of R_i, M_i, and N_i (respectively denoted by R, M, and N). The tetrakaidecahedral unit cell can be regarded as the summation of the simple cubic unite cell ($Z = 6$) and a scaled version of the BCC cell ($Z = 8$). It is obtained by truncating the BCC members with an octahedron featuring 14 faces and 36 edges of equal length a. In this case, the members of the parent simple cubic cell have equal length $R_1 = \sqrt{2}a$ and equal compliances M_1 and N_1; while the members of the parent BCC cell have equal length $R_2 = \sqrt{3/2}\,a$ and equal compliances M_2 and N_2. It is worth noting that, in the stretch-dominated limit ($N_i \to \infty$), the pentamode unit cell ($Z = 4$) has zero shear moduli: ($G = \mu_2 = 0$) and nonzero bulk modulus K.

Table 1. *Unit cells and elastic properties of three-dimensional lattice materials [Norris, 2014]*

unit cell	K	G/K	μ_2/K	V
pentamode (Z=4)	$\dfrac{4R^2}{9MV}$	$\dfrac{9M}{4M+2N}$	$\dfrac{3M}{2N}$	$\dfrac{64}{3\sqrt{3}}R^3$
simple cubic (Z=6)	$\dfrac{2R^2}{3MV}$	$\dfrac{3M}{2N}$	$3/2$	$8R^3$
BCC (Z=8)	$\dfrac{8R^2}{9MV}$	$1+\dfrac{M}{2N}$	$\dfrac{3M}{2N}$	$\dfrac{32}{3\sqrt{3}}R^3$
FCC octet truss (Z=12)	$\dfrac{4R^2}{3MV}$	$\dfrac{3}{4}+\dfrac{3M}{4N}$	$\dfrac{3}{8}+\dfrac{9M}{8N}$	$4\sqrt{2}R^3$
tetrakaidecahedral (Z=14)	$\dfrac{1}{9V}\left[\dfrac{6R_1^2}{M_1}+\dfrac{8R_2^2}{M_2}\right]$	$\dfrac{3}{2}\dfrac{1/M_1+1/N_2}{1/M_1+1/M_2}$	$\dfrac{1/N_2+2/M_2+3/N_1}{2(1/M_1+1/M_2)}$	$8\sqrt{2}a^3$

This means that such a lattice material can be regarded as a "solid water" [Milton and Cherkaev, 1995], [Schittny *et al.,* 2013], [Kadic *et al.,* 2012], which is well suited for the manufacturing of next generation seismic isolation devices.

3. USE OF PENTAMODE LATTICES FOR BASE ISOLATION DEVICES

Let us refer to the representative pentamode element shown in Fig. 1, which is composed of four unit cells endowed with rods composed of two truncated bi-cones. The latter show a small-size diameter d at the extremities of the rods, and a larger diameter D at the mid-span of the rods. The lattice constant a is related to the rod length R through:

$$a = \frac{4R}{\sqrt{3}} \qquad (2)$$

where $r_{min}=d/2$ and $r_{max}=D/2$. On using the above relationships, and taking into account that the cross-section area and the moment of inertia of the rods are respectively given by $A(x)=\pi[r(x)]^2$ and $I(x)=\pi[r(x)]^4/4$, we finally obtain the following expressions of the axial and bending compliances of the generic rod:
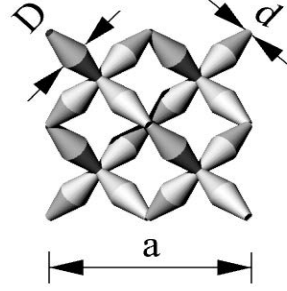
Figure 1. *Geometry of a pentamode module formed by four unit cells*

$$M = \frac{R}{\pi E \ r_{max} r_{min}},$$

$$N = \frac{R^3 \left(2r_{max}^2 + r_{max} r_{min} + r_{min}^2\right)}{3\pi E \ r_{max}^3 r_{min}^3}$$

(3)

where E denotes the Young modulus of the rod material. Making use of Equations (3) into the expressions of K and G/K ratio given in Tab. 1 ($Z = 4$), we finally obtain

$$K = \frac{4R^2}{9VM} = \frac{\pi E dD}{64\sqrt{3}R^2}, \quad G = \frac{9\sqrt{3}\pi \left(dD\right)^3 E}{768\left(dDR\right)^2 + 512\left(d^2 + 2D^2 + dD\right)R^4}$$

(4)

$$\frac{G}{K} = \left[\frac{4}{9} + \frac{8\left(2D + dD + d^2\right)R^2}{27d^2D^2}\right]^{-1}$$

(5)

It is worth comparing the analytic prediction of the G/K ratio provided by Equation (5), with the numerical estimate of the same ratio given in [Kadic *et al.,* 2012], which has been obtained by fitting the results of finite element simulations of pentamode lattices under hydrostatic pressure and simple-shear loading:
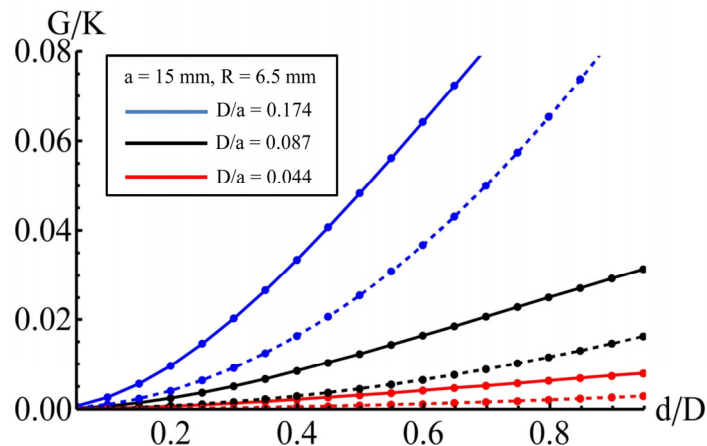

Figure 2. *Curves plotting the G/K ratio of pentamode lattices against the d/D ratio, for $a = 15$ mm and different values of the D/a ratio. The solid curves correspond to the analytic predictions of Equation (7) [Norris, 2014]0, while the dashed curves correspond to the numerical estimates of Equation (8)[Kadic et al., 2012]*

$$\frac{G}{K} = \left[\left(\frac{R}{d} \right)^2 \sqrt{\frac{R}{D}} \right]^{-1} \tag{6}$$

Fig. 2 compares the predictions of Equations (5) and (6) for the G/K ratio, assuming the lattice constant $a = 15$ mm ($R = 6.5$ mm), differen D/a ratios ($D/a = 0.174, 0.087, 0.044$), and letting the d/D ratio vary from zero to one. The limiting cases with $d/D = 0$ and $d/D = 1$ respectively correspond to a stretch-dominated pentamode lattice (no bending effects), and a pentamode lattice showing rods with constant cross-section (cylindrical rods).

The mismatches between the analytic and numerical predictions of the G/K ratio in Fig. 1 are explained by the fact that the analytic formula (5) is based on a beam model for the rods (1D theory), while the numerical estimate (6) accounts for a 3D elastic response of such elements (through fine meshes of tetrahedral finite elements [Kadic *et al.*, 2012]). Both predictions highlight that the shear modulus of pentamode lattices can be finely tuned by properly designing the diameters d and D of the struts [Schittny *et al.*, 2013], [Kadic *et al.*, 2012]. The following section illustrates practical implementations of pentamode lattices for the construction of innovative seismic isolation devices.

3.1 *Practical examples*

Let us compare the mechanical response of pentamode lattices with that of a commercial rubber bearing with diameter $\varnothing 33.5'' \left(0.8509\, m \right)$ and height $13.85'' \left(0.3518\, m \right)$, which is composed of 29 rubber layers of 7 mm each; 28 steel shims (spacers) of 3.04 mm each; two terminal rubber layers of 31.8 mm each and covers, without lead plug (isolator Type E [RB-800] produced by Dynamic Isolation Systems, Inc, McCarran, NV, USA). Figs. 3 and 4 illustrate the hysteretic (low-damping) response of such an isolator in terms of cyclic shear stress (τ) vs. shear strain (γ) curves, and normal stress (σ) vs. axial strain (ε) curves (with preload of $\sigma = 0.31\, MPa$) at constant velocity (courtesy of Caltrans Testing Facility, University of California, San Diego). Such experimental results provide an average shear modulus $\bar{G} = 0.791 MPa$, and an average compression modulus of the rubber-steel composite $\bar{E}_c = 330\, MPa$ [Kelly and Lai, 2011]. Table 2 illustrates the geometrical properties of different pentamode pads, which can be confined between steel plates to form innovative pentamode bearings (PMBs). Such pads are obtained by replicating the pentamode module shown in Fig. 1 $n_a \times n_a$ times in the plane of the pad, and one single time along the thickness ($n_v = 1$), implying pad thickness $t \equiv a$. The lattice struts are made of steel (SPMB1 and SPMB2: $E = 206\, GPa$) or the "FullCure850 VeroGray" polymeric material supported by Stratasys® 3D printers (PPMB1 and PPMB2: $E = 1.4 GPa$ [Schittny et al., 2013]), and show different values of the geometric variables a, D and d. Making use of Equation (4) for the shear modulus of the pentamode pad, and the following formula for the composite, steel-pentamode compression modulus [Kelly and Lai, 2011]:

$$E_c = 6.73\, G\, S_1^2 \tag{7}$$

where $S_1 = L/4t = n_a/4n_v$, we predict $\text{G} = \bar{G} = 0.791 MPa$, $E_c = 341\, MPa$ for all the PMBs based on the pads described in Table 2, i.e., shear and compression moduli almost equal to those of the comparative rubber bearing. Figures 3 and 4 provide comparisons between the experimental stress-strain curves of the analyzed rubber bearing and the linear stress-strain

responses of the PMBs in Table 2 (assuming absence of dissipation in the latter, to a first, simplifying, approximation).
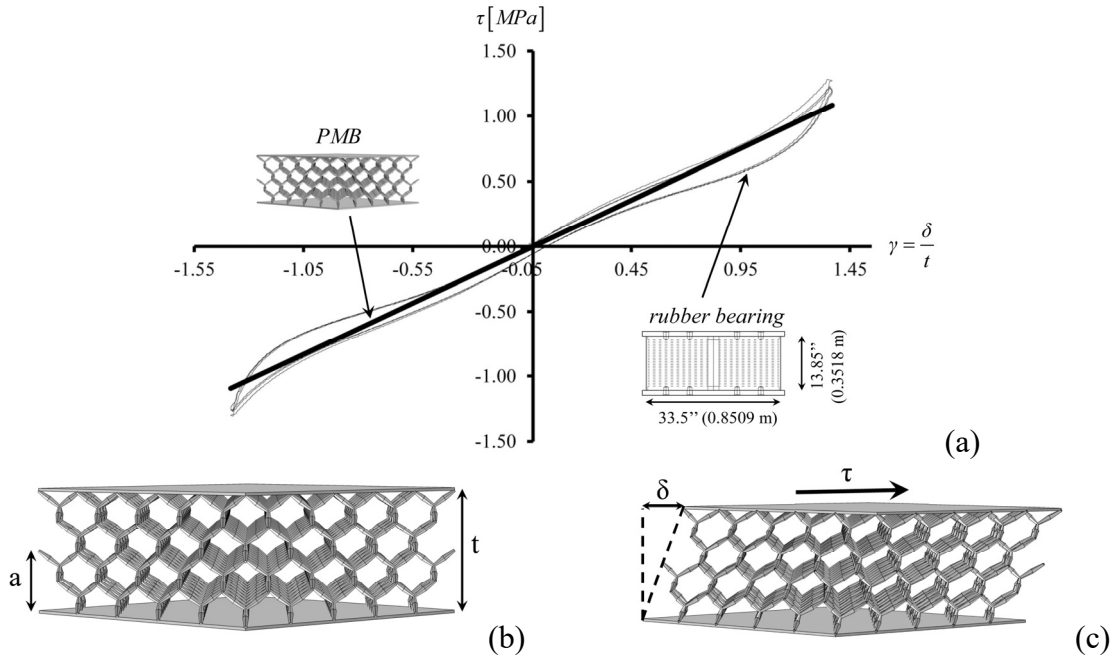
Figure 3. *(a) Comparison between the shear stress vs. shear strain responses of the pentamode bearings (PMBs) in Table 2 and a low-damping rubber bearing; (b-c) undeformed and deformed configurations of a PMB*
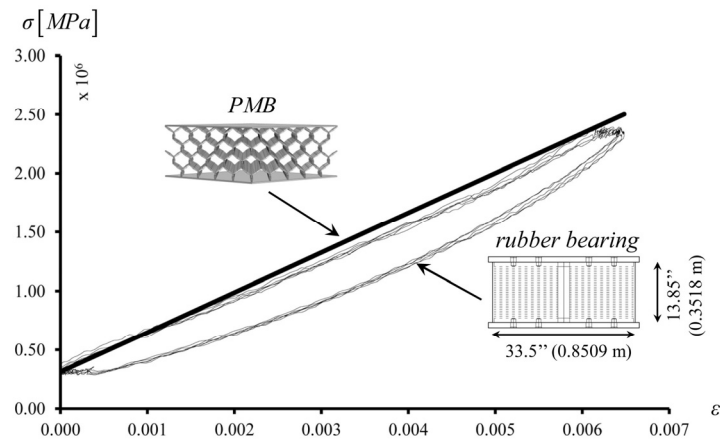
Figure 4. *Comparison between the axial stress vs. axial strain responses of the pentamode bearings (PMBs) in Table 2 and a low-damping rubber bearing*

4. CONCLUSIONS

We have presented novel versions of pentamode materials: artificial structural crystals showing shear moduli markedly smaller than the bulk modulus [Milton and Cherkaev, 1995], [Schittny et al., 2013], [Kadic et al., 2012]. Innovative seismic isolators based on pentamode lattices confined between steel plates have been designed. The soft modes of such materials have been controlled by tuning of the bending moduli and the geometry of members and junctions. We have shown that such novel isolators can exhibit mechanical response similar to that of

conventional rubber bearings, provided that the material and the geometry of the lattice are suitably designed.

Table 2. *Geometric properties of pentamode pads to be employed to form seismic isolators*

Case	$t \equiv a\,[mm]$	$R\,[mm]$	n_a	$L = n_a\,a\,[m]$	$d = \dfrac{D}{2}\,[mm]$
SPMB1	5	2.17	32	0.16	0.19
SPMB2	10	4.33	32	0.32	0.37
PPMB1	5	2.17	32	0.16	0.66
PPMB2	10	4.33	32	0.32	1.32

We may conclude that the main advantages of pentamode bearings over traditional structural bearings [Higashino *et al.*, 2003], [Monaldo-Mercaldo, 1995], [Adebowale, 2012] are the following:
- the mechanical properties of the soft layers forming such devices mainly depend on the geometry of the pentamode lattices, more than on the chemical nature of the employed materials (metallic, ceramic, polymeric, etc.);
- it is easy to adjust the mechanical properties of pentamode bearings to those of the structure to be isolated, by playing with the lattice geometry and the nature of the material (see Equation (6) and Table 2), as opposed to rubber bearings, where instead the achievement of very low shear moduli implies marked reductions of the vertical load carrying capacity, making such devices not particularly convenient in the case of structures with very high fundamental periods of vibrations (such as, e.g., very tall buildings; highly compliant structures; very soft soils; etc.) [Higashino *et al.*, 2003], [Monaldo-Mercaldo, 1995], [Adebowale, 2012];
- the dissipation of pentamode bearings can be conveniently designed through an accurate choice of the material to be used for the pentamode lattices, and inserting, - when necessary, an additional dissipative element within the device (such as, e.g., a lead core);
- the possibility to design and fabricate laminated composite bearings showing layers with different materials, geometries and properties: such a design approach is instead much less effective in the state-of-the-art laminated rubber bearings, where the only lamination variable consists of the type of rubber to be employed for the soft pads (natural rubber or synthetic rubber);
- the freedom in the choice of the materials of the pentamode lattices, by keeping the elastic properties of the device essentially unchanged, allows the designer to adapt the energy dissipation capacity and the life span (i.e., the durability) of the device to the actual use conditions [Monaldo-Mercaldo, 1995], [Adebowale, 2012];
- the possibility to replace the fluid components of the structural bearings and energy absorbing devices currently available on the market (such as, e.g., viscous fluid dampers and tuned mass dampers) with pentamode lattices: such a replacement would lead to significantly reduce the technical issues related to fluid leaking and frequent maintenance, which currently affect the state-of-the-art devices involving fluid materials [Monaldo-Mercaldo, 1995], [Adebowale, 2012];
- the mechanical properties of pentamode bearings can be dynamically adjusted and measured, by equipping selected struts of the pentamode lattices with sensors and/or actuators;

- pentamode bearings directly manufactured from computer-aided design data outputted by a computational material design phase, employing advanced and fast additive manufacturing techniques at different scales and single or multiple materials (metals, polymers, etc.).

Several aspects of the present work pave the way to relevant further investigations and generalizations that we address to future work. First, mechanical models for composite rubber-steel bearings [Kelly and Lai, 2011] need to be generalized to pentamode-steel bearings, accounting for the peculiar deformation models of such systems. Second, physical models of pentamode isolators need to be constructed, employing, e.g., additive manufacturing techniques [Schittny *et al*., 2013], [Kadic *et al*., 2012], and laboratory tested as seismic base-isolation devices [Modano *et al.*, 2015], in order to experimentally asses their isolation and dissipation capabilities arising, e.g., from inelastic response and/or material fracture [Fraternali, 2007]. Another relevant generalization of the present research regards the design of dynamically tunable systems based on the insertion of prestressed cables and/or curved rods within pentamode lattices, with the aim of designing novel metamaterials and bio-inspired lattices tunable by local and global prestress [Amendola *et al*., 2014], [Fraternali *et al*., 2015], [Fraternali *et al*., 2014], [Gurtner and Durand, 2014], [Ascione and Fraternali, 1992], [Fraternali and Bilotti, 1997], [Fraternali *et al*., 2013], [Fraternali *et al.*, 2012], [Fraternali and Marcelli, 2012], [Schmidt and Fraternali, 2012], [Fraternali *et al*., 2014]. Future studies will also address the experimentation of pentamode materials as components of new-generation seismic dampers.

5. REFERENCES

Adebowale Oladimeji F. [2012] "Bridge Bearings - Merits, Demerits, Practical Merits, Demerits, Practical Issues, Maintenance and Extensive Surveys on Bridge Bearings", PhD Thesis, MSc Thesis , Royal Institute of Technology (KTH), Department of Civil and Architectural Engineering, Division of Structural Engineering and Bridges, Stockholm, Sweden.

Amendola A., Carpentieri G., de Oliveira M., Skelton R.E., Fraternali F. [2014] "Experimental investigation of the softening stiffening response of tensegrity prisms under compressive loading", *Composite Structures*, 117, 234–243.

Ascione L., Fraternali F. [1992] "A penalty model for the analysis of composite curved beams", *Computers & Structures*, 45, 985-999.

Bückmann T., Thiel M., Kadic M., Schittny R., Wegener M. [2014] "An elastomechanical unfeelability cloak made of pentamode metamaterials", *Nature Communications,* 5, 4130.

Daraio, C., Ngo, D., Nesterenko, V.F. , Fraternali, F. [2010] "Highly nonlinear pulse splitting and recombination in a two dimensional granular network", *Physical Review E*, 82, 036603.

Fraternali F. [2007] "Free Discontinuity Finite element models in two-dimensions for in-plane crack problems", *Theoretical and Applied Fracture Mechanics*, 47, 274–282.

Fraternali F., Bilotti G. [1997] "Non-linear elastic stress analysis in curved composite beams", *Computers & Structures*, 62, 837-869.

Fraternali F., Carpentieri G., Amendola A. [2015] "On the mechanical modeling of the extreme softening/stiffening response of axially loaded tensegrity prisms", *Journal of the Mechanics and Physics of Solids*, 74, 136–157.

Fraternali F., Carpentieri G., Amendola A., Skelton R.E., Nesterenko V.F. [2014] "Multiscale tunability of solitary wave dynamics in tensegrity metamaterials", *Applied Physics Letters*, 105, 201903.

Fraternali F., Farina I., Carpentieri G. [2014] "A discrete-to-continuum approach to the curvatures of membrane networks and parametric surfaces", *Mechanics Research Communications*, 56, 18-15.

Fraternali F., Lorenz C.D, Marcelli G. [2012] "On the estimation of the curvatures and bending rigidity of membrane networks via a local maximum-entropy approach", Journal of *Computational Physics*, 231, 528-540.

Fraternali F., Marcelli G. [2012] "A multiscale approach to the elastic moduli of biomembrane networks", *Biomechanics and Modeling in Mechanobiology*, 11 (7), 1097-1108.

Fraternali, F., Senatore L., Daraio C. [2012] "Solitary waves on tensegrity lattices", *Journal of the Mechanics and Physics of Solids*, 60, 1137-1144.

Fraternali F., Spadea S., Ascione L. [2013] "Buckling behavior of curved composite beams with different elastic response in tension and compression", *Composite Structures*, 100, 280-289.

Gurtner G., Durand M. [2014] "Stiffest elastic networks", *Proceedings of the Royal Society of London A*, 470, 20130611.

Higashino M., Hamaguchi H., Minewaki S., Aizawa S. [2003] "Basic characteristics and durability of low-friction sliding bearings for base isolation", *Earthquake Engineering and Engineering Seismology*, 4, 1, 95-105.

Kadic M., Bückmann T., Stenger N., Thiel M., Wegener M. [2012] "On the practicability of pentamode mechanical metamaterials", *Applied Physics Letters,* 100, 191901.

Kelly J.M., Lai J.-W [2011] "The use of tests on high-shape-factor bearings to estimate the bulk modulus of natural rubber", *Seismic Isolation and Protective Systems*, 2, 1, 21-33.

Lu M.H., Feng L., Chen Y.F. [2009] "Phononic crystals and acoustic metamaterials", *Materials Today*, 12, 34-42.

Maldovan M. [2013] "Sound and heat revolution in phononics", *Nature*, 503, 209-217.

Meza L.R., Das S., Greer J.R. [2014] "Strong, lightweight, and recoverable three-dimensional ceramic nanolattices", *Science*, 345, 1322-1326.

Milton G.W., Cherkaev A.V. [1995] "Which Elasticity Tensors are Realizable?", *Journal of Engineering Materials and Technology,* 117, 4, 483-493.

Modano M., Fabbrocino F., Gesualdo A., Matrone G., Farina I., Fraternali F. [2015] "On the forced vibration test by vibrodyne", *CompDyn*, 25-27 May.

Monaldo-Mercaldo J.C. [1995] "Passive and Active Control of Structures", MSc Thesis in Civil and Environmental Engineering, Massachusetts Institute of Technology, USA.

Norris A.N. [2014] "Mechanics of elastic networks". *Proceedings of the Royal Society of London A*, 470, 20140522.

Schittny M., Bückmann T., Kadic M., Wegener M. [2013] "Elastic measurements on macroscopic three-dimensional pentamode metamaterials", *Applied Physics Letters,* 103, 231905.

Schmidt B., Fraternali F. [2012] "Universal formulae for the limiting elastic energy of membrane networks", *Journal of the Mechanics and Physics of Solids*, 60, 172-180.

Zheng X., Lee H., Weisgraber T.H., Shusteff M., Deotte J., Duoss E.B., Kuntz J.D., M. Biener M., Ge Q., Jackson J.A., Kucheyev S.O., Fang N.X., Spadaccini C.M. [2014] "Ultralight, ultrastiff mechanical metamaterials", *Science*, 344, 6190.

RISPOSTA MECCANICA E APPLICAZIONI SISMICHE DI STRUTTURE PENTAMODE

Francesco Fabbrocino[1], Ada Amendola[2], Gianmario Benzoni[3], Fernando Fraternali[2]

[1] Department of Engineering, Pegaso University, Napoli, Italy
[2] Department of Civil Engineering, University of Salerno, Fisciano (SA), Italy
[3] Department of Structural Engineering, University of California San Diego, CA, USA

SOMMARIO: *La categoria dei "metamateriali estremi" è stata introdotta in letteratura per definire materiali che esibiscano, contemporaneamente, modi di deformazione molto "soffici" e modi "rigidi" (materiali unimode, bimode, trimode, quadramode e pentamode, a seconda del numero di modi soffici). Questa definizione può essere applicata a classi speciali di metamateriali meccanici, quali, ad esempio, materiali compositi, schiume strutturali, materiali cellulari, ecc., che siano dotati di proprietà meccaniche speciali, non rinvenibili nei materiali ordinari. Sistemi pentamode sono stati proposti per realizzare l'isolamento dalle onde meccaniche dei corpi ("elasto-mechanical cloak"), mediante avvolgimento del corpo da isolare con membrane elastiche a struttura reticolare pentamode. Tuttavia, il potenziale ingegneristico di tali materiali è stato sinora solo parzialmente esplorato. Il presente lavoro presenta nuove versioni di materiali pentamode, ossia cristalli strutturali artificiali che esibiscano moduli di elasticità tangenziale marcatamente più bassi dei moduli di comprimibilità uniassiale e volumetrica.. Architetture tensegrity sono impiegate per controllare i modi soffici e le proprietà meccaniche dei reticoli pentamode, attraverso l'inserimento di attuatori e cavi precompressi all'interno delle celle unitarie. Tali strutture sono proposte come dispositivi di isolamento sismico di tipo innovativo, che presentino proprietà di isolamento regolabili in base alle proprietà dinamiche struttura da isolare.*

*Corresponding author: Fernando Fraternali, Department of Civil Engineering, University of Salerno, Fisciano, Italy.
Email: f.fraternali@unisa.it

CRITICAL REVIEW OF SEISMIC DESIGN CRITERIA FOR CHEVRON CONCENTRICALLY BRACED FRAMES: THE ROLE OF THE BRACE-INTERCEPTED BEAM

Silvia Costanzo*, Mario D'Aniello, Raffaele Landolfo

Department of Structures for Engineering and Architecture, University of Naples Federico II, Naples, Italy

SUMMARY: *Steel chevron concentrically braced frames are expected to dissipate seismic energy by yielding of the brace under tension, while both beam and columns behave elastically. Besides the strength, also the stiffness of the brace-intercepted beam plays a key role to avoid unfavourable mechanisms. However, no codified requirements are provided to assure adequate beam rigidity. In order to examine this aspect, in the first part of this paper the main results of a numerical parametric study devoted to investigate the mutual interaction between the beam vertical deflection and the brace ductility demand are described. The second part of this article investigates the efficiency of both EC8 and AISC341-10 seismic provisions on the global performance of chevron bracings, particularly focusing on the design of the beam of the braced bays. The results of incremental dynamic analyses performed on several structures confirm the primary importance of the flexural stiffness of the beam.*

KEYWORDS: *Chevron concentrically braced frames, capacity design, stiffness, ductility demand, brace buckling*

1. INTRODUCTION

Chevron concentric bracings (CCBs), also known as inverted-V concentric bracings, are commonly used in the seismic design of multi-storey steel buildings owing to both their architectural functionality and structural efficiency. Indeed, structures equipped with CCBs are generally characterized by large lateral stiffness, which guarantees the fulfilment of both codified drift limitations and stability criteria (namely P-Delta effects). On the other hand, the structural performance against strong seismic action, involving large plastic engagement, is strongly dependent on the design requirements and provisions devoted to assure the achievement of a ductile global failure mechanism.

Differently from other typologies (e.g. X-CBFs or diagonal bracings [Longo *et al.,* 2006; Giugliano *et al.,* 2010; Giugliano *et al.,* 2011; Bosco *et al.,* 2013; Bosco *et al.,* 2014*;* Faggiano *et al*., 2014; Longo *et al.,* 2014; Longo *et al.,* 2015]), the nonlinear response of steel frames equipped with bracings in chevron configuration is deeply affected by the bending-axial force interaction behaviour of the beam connected to the diagonal members [Fukuta *et al.,* 1989; Yamanouchi *et al.,* 1989; Shen *et al.,* 2014; D'Aniello *et al.,* 2015; Shen *et al.,* 2015]. Indeed, following the buckling of the brace in compression, an unbalanced vertical

_____

*Corresponding author: Silvia Costanzo, Department of Structures for Engineering and Architecture, University of Naples Federico II, Naples, Italy
Email: silvia.costanzo@unina.it

force resulting from the axial forces transmitted by both braces is applied on the beam, inducing a significant bending moment at the brace-intercepted section. In such situation the flexural yielding of the beam must be avoided, because it entails significant loss of strength and stiffness. Conversely, larger energy dissipation can be recognized in case of inelastic deformation experienced by the brace under tension, with the beam behaving elastically [Khatib *et al.,* 1989; Tremblay and Robert, 2001].

In light of these considerations, current seismic codes (e.g. EN1998-1, AISC341) provide capacity design criteria to achieve the "strong-beam mechanism". However, analysing the results from literature, it can be observed that in the most of cases, capacity curves of this type of structures are characterized by negative stiffness in post-buckling range and soft storey mechanisms cannot be avoided [Kim and Choi, 2005; Longo *et al.,* 2008]. Moreover, numerical analyses showed very poor seismic performance with tensioned bracings mostly in elastic field, and suffering severe damage in diagonals under compression [Kim and Choi, 2005; Longo *et al.,* 2008].

This poor dissipative behaviour mainly depends on the design rules, which are generally focused on the strength of the beam connected to the bracing members, without accounting for its flexural stiffness. Conversely, the beam flexural stiffness plays a key role in the performance of CCBs, being the flexural response of the beam and the brace deformation in compression correlated phenomena [D'Aniello *et al.,* 2015]. Indeed, as depicted in Fig. 1, the elastic deflection caused by the unbalanced force can be large enough to prevent yielding of the brace in tension and to concentrate the damage in the compression diagonal, thus leading to a very poor overall performance due to the brace deterioration. Recent studies [Shen *et al.,* 2014; D'Aniello *et al.,* 2015; Shen *et al.,* 2015] already underlined that the brace-intercepted beams designed with the minimum possible required strength permitted by seismic codes, could experience severe vertical deflection for interstorey drift ratios ranging in [0.02, 0.04]. Moreover, D'Aniello *et al.* [D'Aniello *et al.,* 2015] show that in frames with very flexible beams, this mechanism becomes dominant and for large drift (e.g. $\theta > 2\%$) both braces are even under compression. Such results were also confirmed in the framework of a recent European research project HSS-SERF RFSR-CT-2009-00024 [Vulcu *et al.,* 2014], aimed at investigating the potential benefits of the combined use of high strength steel for non-dissipative members, and mild-carbon steel for dissipative zones. Indeed, the possibility to use high strength steel for beams leads to over-strong but flexible beams, showing very poor overall performance. Former studies [Marino and Nakashima, 2006; Marino, 2014; Longo *et al.,* 2015] have deeply investigated the seismic performance of CCBs, also proposing new design criteria. However, limited attention was focused on the role of the beam belonging to the braced span. In light of the above considerations, the main aim of this paper is to discuss the seismic behaviour and design criteria for steel chevron concentrically braced frames, with special reference to the design of the brace-intercepted beam. With this regard, in the first part of this article, results carried out by the Authors in previous studies specifically devoted to investigate the role of the beam flexural behaviour, are summarized and further discussed. On the basis of these results, in the second part of this paper, a critical review of seismic design requirements given by EN1998-1 and AISC341-10 for CCBs is provided in order to examine the effectiveness of the relevant provisions in the design of the brace-intercepted beam. To this aim, a reference building was selected as case study and alternatively designed according to both examined codes. Incremental dynamic analyses (IDAs) were performed and the relevant main results are discussed and compared.
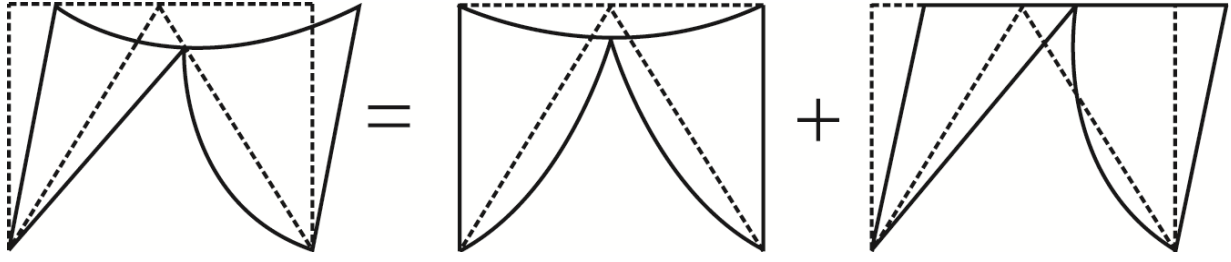
Figure 1. *Shape of lateral displacements for CCBs: a) contribution of the vertical displacements; b) contribution of the horizontal displacements*

2. THE INFLUENCE OF THE BEAM FLEXURAL STIFFNESS

2.1 *Investigated parameters*

D'Aniello et al. [D'Aniello et al., 2015] specifically investigated the influence of the beam flexural stiffness on the seismic performance of CCBs by performing an extent parametric study on a one-storey-one-bay chevron CBF prototype. The examined key parameter is the mutual beam-to-brace stiffness ratio (in the following referred as K_F) ranging from zero to infinitive by varying both geometrical and mechanical properties. The brace-to-beam stiffness ratio was defined according to the Eq. (1):

$$K_F = \frac{k_b}{k_{br}} \tag{1}$$

where k_b is the beam flexural stiffness at the intersection with braces and k_{br} is the vertical stiffness of the bracing members. In particular, the former is given by:

$$k_b = 48\zeta \frac{EI_b}{L_b^3} \tag{2}$$

where E is the elastic modulus of steel, I_b is the second moment of area of the beam section, L_b is the beam length and ζ is a factor depending on the beam boundary condition, namely $\zeta = 4$ for fixed ends and $\zeta = 1$ for pinned ends. The vertical stiffness of the bracings is given by:

$$k_{br} = 2\frac{A_{br}E}{L_{br}} sen^2\alpha \tag{3}$$

where A_{br} is the area of the brace section, L_{br} is the brace length and α is the tilt angle of the brace. In Table 1 all parameters and their relevant variations are summarized and described:

Table 1. *Parameters of variation.*

Parameter	Units	Variations
K_F	[-]	upper bound = ∞ – lower bound = 0
Beam	[-]	IPE (*) – HEA (**) – HEB (**) – HEM (**) upper bound ($k_b = \infty$) – lower bound ($k_b = 0$)
$tg\alpha$ (aspect ratio: tilt of bracing members h/L)	[-]	0.6 – 0.7 – 0.75 – 0.8 – 0.875 – 1 – 1.167 – 1.333
Braces Slenderness ($\bar{\lambda}$)	[-]	0.6 – 0.8 – 1 – 1.2 – 1.4 – 1.6 – 1.8 – 2
Interstorey height (h)	[m]	3 – 3.5 – 4
Span length (L)	[m]	6 – 8 – 10
(*) beam depth from 240 mm to 600 mm (i.e. n. 10 profiles) (**) beam depth from 240 mm to 1000 mm (i.e. n. 18×3 profiles)		

2.2 Monitored mechanical parameters

Both global and local response parameters were selected to characterize the behaviour of CCBs and monitored during each analysis. The monitored parameters are summarized as follow:

- The normalized unbalanced force (β) applied to the beam when the buckling of the brace in compression occurs. This parameter is defined as:

$$\beta = \frac{N_{T,br} - N_{C,br}}{N_{pl,br}}$$ (4)

Where $N_{T,br}$ is the brace axial force in tension; $N_{C,br}$ is the brace axial force in compression; $N_{pl,br}$ is the brace plastic axial strength.

- The brace ductility (μ) both in tension and in compression, given by the ratio d/d_y being d the brace axial displacement and d_y the displacement of the brace at yielding.
- The storey drift ratio (θ_y) corresponding to the brace yielding.
- The beam flexural yielding.

2.3 Discussion of results

Results obtained from both monotonic and pseudo-static cyclic analyses clearly show that the better performance in terms of brace ductility demand, namely yielding in tension and limited damage in compression, is experienced for the structures with the higher values of beam-to-brace vertical stiffness ratio K_F.

This feature can be explained considering that the stiffer the beam, the smaller is its vertical displacement, thus limiting the deformation demand in the brace under compression (see Figs. 1.1 and 2.1). As a general remark, from Fig. 2b it can be observed that the higher the K_F value, the lower is the drift ratio for which yielding occurs. In the cases with $K_F = \infty$ the yielding of the brace in tension occurs at a drift ratio ranging from 0.1 % (for $tg\alpha = 1.33$) to 0.3% (for $tg\alpha = 0.6$).

Monotonic pushover analyses show that $K_F = 0.1$ is the threshold value that delimits two different structural performances. Indeed, for $K_F > 0.1$ brace yielding in tension can be observed at drift ratios within the range of 2-3%, depending on the frame aspect ratio $tg\alpha$ (see Fig. 2b). On the contrary, for $K_F < 0.1$ the bracing does not yield in tension and at large drift ratios (e.g. $\theta > 2\%$) both diagonal elements can be subjected to compression forces.

This behaviour is more evident for very flexible beams ($0 < K_F < 0.02$) (see Fig. 2b). Pseudo-static cyclic analyses confirm these results as shown in Fig. 2c. As it can be observed, the braces in structures with deformable beams are subjected to axial shortening in both directions of the cyclic action. Only for $K_F > 0.02$ the bracings are subjected to alternate tension and compression. Regarding the beam response, the bending demand at the beam mid-length is mainly due to the vertical unbalanced force occurring after the buckling of the brace in compression. As shown in Fig. 3 (where only the case with $tg\alpha = 0.6$ is reported), the plastic hinge develops in the beam at about 2% of drift ratio for all cases with K_F within the range [0.02, 0.1].

For $K_F > 0.1$ the beam tends to behave elastically because increasing the beam stiffness implies enlarging the flexural strength. In addition, at larger K_F both the full yielding of the brace in tension and deterioration of brace in post-buckling range occur; in such condition, the unbalanced force cannot be larger than the value corresponding to the development of the plastic capacity of the connected braces, and the bending moment acting on the beam cannot increase.
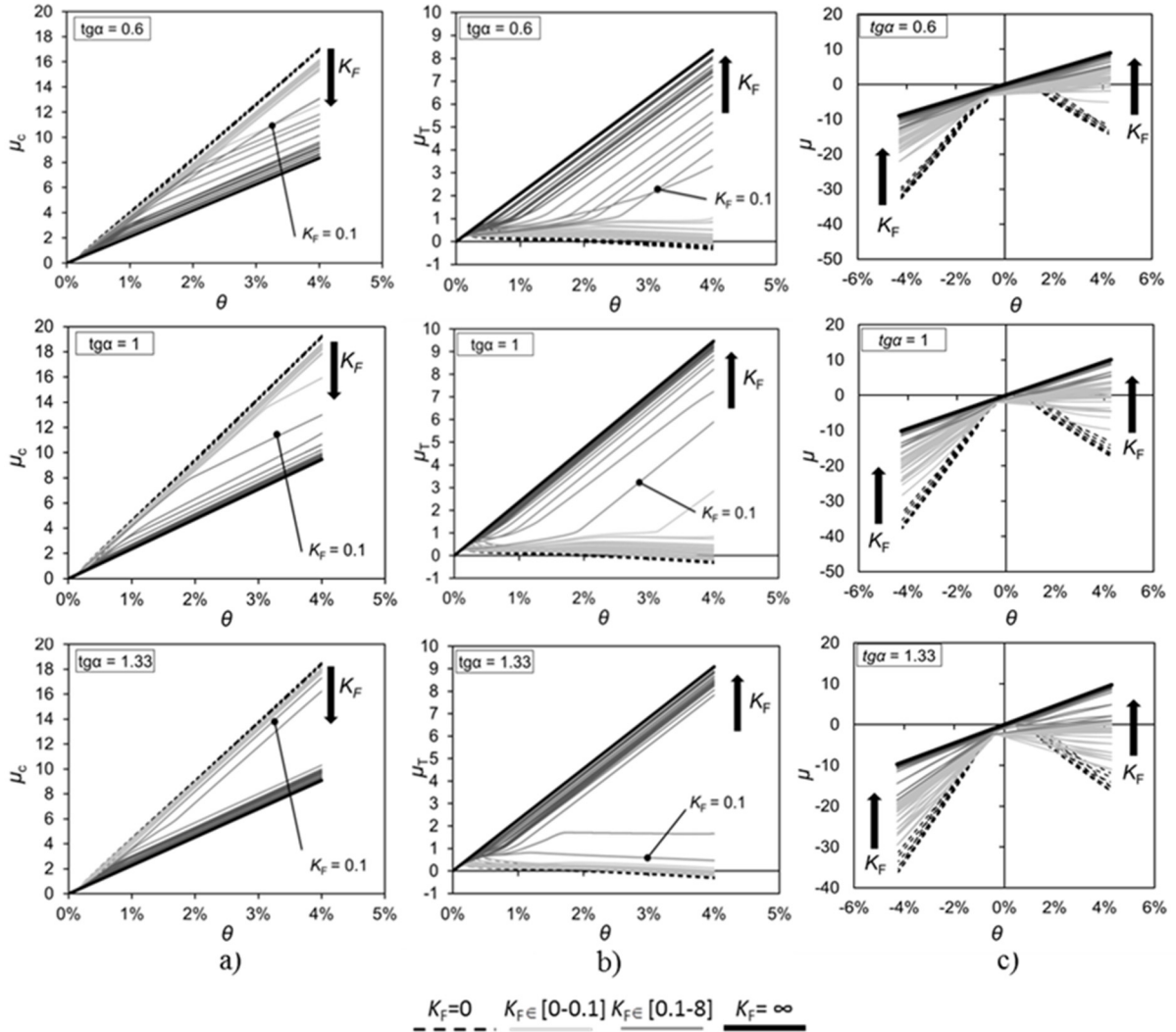
Figure 2. *a) Brace ductility in compression from monotonic analyses; b) brace ductility in tension from monotonic analyses; c) brace ductility from cyclic analyses*

For K_F within the range [0, 0.02] (very flexible beams) the beam behaves elastically even beyond the 4% of drift ratio. This result can be explained considering that both bracing members are under compression and negligible values of the unbalanced force can be developed even at very large storey displacements.

2.4 Empirical equations

On the basis of multiple regression of the numerical results [D'Aniello *et al.,* 2015] shown in Section 2.3, analytical equations were obtained to select the optimal beam stiffness depending on both the brace ductility and interstorey drift ratio demands.

Fig. 4 shows the relationship between the drift ratio corresponding to the yielding of the brace in tension (θ_y) and K_F. The interpolating curve fitting the numerical data is a hyperbolic function given as follows:

$$\theta_y(K_F) = \frac{0.008 \cdot K_F + 0.0013}{1.6 \cdot K_F - 0.08} \qquad \forall K_F \geq 0.1 \qquad (5)$$
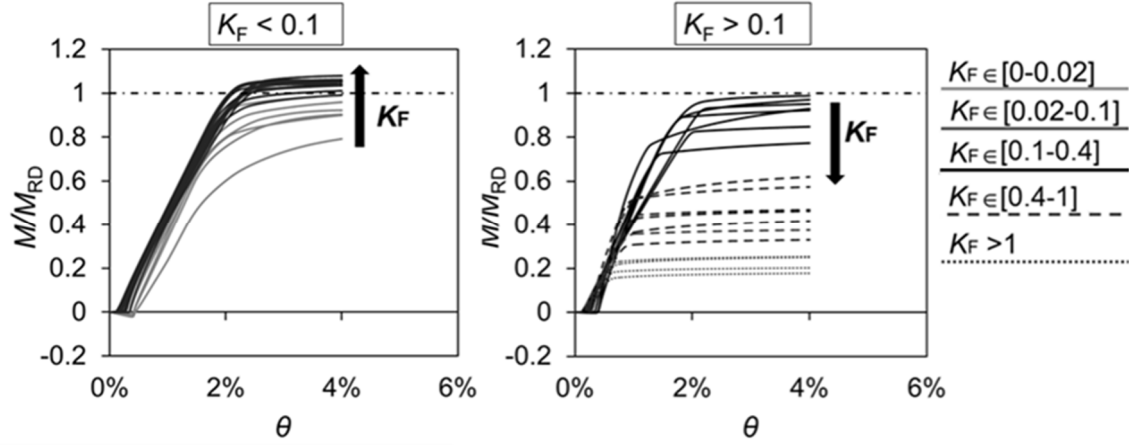
Figure 3. *Beam response: normalised bending moment vs. drift ratio*

This equation is limited to $K_F > 0.1$, because bracing member cannot yield in tension for smaller K_F as previously discussed.

Numerical data for drift ratios in the range of [0.01, 0.04] highlight that the brace ductility demand μ depends on both K_F and $tg\alpha$. As shown in Fig. 5, the ductility demand for the braces in compression and tension is satisfactorily matched by a hyperbolic equation given by:

$$\mu(K_F, \text{tg}\,\alpha, \theta) = \frac{\left[\left(k_3 \cdot \text{tg}\,\alpha^3 + k_2 \cdot \text{tg}\,\alpha^2 + k_1 \cdot \text{tg}\,\alpha + k_0\right) \cdot \theta^2 + \left(p_3 \cdot \text{tg}\,\alpha^3 + p_2 \cdot \text{tg}\,\alpha^2 + p_1 \cdot \text{tg}\,\alpha + p_0\right) \cdot \theta + \left(q_3 \cdot \text{tg}\,\alpha^3 + q_2 \cdot \text{tg}\,\alpha^2 + q_1 \cdot \text{tg}\,\alpha + q_0\right)\right] \cdot K_F + (b_2 \cdot \theta^2 + b_1 \cdot \theta + b_0)}{(c_2 \cdot \theta^2 + c_1 \cdot \theta + c_0) \cdot K_F + (d_2 \cdot \theta^2 + d_1 \cdot \theta + d_0)}$$

(6)

The normalized unbalanced force β (previously defined in Section 2.2) obtained from numerical analyses is plotted against K_F in Fig. 6 The regression function is given by the following:

$$\beta(K_F, \theta) = \frac{a \cdot K_F}{(c_2 \cdot \theta^2 + c_1 \cdot \theta + c_0) \cdot K_F + (d_3 \cdot \theta^3 + d_2 \cdot \theta^2 + d_1 \cdot \theta + d_0)}$$

(7)

The Reader can found the values of the coefficients in Eqs. (6) and (7) and the corresponding R^2 indexes in [D'Aniello *et al.,* 2015].
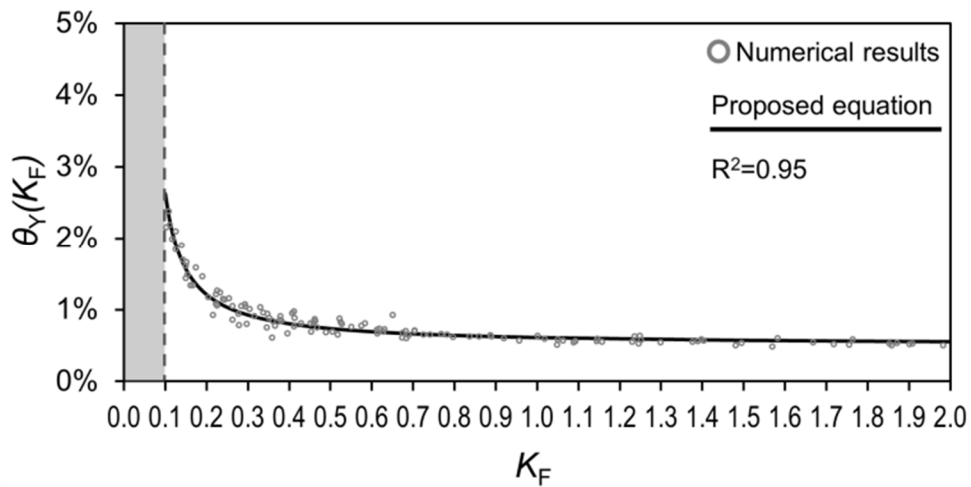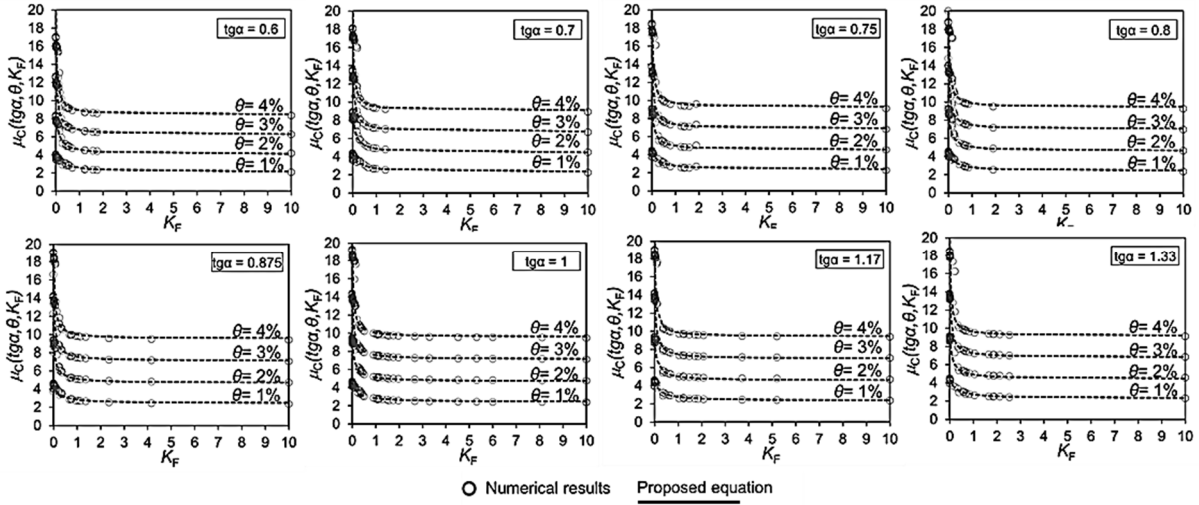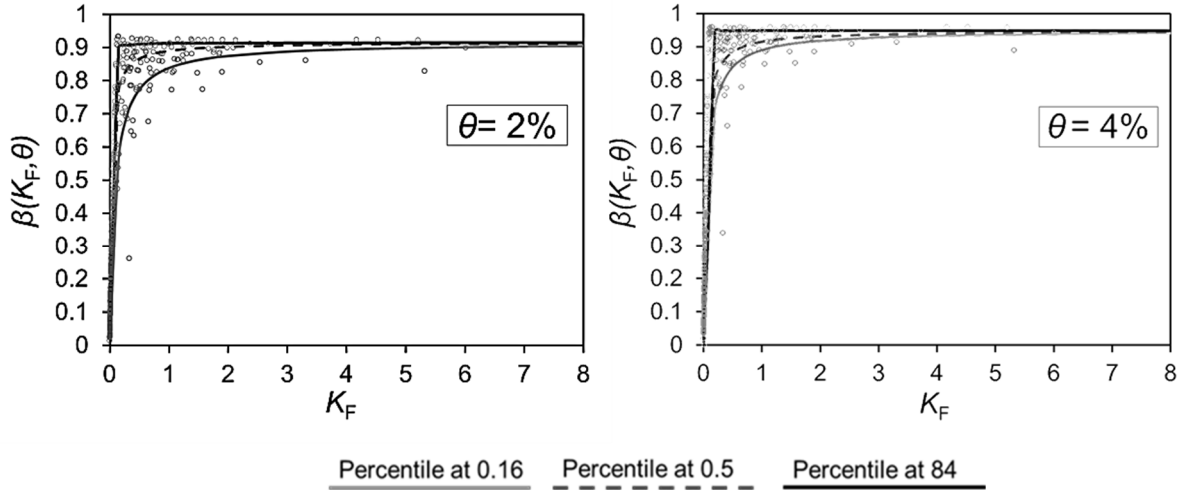

Figure 4. *Brace yielding drift ratio vs. K_F: numerical results and proposed equation*

Figure 5. *Brace ductility demand in compression (μC) vs. KF*

Figure 6. *Unbalanced force β vs. KF (given as example for θ = 2% and θ = 4%)*

It should be noted that the case of *β* = 0.7 corresponds to the unbalance force recommended by EN1998-1 for symmetric CCB configuration. Fig. 6 clearly highlights that in most of cases (those having *β* > 0.7) the requirement of EN1998-1 is not conservative.

3. CODIFIED DESIGN CRITERIA FOR THE CHEVRON BRACED FRAMES: EUROPEAN VS US CODES

3.1 Generality

Even though, both European and US codes are based on capacity design philosophy, different requirements are recommended to guarantee the hierarchy of resistances between dissipative and non-dissipative zones, resulting in dissimilar strength and stiffness ratios between the elements and, as a consequence, different overall response.
Both EN1998-1 and AISC341-10 consider different ductility classes depending on the level of plastic engagement ensured in the dissipative zones and a force reduction factor is assigned

per ductility class in order to directly account for the energy dissipation capacity of the system.

EN1998-1 (in the following also referred as EC8 or Eurocode 8) considers three ductility classes: (i) low ductility class (DCL); (ii) medium ductility class (DCM); (iii) and high ductility class (DCH). In case of DCL poor plastic deformations are expected and the code allows performing global elastic analysis using a behaviour factor q within [1.5, 2.0]; the strength of elements (both members and connections) is verified according to EN 1993:1-1 (Eurocode 3: Design of Steel Structures) without accounting for capacity design rules (recommended just for low seismic areas). On the contrary, systems designed for DCM or DCH are expected to have moderate (a q factor ranging from 2.0 to 4.0 is assumed) or large plastic engagement ($q > 4.0$) in dissipative parts, respectively.

In EN1998-1 CCBs are allowed in DCM and DCH, designed with $q = 2$ and $q = 2.5$ respectively. It is worth to note that it is unclear the reason why the European codes states to assume $q=2.5$ for CCBs in high ductility class, although according to the ductility classification given in EN1998-1 Section 6.1.2, such value of q factor should be adopted for DCM.

AISC 341 provides two different categories based on their expected energy-dissipation capacity: (i) special concentrically braced frames (SCBFs), which are expected to provide significant ductility; and (ii) ordinary concentrically braced frames (OCBFs), characterized by smaller energy dissipation capacity. Similarly to EN1998-1, also for US codes [AISC 341, 2010; ASCE/SEI 7-10, 2010; FEMA P-750, 2009] the behaviour factor (i.e. the reduction factor R) differs with the ductility class, but even larger values are recommended, namely equal to 3.25 for OCBFs and 6.0 for SCBFs.

3.2 Design criteria for brace-intercepted beam

Both European and US codes recommend performing plastic mechanisms analysis in order to evaluate the required strength of the brace-intercepted beam.

Indeed, the beam may experiences the most severe bending moment following the buckling of the compression diagonal. At this stage, an unbalanced vertical force, due to the vertical component of the resultant force transmitted by the tension and compression braces, is applied at the brace-intercepted section.

According to EN1998-1, the beam belonging to the braced bay should be designed to withstand the following action: (i) all non-seismic action without considering the intermediate support given by the diagonal members (ii) the unbalanced vertical force occurring in the post-buckling range. The unbalanced force is evaluated by assuming that the tensioned brace transfers its design plastic resistance ($N_{pl,br,Rd}$) and brace under compression attains its post-buckling compression strength, estimated equal to $\gamma_{pb}N_{pl,br,Rd}$. The value of the reduction coefficient γ_{pb} has to be found in the National annexes; EN 1998-1 recommends $\gamma_{pb}=0.3$.

According to AISC 341, the required strength for beams in SCBFs should be determined by considering the most severe condition between: (i) the seismic induced effects evaluated by performing a linear elastic analysis and magnified by the overstrength factor Ω_o fixed equal to 2; (ii) the forces evaluated by performing plastic mechanism analysis assuming full expected plastic strength (corresponding to $\gamma_{ov}N_{pl,br}$) acting in the brace under tension and the 30% of the expected buckling resistance for the brace under compression (i.e. corresponding to 0.3 $\gamma_{ov}\chi N_{pl,br}$).

It can be easily recognized that both European and US codes recommend similar design rules, but they follow different approaches to quantify the compression strength degradation in the post-buckling range. In particular, EN1998-1 assumes the largest value for the post-buckling compression strength, potentially leading to weaker beams (i.e. a smaller unbalanced force is accounted for). In addition, the rule given by the European codes may lead to evaluate design forces that are inconsistent if very slender brace are used: indeed, for normalized slenderness values close to the upper bound limit ($\bar{\lambda} \leq 2$) stated by the Code, the brace buckling strength tends to the 20% (namely $\chi=0.2$) of the plastic strength, thus resulting smaller than the value proposed for the compression strength in the post-buckling range.

Another important aspect is related to the beam-to-column connections in the braced bays: indeed, US codes requires moment-resisting connections for the braced bays in order to improve the degree of redundancy and enhancing the distribution of damage along the building height; such requirement is absent in the European code in which the redistribution of damage is assured by limiting the range of variation of the overstrength of the braces at each storey. Thereby, the brace-intercepted beams are generally conceived using different boundary conditions, namely: (i) double pinned in the chevron CBFs compliant to EN1998-1 and (ii) fixed at both ends according to AISC 341, thus resulting in significantly stiffer beams respect to the European case.

3.3 Case study

In order to examine the influence on the overall response of the different codified requirements described in the previous Section, a case study was selected and alternatively designed according to both European and US codes.

As shown in Fig. 7, the reference structure is a 2D frame equipped with CCBs extracted from a six-storey residential building with rectangular plan measuring 24 x 24 m (3 bays of 8m span per direction). The interstorey height is equal to 3.50 m with exception of the first floor, which is assumed equal to 4.00 m. Rigid diaphragms are assumed at each floor and circular hollow hot formed sections were used for all diagonal members.

The EC8-compliant frame was designed for DCH (Ductility Class High) concept and a behaviour factor $q = 2.5$ was assumed; the AISC-compliant frame was designed according to the SCBFs (Special Concentrically Braced Frames) concept and a force reduction factor $R = 6$ was adopted. In order to have consistent results allowing a profitable comparison, both cases were designed for the same hazard level, considering a reference peak ground acceleration equal to $a_{gR} = 0.35$ g, a soil type C, a type 1 spectral shape as given by EN1998-1. The members resulting from both EC8 and AISC design procedures are reported in Table 2. It is trivial to observe (see Fig. 8), that the frame designed according EN1998-1 is characterized by stockier braces with intermediate normalized slenderness $\bar{\lambda}$ varying between 0.8 and 1.2. The AISC-compliant case has more slender braces with $\bar{\lambda}$ varying between 1.3 and 2. In addition, the design procedure provided by EN1998-1 also leads to heavier profiles for beams and columns. This difference can be easily explained by considering the smaller value of the force reduction factor accounted for by the European code. Moreover, this difference is further exasperated considering that in the US codes the dissipative members are designed according their "expected" capacities, namely evaluated using the average yield stress of the material, while the design value (namely the characteristic value also reduced by using a proper partial safety factor) is implemented in the calculation of the resistance of diagonal members according to EN1998-1.
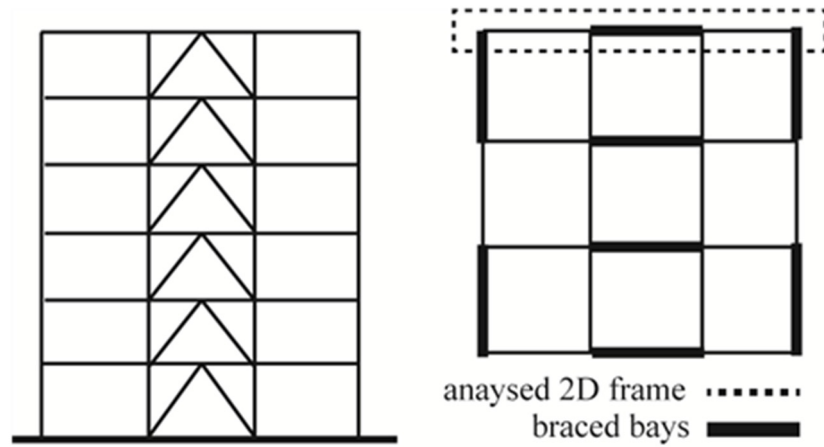
Figure 7. *Structural layout of the examined cases and location of CCBs*

Table 2. *Members of the structures designed according to EN1998-1 and AISC 341*

STOREY	COLUMNS		BEAMS		BRACES (d x t)	
	EC8	AISC	EC8	AISC	EC8	AISC
	S355	*S355*	*S460*	*S460*	*S355*	*S355*
6	HE 400 A	HE 320 A	HE 400 A	HE 360 B	168.3 x 6	139.7 x 5
5	HE 400 A	HE 320 A	HE 450 B	HE 450 B	193.7 x 8	168.3 x 6
4	HE 450 B	HE 360 A	HE 500 B	HE 450 B	219.1 x 10	168.3 x 6
3	HE 450 B	HE 360 A	HE 550 B	HE 500 A	244.5 x 10	177.8 x 6
2	HD 400 x 347•/+	HE 400 M	HE 600 B	HE 500 B	244.5 x 12	177.8 x 8
1	HD 400 x 347•/+	HE 400 M	HE 600 M	HE 550 B	273 x 12	177.8 x 8

However, beside the size of the members, it is interesting to note that, even though the AISC-compliant frame is characterized by smaller cross sections of the members, the relative beam-to-brace stiffness is larger if compared to the European case.
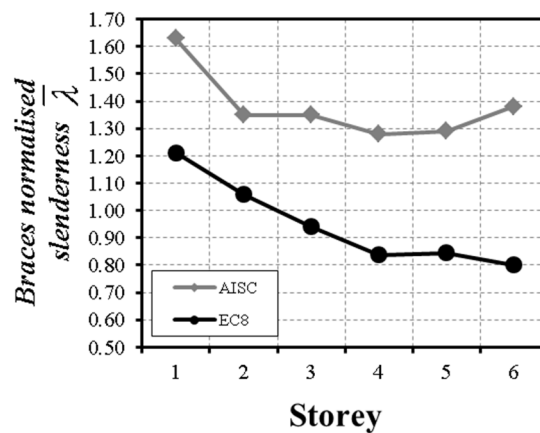

Figure 8. *Normalized slenderness of braces at each storey: comparison between AISC341 and EC8 compliant cases*
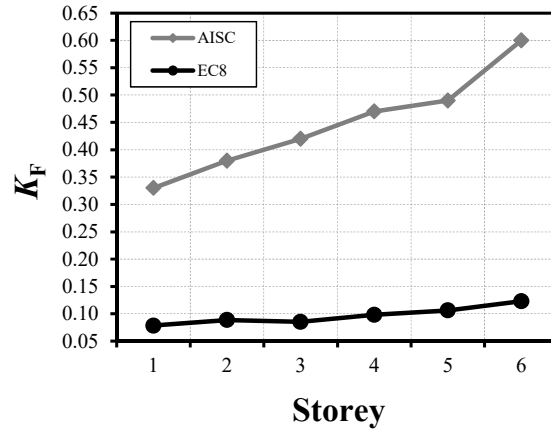
Figure 9. *Beam-to-brace stiffness ratios at each storey: comparison between AISC341 and EC8 compliant cases*

Fig. 9 shows the beam-to-braces stiffness ratios (as defined in Section 2) at each storey for both examined cases. As it can be observed, AISC341-10 leads to the largest values of K_F.

A set of nonlinear dynamic time history analyses was performed in order to investigate the influence of the applied design criteria on the dissipative capacity of the examined CCBs.

A set of 14 natural earthquake acceleration records was selected according to the [Fülöp, 2010] in order to match the elastic acceleration spectrum provided for by EN1998-1. The records were obtained from the RESORCE ground-motion database [Akkar *et al.,* 2014]; the relevant data are summarized in Table 3, and the comparison with the codified elastic spectrum is shown in Fig. 10.

Table 3. *Selected ground motion records data*

| Earthquake name	Date	Station Name	Station Country	Magnitude Mw	Fault mechanism
Alkion	24.02.1981	Xylokastro-O.T.E.	Greece	6.6	Normal
Montenegro	24.05.1979	Bar-Skupstina Opstine	Montenegro	6.2	Reverse
Izmit	13.09.1999	Yarimca (Eri)	Turkey	5.8	Strike-Slip
Izmit	13.09.1999	Usgs Golden Station Kor	Turkey	5.8	Strike-Slip
Faial	09.07.1998	Horta	Portugal	6.1	Strike-Slip
L'Aquila	06.04.2009	L'Aquila - V. Aterno - Aquila Park In	Italy	6.3	Normal
Aigion	15.06.1995	Aigio-OTE	Greece	6.5	Normal
Alkion	24.02.1981	Korinthos-OTE Building	Greece	6.6	Normal
Umbria-Marche	26.09.1997	Castelnuovo-Assisi	Italy	6.0	Normal
Izmit	17.08.1999	Heybeliada-Senatoryum	Turkey	7.4	Strike-Slip
Izmit	17.08.1999	Istanbul-Zeytinburnu	Turkey	7.4	Strike-Slip
Ishakli	03.02.2002	Afyon-Bayindirlik ve Iskan	Turkey	5.8	Normal
Olfus	29.05.2008	Ljosafoss-Hydroelectric Power	Iceland	6.3	Strike-Slip
Olfus	29.05.2008	Selfoss-City Hall	Iceland	6.3	Strike-Slip
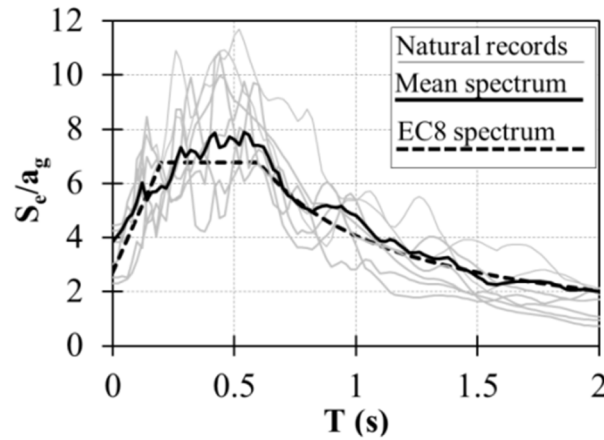
Figure 10. *Comparison between natural signals and EC8 design spectrum*

The analyses were performed by using Seismostruct computational platform [Seismosoft, 2011]. Masses were considered as lumped into a selected master joint at each floor, because the floor diaphragms may be taken as rigid in their planes. The beam section at the brace intersection can deform axially: in such a way, the catenary effect can develop when the beam bends under large deformations. Fiber distributed plasticity elements were used to model beam and column members; the differently-section behaviour is also reproduced by means of the fibre approach, by assigning a uniaxial stress–strain relationship at each fibre. The Menegotto–Pinto (MP) hysteretic model [Menegotto and Pinto, 1973] was selected to simulate the steel behaviour. The average value of yield steel stress was assumed for all members, which was obtained by multiplying the nominal value of the yield stress of the material by the randomness coefficient γ_{ov} (set equal to 1.25 as recommended by EN1998-1). Physical-theory models (PTM) were used to simulate the braces response as reported by [D'Aniello *et al.,* 2013; D'Aniello *et al.,* 2015]. The P–Δ effects were accounted for by assigning the gravity loads on the interior frames to fictitious column, connected to the main frame using pinned rigid links. A 2% Rayleigh tangent stiffness damping was used at both first and second modes. The numerical model was calibrated on the basis of experimental results carried out by Uriz and Mahin [Uriz and Mahin, 2008]. As it can be observed, the simulated behaviour satisfactorily matches the test results, thereby predicting buckling, post-buckling and fractures of braces (see Fig. 11). The seismic performance of the examined cases was compared by monitoring both global (i.e. interstorey drift ratios) and local (i.e. braces ductility demand) response parameters with reference to the three limit states Damage Limitation (DL), Severe Damage (SD) and Near Collapse (NC) defined in EN1998-3. Fig. 12 depicts the average demand of interstorey drift θ along the building height. It should be noted that both EC8 and AISC341 compliant frames experience satisfactorily performance in terms of lateral displacement against earthquake for DL limit state. However, the AISC-compliant frame shows better response, characterized by a more uniform distribution of drift demand along the building height. Indeed, different displacement shapes can be recognized, namely cantilever shape for EC8-compliant case, and shear-type for AISC-compliant frame. Consistently with the relevant displacement shapes, the ductility demand for braces shows different damage distribution (see Fig. 13). It should be noted that the structure designed in compliance with EN1998-1 does not experience any yielding phenomenon in the braces under tension up to NC limit state.
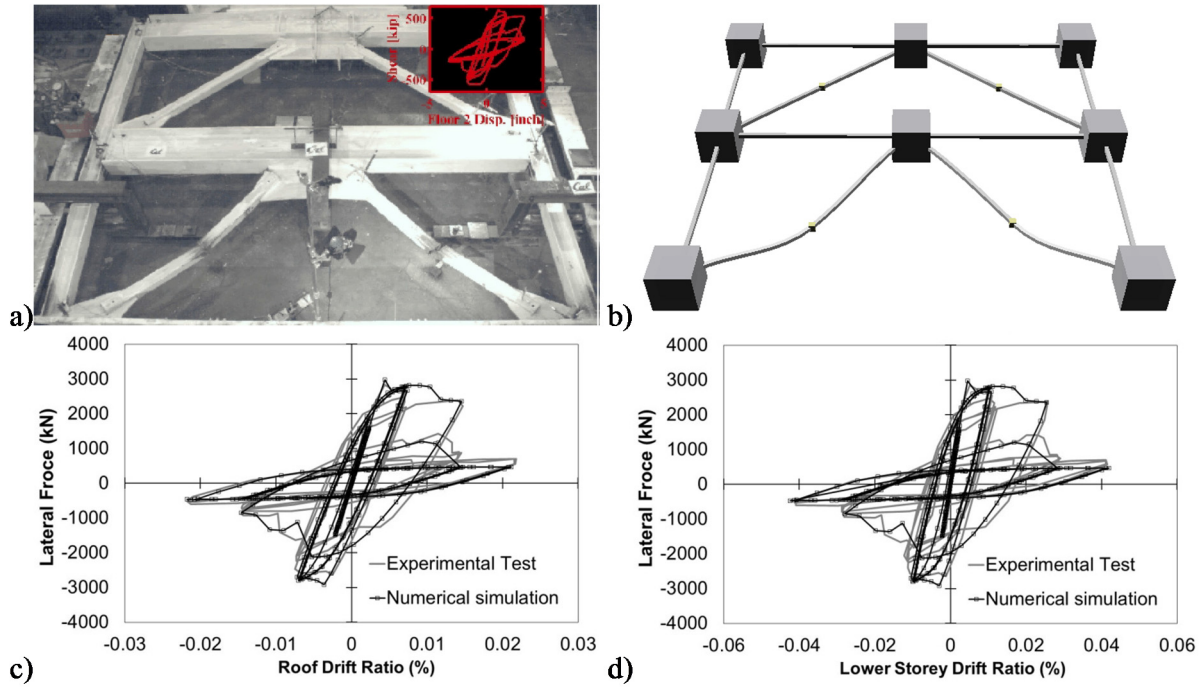
Figure 11. *Numerical vs. experimental cyclic pseudo-static behaviour of the frame tested by Uriz and Mahin (2008)*
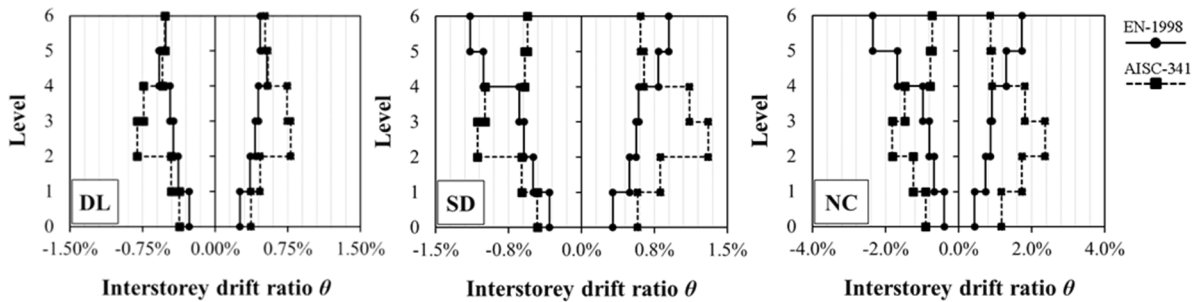

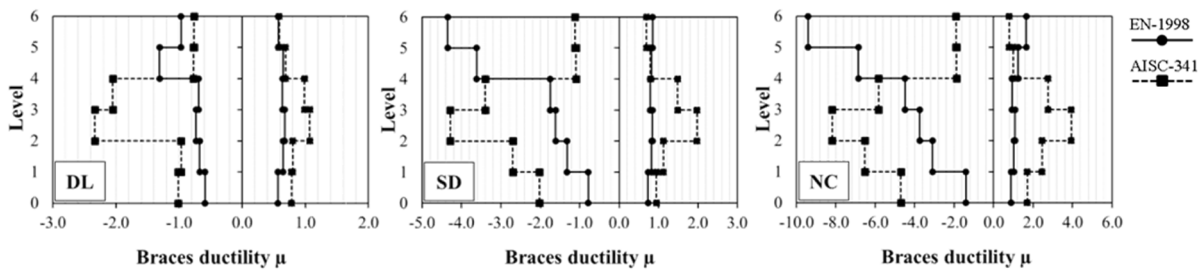Figure 12. *Interstorey drift ratio: EN1998-1 vs. AISC 341-10*

Figure 13. *Braces ductility demand: EN1998-1 vs. AISC 341-10*

On the contrary, plastic deformations under tension can be recognized for the AISC-compliant case even at DL limit state. In addition, the latter also experiences more uniform distribution of damage in compression along the building height. As already mentioned, the requirement on moment resisting beam-to-column connections for braced bay provided by AISC 341, strongly contributes to increase the stiffness of brace-intercepted beams respect to the European case. In order to clarify this aspect, in Figs. 14 and 15 the seismic performance

of AISC-compliant frame is shown by varying the connections typology at the same cross sections of beams. Even though no appreciable differences can be recognized at global level, namely in terms of interstorey drift ratios (see Fig. 14), an improved energy dissipation capacity can be observed for the case with moment-resisting connections, with more plastic engagement for braces under tension and more limited damage under compression (see Fig. 15). However, beside the stiffness of the beams, moment resisting beam-to-column connections in the braced bay also increases the redundancy of the structural system, favouring the distribution of damage along the building height and thus enhancing the global performance. In order to clearly identify which parameter, among K_F and redundancy, mostly affects the response of the system, the performance of AISC-compliant frame was also assessed by varying the connections typology (namely fixed and pinned beams) at the same K_F stiffness ratio. With this aim, a further structure was designed and analysed as follows: AISC 341 provisions were met in the design of both dissipative and non-dissipative elements but the requirement on the moment-resisting connections of the braced bay was disregarded; in addition the beams connected to the diagonals members were designed to have K_F ratios at least equivalent to the values obtained for the AISC-compliant frame with the moment resisting connections (namely for the beams fixed at both ends).
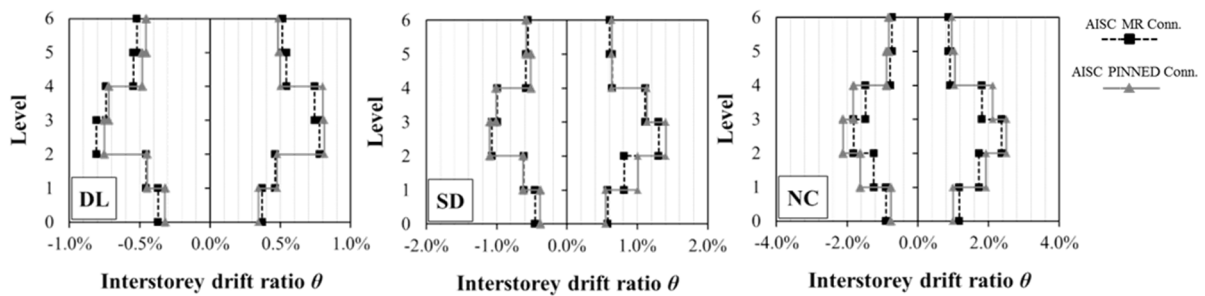

Figure 14. *Interstorey drift ratio: AISC 341, Moment Resisting vs Pinned connection*
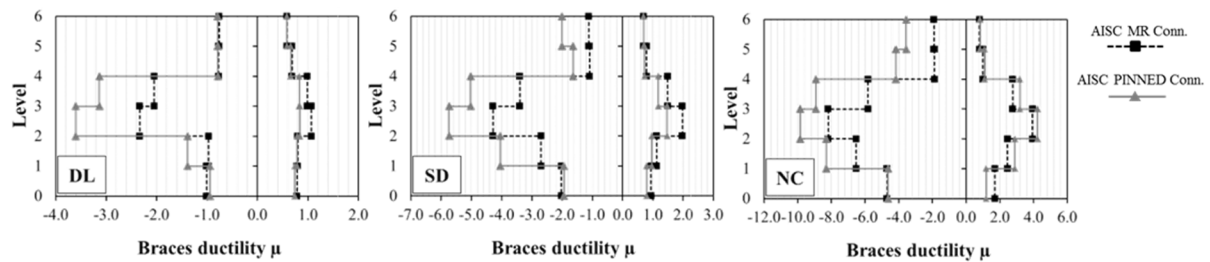

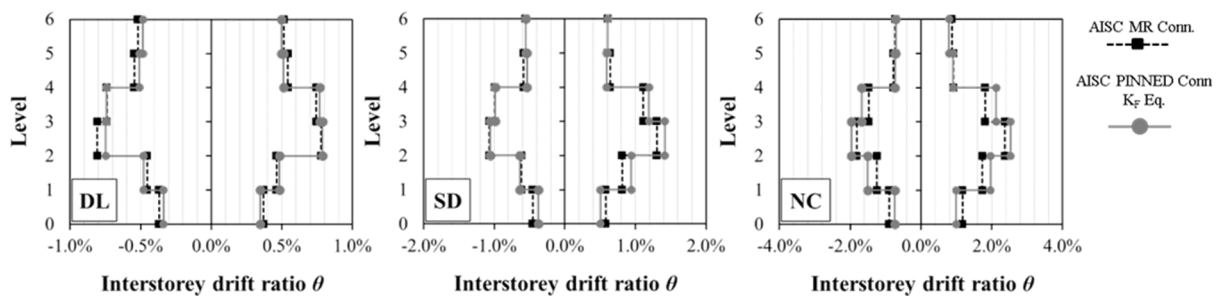Figure 15. *Braces ductility demand: AISC 341, Moment Resisting vs Pinned connection*

Figure 16. *Interstorey drift ratio: AISC 341, Moment Resisting vs Pinned connection with equivalent K_F*
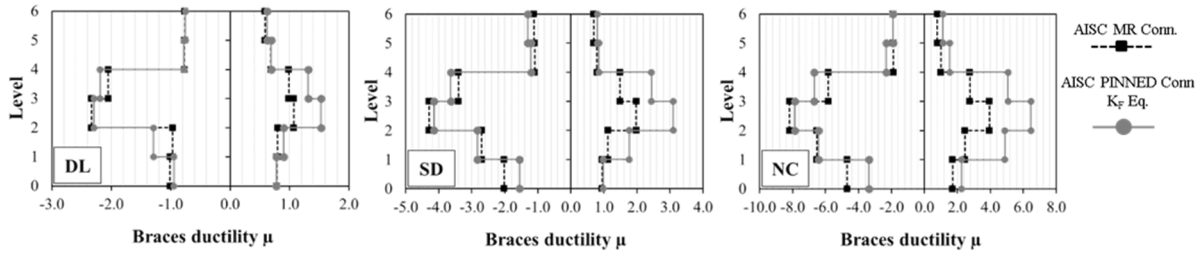
Figure 17. *Braces ductility demand: AISC 341, Moment Resisting vs Pinned connection with equivalent K_F*
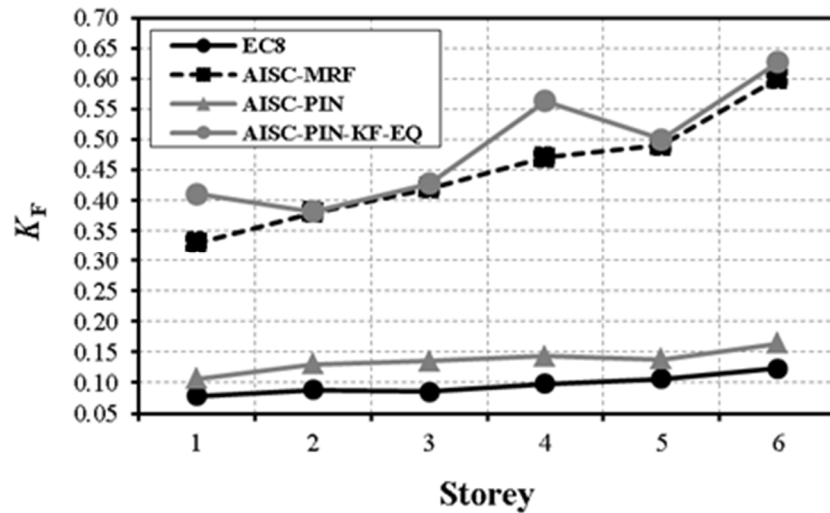

Figure 18. *Examined cases: K_F ratios comparison*

Also in this case (see Fig. 16), no appreciable differences can be recognized at global level, namely in terms of interstorey drift ratio. At local level (see Fig. 17), similar responses can be noted in terms of damage of the braces under compression. However the case with pinned connections exhibits improved plastic engagement in the tension braces even at DL limit state. The enhanced performance can be explained considering that: i) K_F ratios of the pinned-case are slightly larger than those of the fixed-one (see Fig. 18); ii) the pinned-case is slightly more deformable and experiences larger horizontal displacements favouring the elongation of the tension braces at small beams deflection. Therefore, the comparison of the examined cases (Fig. 12-17 and Fig. 18) confirms that the beam-to-brace vertical stiffness ratio K_F is the feature mostly influencing the seismic performance of chevron bracing.

4. CONCLUSION

The design issues influencing the seismic behaviour of chevron concentrically braced frames have been analysed and critically discussed, particularly focusing on the features of the brace-intercepted beams.
In order to specifically investigate the influence of the ratio K_F between the flexural stiffness of the brace-intercepted beam over the axial stiffness of braces on the seismic response of chevron concentrically braced frames, the results of a former parametric study based on

nonlinear monotonic and cyclic analyses [D'Aniello *et al.,* 2015] were described and discussed. The interpretation of numerical data inferred the following remarks:

- The higher the K_F value, the lower is the drift ratio for which yielding occurs. In the cases with $K_F = \infty$ the yielding of the brace in tension occurs at interstorey drift ratio ranging from 0.1 % to 0.3% depending on the tilt angle of the bracing members.
- $K_F = 0.1$ is the threshold value that delimits two different structural performances. For $K_F > 0.1$ the brace yielding in tension can be observed, occurring at interstorey drift ratios within the range 2-3% depending on the tilt angle of the bracing members. On the contrary, for $K_F < 0.1$ the bracing members cannot yield in tension and at larger interstorey drift ratios (e.g. $\theta > 2\%$) both diagonal elements can be subjected to compression. For $0 < K_F < 0.02$ both diagonal members are in compression at any interstorey drift ratio.
- The capacity design rule for beams given by EN1998-1 is not conservative in the most of cases, being the unbalanced force resulting from the analyses larger than the value recommended by the code.
- The numerical analysis results allowed also developing empirical equations able (i) to predict with satisfactory accuracy the brace ductility demand and (ii) the drift ratio corresponding to brace yielding in tension, (iii) to provide the unbalance force acting on the beam of the braced span and (iv) to provide the appropriate beam flexural stiffness for the brace ductility corresponding to the required interstorey drift ratio.
- The provided empirical formulations can be used to control the braces ductility demand and the plastic mechanism at different performance levels. More details about this issue can be found in [D'Aniello *et al.,* 2015].

In light of the main outcomes of the parametric study, the design provisions given by EN1998-1 and AISC341-10 were critically discussed and compared. In order to examine the influence of both codified design criteria, a case study was selected and alternatively designed according to either European or US code. Incremental dynamic analyses were performed on the selected building. The observation of the results led to the following observations:

- The structure designed according to EN1998-1 is generally characterized by stockier braces and heavier cross-sections for beams and columns.
- The beam-to-brace stiffness mutual ratio K_F assumes significantly larger values in the AISC-compliant frame, also due to the requirements on the connections of the braced bays which should be moment-resisting type, thus leading to K_F ratios 4 times larger at the same cross sections of structural members.
- The frame designed according to AISC 341 shows more uniform distribution in terms of interstorey drift ratios, and larger plastic engagement of the braces under tension, respect to the European case.
- Therefore, the comparison confirms that the beam-to-brace vertical stiffness ratio K_F is the design parameter mostly influencing the seismic performance of chevron concentrically braced frames.

5. REFERENCES

Akkar S., Sandıkkaya M.A., Şenyurt M., Azari Sisi A., Ay B.Ö., Traversa P., Douglas J.,Cotton F., Luzi L., Hernandez B., Godey S., [2014] "Reference database for seismic groundmotion in Europe (RESORCE)," *Bulletin of earthquake engineering* **12** (1) (2014) 311–339.

American Institute of Steel Construction, Inc. (AISC) [2010] Seismic Provisions for Structural Steel Buildings. *ANSI/AISC Standard 341-10*. AISC, Chicago, Illinois

ASCE [2010] Minimum design loads for buildings and other structures (ASCE/SEI 7-10), American Society of Civil Engineers, Reston, VA.

Bosco, M., Ghersi, A., Marino, E.M., Rossi, P.P. [2013] "Prediction of the seismic response of steel frames with concentric diagonal bracings*," Open Construction and Building Technology Journal* **7**, pp. 118-128

Bosco, M., Ghersi, A., Marino, E.M., Rossi, P.P. [2014] "A capacity design procedure for columns of steel structures with diagonals braces," *Open Construction and Building Technology Journal* **8**, pp. 196-207

D'Aniello M., Costanzo S., Landolfo R., [2015] "The influence of beam stiffness on seismic response of chevron concentric bracings," *Journal of Constructional Steel Research* **112** 305–324

D'Aniello M., La Manna Ambrosino G., Portioli F., Landolfo R. [2013] "Modelling aspects of the seismic response of steel concentric braced frames," *Steel & Composite Structures, An International Journal* **15**(5): 539-566

D'Aniello M., La Manna Ambrosino G., Portioli F., Landolfo R. [2015] "The influence of out-of-straightness imperfection in Physical-Theory models of bracing members on seismic performance assessment of concentric braced structures" *The Structural Design of Tall and Special Buildings* **24**(3), 176-197, 2015.

EN 1993 [2005] Eurocode 3: Design of steel structures – Part 1-1: General rules and rules for buildings. CEN.

EN1998-1-1 [2005] Eurocode 8: Design of structures for earthquake resistance – Part 1: General rules, seismic actions and rules for buildings. CEN

Faggiano B., Fiorino L., Formisano A., Macillo V., Castaldo C., Mazzolani F.M. [2014] "Assessment of the Design Provisions for Steel Concentric X Bracing Frames with Reference to Italian and European Codes," *The Open Construction and Building Technology Journal* **8**, (Suppl 1: M3): 208-215.

FEMA P-750 [2009] Recommended Seismic Provisions for New Buildings and Other Structures. Federal Emergency Management Agency - U.S. Department of Homeland Security - Building Seismic Safety Council of the National Institute of Building Sciences

Fukuta T., Nishiyama I., Yamanouchi H., Kato B. [1989] "Seismic performance of steel frames with inverted V braces," *Journal of Structural Engineering, ASCE*, **115**(8): 2016- 2028

Fülöp L.A. [2010] "Selection of earthquake records for the parametric analysis," *Research report* VTT-R-03238-10, VTT, Espoo.

Giugliano M.T., Longo A., Montuori R., Piluso V. [2010] "Plastic design of CB-frames with reduced section solution for bracing members, *Journal of Constructional Steel Research* **66** (5) (2010) 611–621.

Giugliano M.T., Longo A., Montuori R., Piluso V. [2011] "Seismic reliability of traditional and innovative concentrically braced frames," *Earthquake Engineering and Structural Dynamics*. **40** (13) (2011) 1455–1474.

Khatib I.F., Mahin S.A., Pister K.S. [1989] "Seismic behavior of concentrically braced steel frames. *Report UCB/EERC-88/01*, Earthquake Engineering Research Center, University of California, Berkeley, CA

Kim J., Choi H. [2005] "Response modification factors of chevron-braced frames," *Engineering Structures* **27** (2005) 285–300

Longo A., Montuori R., Piluso V. [2006] "Failure mode control of X-braced frames under seismic actions, *Journal of Earthquake Engineering* **12** (5) 728–759.

Longo A., Montuori R., Piluso V. [2008] "Plastic design of seismic resistant V-braced frames," *Journal of Earthquake Engineering* **12** (8) 1246–1266.

Longo, A., Montuori, R., Piluso, V. [2015] "Moment frames – concentrically braced frames dual systems: analysis of different design criteria," *Structure and Infrastructure Engineering* **12** (1), pp. 122-141

Longo, A., Montuori, R., Piluso, V. [2015] "Seismic design of chevron braces coupled with MRF fail safe systems" *Earthquake and Structures* **8** (5), pp. 1215-1239

Longo, A., Montuori, R., Piluso, V. [2014] "Theory of plastic mechanism control for MRF CBF dual systems and its validation," *Bulletin of Earthquake Engineering* **12** (6), pp. 2745-2775

Marino E.M. [2014] "A unified approach for the design of high ductility steel frames with concentric braces in the framework of Eurocode 8," *Earthquake Engineering and Structural Dynamics* **43** 97–118.

Marino E.M., Nakashima M. [2006] "Seismic performance and new design procedure for chevron-braced fames," *Earthquake Engineering and Structural Dynamics* **35** (2006) 433–452.

Menegotto M., Pinto P.E. [1973] "Method of analysis for cyclically loaded R.C. plane frames including changes in geometry and non-elastic behaviour of elements under combined normal force and bending," *Symposium on the Resistance and UltimatDeformability of Structures Acted on by Well Defined Repeated Loads.*

Seismosoft [2011] SeismoStruct - A computer program for static and dynamic nonlinear analysis of framed structures. Available from URL: www.seismosoft.com.

Shen J., Wen R., Akbas B. [2015] "Mechanisms in two-story X-braced frames, *Journal of Constructional Steel Research,"* **106** 258–277.

Shen J., Wen R., Akbas B., Doran B., Uckan E. [2014], "Seismic demand on brace-intersected beams in two-story X-braced frames," *Engineering Structures* **76** 295–312.

Tremblay R., Robert N. [2001] "Seismic performance of low- and medium-rise chevron braced steel frames," *Canadian Journal of Civil Engineering*, **28**: 699-714, 2001

Uriz P., Mahin S.A. [2008] "Toward earthquake-resistant design of concentrically braced steel-frame structures," *Pacific Earthquake Engineering Research Center, College of Engineering, Univ. of California, Berkeley* PEER Rep. No.2008/08

Vulcu C., Stratan A., Dubina D., D'Aniello M., Landolfo R., Cermelj B., Beg D., Comeliau L., Demonceau J.F., Long V.H., Kleiner A., Kuhlmann U., Fülöp L.A. [2014] "Guidelines for seismic design and performance based evaluation of dual steel building frames", Deliverable WP6 High Strength Steel in Seismic Resistant Building Frames (HSSSERF) 2014. (Doc. ID: hss-d-0006-wp6-vtt-v13)

Yamanouchi H., Midorikawa M., Nishiyama I., Watabe M. [1989] "Seismic behavior of full-scale concentrically braced steel building structure," *Journal of Structural Engineering, ASCE*, **115**(8): 1917-1929

REVISIONE CRITICA DEI CRITERI DI PROGETTO PER I CONTROVENTI CONCENTRICI A V ROVESCIA: IL RUOLO DELLA TRAVE DELLA CAMPATA CONTROVENTATA

Silvia Costanzo*, Mario D'Aniello, Raffaele Landolfo

Department of Structures for Engineering and Architecture, University of Naples Federico II, Naples, Italy

SOMMARIO: *Le strutture di acciaio con controventi concentrici a V rovescia sono concepite per dissipare l'energia sismica attraverso la plasticizzazione delle diagonali di controvento, mentre sia travi che colonne devono rimanere in campo elastico. Le attuali norme sismiche forniscono regole di progetto al fine di garantire questo tipo di meccanismo plastico in modo da contenere le deformazioni plastiche solo nelle diagonali. Tuttavia, a causa dell'interazione esistente tra la trave ed i controventi ad essa collegati, tali strutture evidenziano una bassa capacità di dissipazione e meccanismi di piano soffice, come confermato da alcuni esistenti studi. Infatti, oltre alla resistenza necessaria per evitare meccanismi di collasso indesiderati, anche la rigidezza flessionale della trave è un parametro molto importante di cui, però, le norme non tengono conto. Al fine di investigare questo aspetto, nella prima parte di questo articolo sono descritti i risultati di uno studio parametrico teso a determinare la relazione che intercorre tra la richiesta di duttilità delle diagonali e la rigidezza della trave. Sulla base di questi risultati, nella seconda parte del lavoro viene investigata l'efficienza delle regole di progetto dettare dall'Eurocodice 8 e dall'AISC341-10 sulla prestazione sismica delle strutture con controventi a V rovescia. In aggiunta, un caso studio è stato progettato alternativamente in accordo ai due codici esaminati e, successivamente, analizzato al fine di valutare l'efficacia dei relativi dettami. I risultati delle analisi dinamiche non lineari condotte sul caso studio confermano il ruolo primario della rigidezza della trave: in particolare emerge che il rapporto K_F tra la rigidezza flessionale della trave e quella assiale delle diagonali è in parametro che influenza maggiormente la prestazione sismica di tali strutture.*

*Corresponding author: Silvia Costanzo, Department of Structures for Engineering and Architecture, University of Naples Federico II, Naples, Italy
Email: silvia.costanzo@unina.it

INFLUENCE OF THE CYCLIC BEHAVIOUR OF BEAM-TO-COLUMN CONNECTION ON THE SEISMIC RESPONSE OF REGULAR STEEL FRAMES

Rosario Montuori, Elide Nastri*, Vincenzo Piluso, Marina Troisi

Department of Civil Engineering, University of Salerno

SUMMARY: *The work presented is aimed at the investigation of the influence of beam-to-column connection typologies on the seismic response of MR-Frames designed according to the Theory of Plastic Mechanism Control (TPMC). The investigated typologies are four partial strength connections designed in order to obtain the same flexural resistance. The first three joints are partial-strength semi-rigid connections while the fourth one is a beam-to-column connection equipped with friction pads properly designed to assure the earthquake input energy dissipation. Beam-to-column joints are modelled by means of rotational inelastic spring elements located at the ends of the beams whose moment-rotation curve is characterized by a cyclic behaviour accounting for stiffness and strength degradation and pinching phenomenon. The parameters characterizing the joints cyclic hysteretic behaviour have been calibrated on the base of experimental results aiming to the best fitting. The prediction of the structural response has been carried out by means of IDA analyses.*

KEYWORDS: *Partial strength connections, dissipation, MRFs, friction dampers, beam-to-column connections*

1. INTRODUCTION

As it is known, modern seismic codes [CEN, 2005] promote the dissipation of seismic input energy by properly designed so-called dissipative zones that are some zones of structural members engaged in plastic range, properly detailed in order to assure wide and stable hysteresis loops [Formisano *et al.* 2006a]. To this scope various design methodology have been proposed [Mazzolani and Piluso, 1997, Castaldo, 2014, De Iuliis and Castaldo, 2012, Castaldo and De Iuliis, 2014, Ferraioli *et al.* 2014a, 2014b, Formisano *et al.* 2013] in order to design dissipative structures. However, it is important to promote the plastic engagement of the greatest number of dissipative zones by properly controlling the failure mode [Montuori *et al.*, 2014a]. As the plastic engagement of columns can lead to non-dissipative collapse mechanisms, modern seismic codes, such as Eurocode 8, suggest the application of the beam-to-column hierarchy criterion which imposes that, at each joint, the flexural strength of connected columns has to be sufficiently greater than the flexural strength of the connected beams. However, it is important to underline that the fulfilment of this design criterion is not sufficient to assure the development of a collapse mechanism of global type, even if, generally, it allows to prevent the occurrence of soft-storey mechanisms.

*Corresponding author: Elide Nastri, Department of Civil Engineering, University of Salerno, Italy.
   Email: enastri@unisa.it

Depending on the beam-to-column joint typology, the dissipative zones can be located at the beam ends or in the connecting elements. In fact, beam-to-column connections can be designed either as full-strength joints, having sufficient overstrength with respect to the connected beam concentrating dissipative zones at the beams ends [Bruneau *et al.*, 1998; Faella *et al.*, 2000; Moore *et al.*, 1999], or as partial strength joints, so that the seismic input energy is dissipated by means of the plastic engagement of one or more joint components properly selected.

The use of rigid full-strength joints has been always considered the best way to dissipate the seismic input energy, that is why seismic codes provide specific design criteria for them, while there are no detailed recommendations dealing with partial-strength connections. However, in the last years there was a significant use of Reduced Beam Section (RBS) [Montuori, 2014, 2015, Kanyilmaz *et al.*, 2015, Castiglioni *et al.* 2012], that consists in the weakening of the terminal part of beams by properly cutting beam ends. Recently, Eurocode 8 has introduced the use of partial-strength joints for dissipating the seismic input energy in the connecting elements of beam-to-column joints because it has been recognized that semi-rigid partial-strength connections, if properly designed by means of an appropriate choice of the joint components where the dissipation has to occur, can lead to dissipation and ductility capacity compatible with the seismic demand.

The use of partial-strength joints, moreover, allows to avoid the plastic engagement of columns without their over-sizing, leading to convenient structural solutions particularly in case of long span MR-Frames [Faella *et al.*, 1997].

However, beam-to-column connection equipped with friction dampers are full-strength joint whose dissipative capacity is demanded to the damping devices located at beam ends that can be equipped with friction pads made by simple steel or coated with other materials such as thermally sprayed aluminum [Latour *et al.*, 2014; Latour *et al.*, 2015]. In this work friction devices are not adopted to provide supplementary energy dissipation [Castaldo et al., 2016a, Castaldo et al., 2016b, Castaldo et al., 2016c, Palazzo *et al.*, 2015, Castaldo and Tubaldi, 2015; Castaldo *et al.*, 2015; Palazzo *et al.*, 2014; Montuori *et al.*, 2014b; Piluso *et al.*, 2014, Longo *et al.*, 2012a, 2012b, De Matteis *et al.,* 2011, Formisano *et al.*, 2006b] but they are rather used to properly substitute the traditional dissipative zones of MR-Frames.

Given the above, the main purposes of this paper are, on one end, the evaluation of the influence of beam-to-column connections on the seismic response of regular MR-Frames, and on the other end, the estimation of the performances of MRFs equipped with the investigated partial strength connections. After a proper calibration of the behaviour of the partial strength connections, the seismic performances of the investigated structures are carried out by means of IDA analyses using Seismostruct computer program.

2. EXAMINED BEAM-TO-COLUMN CONNECTIONS AND THEIR MODELLING

The first three beam-to-column typologies herein investigated are semi-rigid partial-strength connections whose structural detail has been designed by means of the component approach, aiming to obtain the same flexural resistance, but changing the weakest component. Therefore, they are characterized by different locations of the weakest joint component, leading to different values of the joint rotational stiffness and of the plastic rotation supply.

The fourth investigated typology is a beam-to-column connections equipped with friction pads. The use of beam-to-column joints equipped with friction dampers allows to obtain MR-Frames where the dissipative zones are constituted by damping devices located at the beam ends. The reason for investigating these beam-to-column joints is related to the availability of results

dealing with their cyclic rotational response, tested as structural sub-assemblages at the Materials and Structures Laboratory of Salerno University. The structural details of the connections are depicted in Figures 1-4. In order to point out how the cyclic behavior is governed by the location of the structural detail, the tested specimens have been designed aiming to obtain the same flexural strength, but different values of rotational stiffness and plastic rotation supply. The joint non-dimensional resistance $\bar{m}$, given by the ratio between the joint flexural resistance and the beam plastic moment is equal to 0.76 [Iannone *et al.*, 2011]. Specimen EEP-CYC 02 (Figure 1) was designed aiming to obtain the aforementioned value of the non-dimensional resistance and relying on the ductility supply of the end-plate, by properly designing its thickness and bolt location [Piluso *et al.*, 2001]. The first component to be designed is the weakest component, i.e. the end-plate, whose design resistance is obtained as the ratio between the desired joint flexural resistance and the lever arm. Successively, the other components are designed to have sufficient overstrength aiming to avoid their plastic engage. Specimen EEP-DB-CYC 03 (Figure 2) is an extended end-plate connection, whose design is aimed at the investigation of the energy dissipation capacity of beams. However, aiming to obtain the same flexural resistance of the previous specimen, RBS (Reduced Beam Section) strategy, called also "dog-bone", has been adopted. The corresponding structural detail has been designed according to [Moore *et al.*, 1999]. Specimen TS-CYC 04 (Figure 3) is a partial-strength joint with a couple of T-stubs bolted to the beam flanges and to the column flanges and designed to be the main source of plastic deformation capacity. The design goal is to avoid the plastic engage of the components related to the column web panel, the column web in compression/tension and the panel zone in shear. The main advantage of double split tee connections is due to their easy repair. In fact, if the panel zone is designed with adequate overstrength, it is possible to substitute only the end T-stubs after a seismic event. Also in this case the same flexural resistance of the other joints was imposed requiring, in addition, a plastic rotation supply of about 0.08 rad. The plastic deformation supply of the T-stub components has been predicted as suggested by [Piluso *et al.*, 2001]. The last specimen, TS-M2-460-CYC 09, is a bolted double split tee beam-to-column connections equipped with friction dampers designed to slip before the yielding of the beam (Figure 4) where the energy is dissipated through the slippage between the stem of bolted tee stubs and the beam flange with an interposed friction pad [Latour *et al.*, 2012; Latour *et al.*, 2013] which are clamped by means of high strength bolts that allow to apply a constant force on the surfaces in contact by simply governing the value of the tightening torque and the number and diameter of the bolts. In particular, the structural detail depicted in Figure 4 has been subjected to experimental tests at the Material and Structure laboratory of Salerno University [Latour *et al.*, 2012; Latour *et al.*, 2013], by investigating the influence of different materials adopted as friction pads.

In order to evaluate the seismic performance of MRFs it is of preliminary importance to set up an appropriate model to accurately represent the cyclic rotational behavior of connections. In particular, hysteretic behavior of semi-rigid partial strength connections are affected by both the development of strength and stiffness degradation and pinching phenomena as far as the number of cycles increases. As the rules describing these phenomena cannot be deduced by means of theoretical approaches, a sufficient experimental data aiming to develop adequately accurate semi-analytical models are needed where the monotonic envelope is predicted by means of the use of mechanical models based on the component method, while the degradation rules are empirically derived by means of the available experimental results.

Table 1. *First class parameters (strength, stiffness and ductility parameters) of the SHM spring element adopted for modelling the four connection typologies in SeismoStruct*

CONNECTION	Initial Rotational Stiffness	First Yielding Moment	Plastic Moment	Yield Rotation	Ultimate Rotation	Post Yield stiffness ratio as % of elastic
	EI (kN/mm²)	PCP/PCN (kN mm)	PYP/PYN (kN mm)	UYP/UYN (rad)	UUP/UUN (rad)	EI3P/EI3N (-)
EEP-CYC 02	41411466	116463/-130074	157000/-173000	0.01/-0.01	0.04/-0.04	0.0307/0.0352
EEP-DB-CYC 03	47238740	150000/-145000	201000/-207000	0.013/-0.017	0.06/-0.06	0.009/0.001
TS-CYC 04	20000000	185000/-190000	190000/-200000	0.022/-0.022	0.07/-0.07	0.025/0.055
TS-M2-460-CYC 09	30000000	90000/-100000	100000/-120000	0.013/-0.015	0.10/-0.10	0.03/0.03

Table 2. *Second class parameters (Hysteresis shape parameters) of the SHM spring element adopted for modelling the four connection typologies in SeismoStruct*

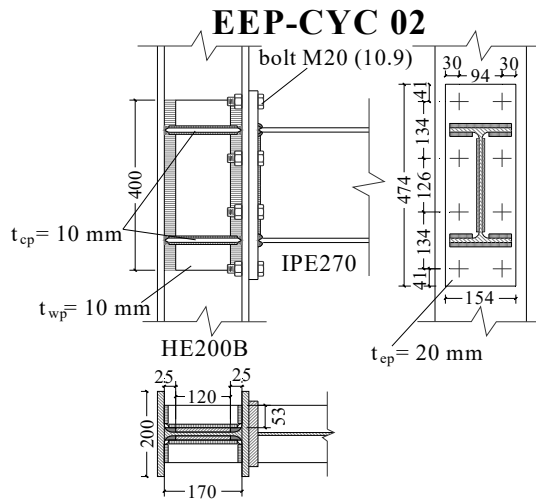| CONNECTION	HC	HBD	HBE	NTRANS	ETA	HSR	HSS	HSM	NGAP	PHIGAP	STIFFGAP
EEP-CYC 02	2	0.001	0.015	1.2	1.8	0.25	0.04	0.51	0.2	0.2	5
EEP-DB-CYC 03	12.5	0.01	0.1	0.75	0.5	0.10	10	1	0.2	0.2	0.2
TS-CYC 04	200	0.003	0.06	1	0.5	0.38	0.2	0.45	0.2	0.2	0.2
TS-M2-460-CYC 09	75	0.10	0.26	5	0.5	0.25	100	0.4	2	1000	2

Figure 1. *Structural details of EEP-CYC 02 connection*
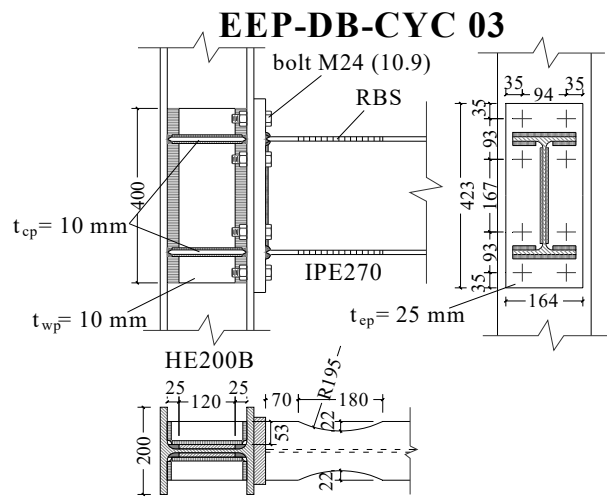
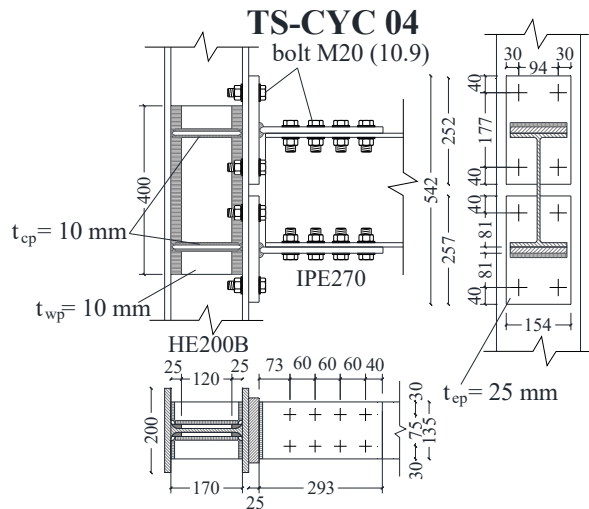

Figure 2. *Structural details of EEP-DB-CYC 03connection*

TS-CYC 04

Figure 3. *Structural details of TS-CYC 04*
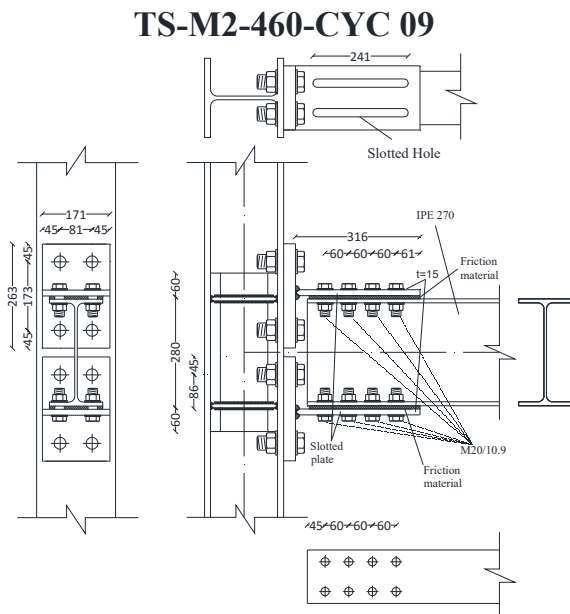
TS-M2-460-CYC 09

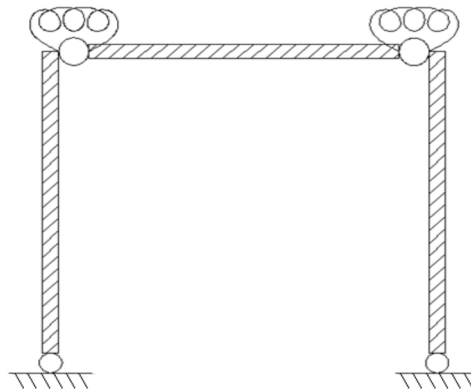Figure 4. *Structural details of TS-M2-460-CYC 09*

Figure 5. *Structural scheme adopted for spring elements calibration*

Therefore, it is possible to apply to such structural model a displacement time-history exactly reproducing that adopted in testing beam-to-column joint sub-assemblages and to compare the cyclic moment-rotation response of the spring element with the one obtained from experimental tests. By properly modifying the parameters modelling strength and stiffness degradation and pinching phenomena, it has been possible to select, for each tested specimen, the connection model leading to the best fitting between the analytical model and experimental test results. In particular, the adopted hysteretic model is the Smooth Hysteretic Model (SHM) [Bouc, 1967; Wen, 1976; Sivaselvan and Reinhorn, 2001; Sivaselvan and Reinhorn, 1999], available in the finite element library of SeismoStruct computer program. The hysteretic behaviour of the rotational spring depends on two class of parameters. The first class is related to the strength, stiffness and rotation parameters, while the second class is related to all the parameters influencing the shape of the hysteresis loops and also the pinching phenomenon.
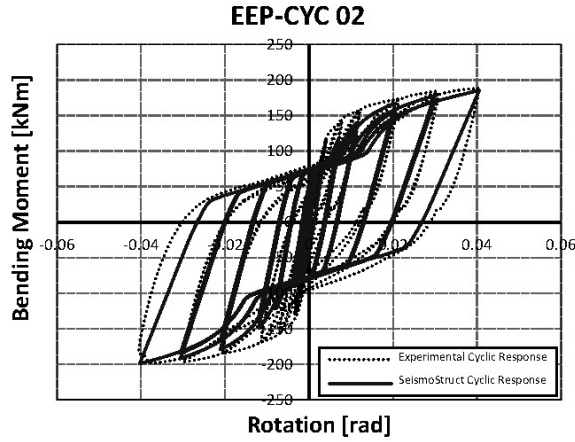
Figure 6. *Comparison between the SHM cyclic moment-rotation response of the spring elements with the experimental tests for EEP-CYC 02 connection*
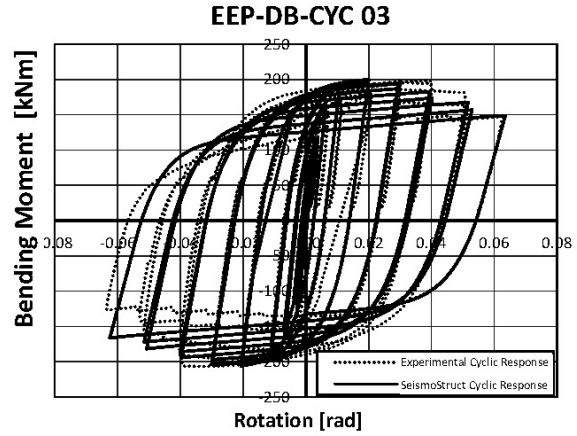
Figure 7. *Comparison between the SHM cyclic moment-rotation response of the spring elements with the experimental tests for EEP-CYC 03 connection*
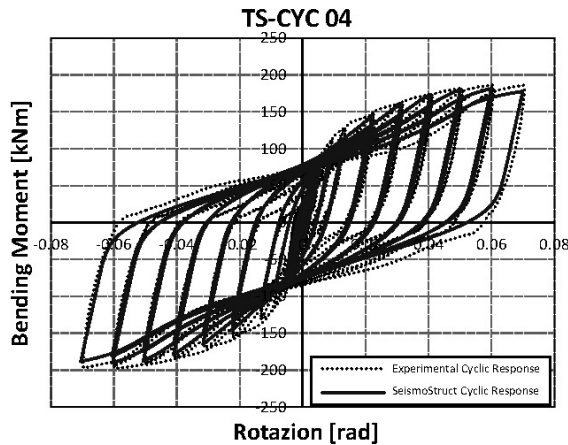

Figure 8. *Comparison between the SHM cyclic moment-rotation response of the spring elements with the experimental tests for TS-CYC 04 connection*
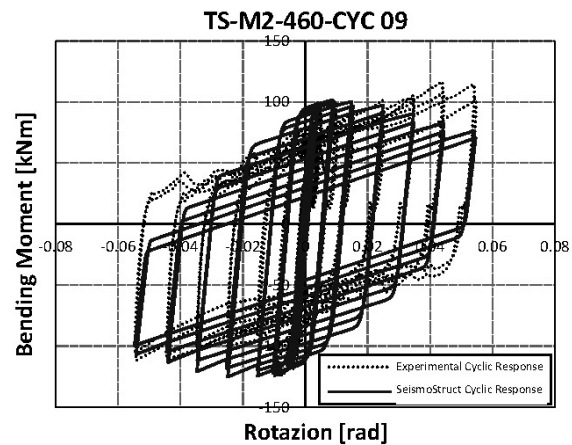
Figure 9. *Comparison between the SHM cyclic moment-rotation response of the spring elements with the experimental tests for TS-M2-460-CYC 09 connection*

In Table 1 all this first class parameters are reported. In particular they are EI (Initial Stiffness), PCP (first yield moment positive), PCN (first yield moment negative), PYP (plastic moment positive), PYN (Plastic Moment Negative), UYP (yield rotation positive), UYN (yield rotation negative), UUP (ultimate rotation positive), UUN (Ultimate Rotation Negative), EI3P (post yield stiffness ratio as a percentage of elastic stiffness positive) and EI3N (post yield stiffness ratio as a percentage of elastic stiffness negative). This class of parameters are also suitable for the Polygonal Hysteretic Model.

As testified by the developed experimental tests, the cyclic response of connections in terms of shape of the hysteresis loops, stiffness and strength degradation and resulting dissipation capacity are directly related to the components involved in plastic range, mainly the weakest component.

For this reason, the non-linear cyclic rotational response of beam-to-column joints has been modelled by means of the spring elements included SeismoStruct (version 5.2) software by properly calibrating parameters on the bases of available experimental results to account for both stiffness and strength degradation and for pinching phenomenon. In order to derive the parameters governing the cyclic response of the spring elements, a cyclic push-over analysis under displacement control has been carried out with reference to the structural scheme depicted in Figure 5, having infinitely rigid beam and column elements, whose feature is that its structural response is dependent on the cyclic response of the spring elements only.

Regarding the second class of parameters, HC locates the pivot point, HBD and HBE represent the measure of strength degradation related to ductility and to energy, respectively. In addition, the SHM model is characterized by smoothing parameters which describe the transition from the elastic branch to the plastic branch of the hysteretic cycle. They are: NTRANS which is the parameter governing the elasto-plastic transition (NTRANS=20 corresponds to a bilinear behaviour), ETA which governs the unloading shapes and HSR, HSS, HSM which are the parameters influencing the pinching phenomenon that are the slip length, the slip sharpness and the parameter for the mean moment level of slip. Finally, NGAP, PHIGAP and STIFFGAP take into account the strength increase for high deformation levels. The parameters describing the hysteretic behaviour of the spring element, adopted in the SeismoStruct model, are delivered in Table 2. In addition, the damage phenomena occurring under cyclic loading conditions have been accounted for by calibrating the corresponding parameters by minimizing the scatter in terms of dissipated energy between experimental test results and numerical results obtained with SeismoStruct spring element. The comparison between the cyclic moment-rotation curve of the tested connections, depicted in Figures 1 to 4 and the corresponding rotational response, predicted by SeismoStruct with the spring element modelling parameters given in Table 1 and Table 2 is provided in Figures 6 to 9. From these figures, it can be observed that SeismoStruct provides a satisfactory degree of accuracy in the modelling of the beam-to-column joint cyclic behaviour.

3. ANALYSED MR-FRAME AND ITS STRUCTURAL MODELLING

In this paper, the influence of the constructional detail of beam-to-column joints on the seismic response of a three bays - six storeys MR-Frames with partial-strength connections is investigated. Regarding the design loads, a uniform dead load (G_k) equal to 12.00 kN/m and a uniform live load (Q_k) equal to 6.00 kN/m are applied. The spans of the longitudinal frames are equal to 6.00 m, while the interstorey heights are equal to 3.20 m with the exception of the first storey whose height is equal to 3.50 m. The uniform vertical load adopted for beam design is $q = 1.3G_k + 1.5Q_k = 25.20\ kN/m$. A design value of the beam plastic moment approximately equal to $qL^2/8$ has been chosen and IPE270 profiles made of S275 steel grade have been adopted for the beams. The size of the columns of both regular and irregular structures are selected by adopting a rigorous design procedure assuring a collapse mechanism of global type [Montuori *et al.*, 2014].

Table 1. *Mechanical properties of members*

	$f_{y,f}$ [N/mm²]	$f_{u,f}$ [N/mm²]	$f_{y,w}$ [N/mm²]	$f_{u,w}$ [N/mm²]
Column	430	523	382.5	522
Beam	405	546	387	534
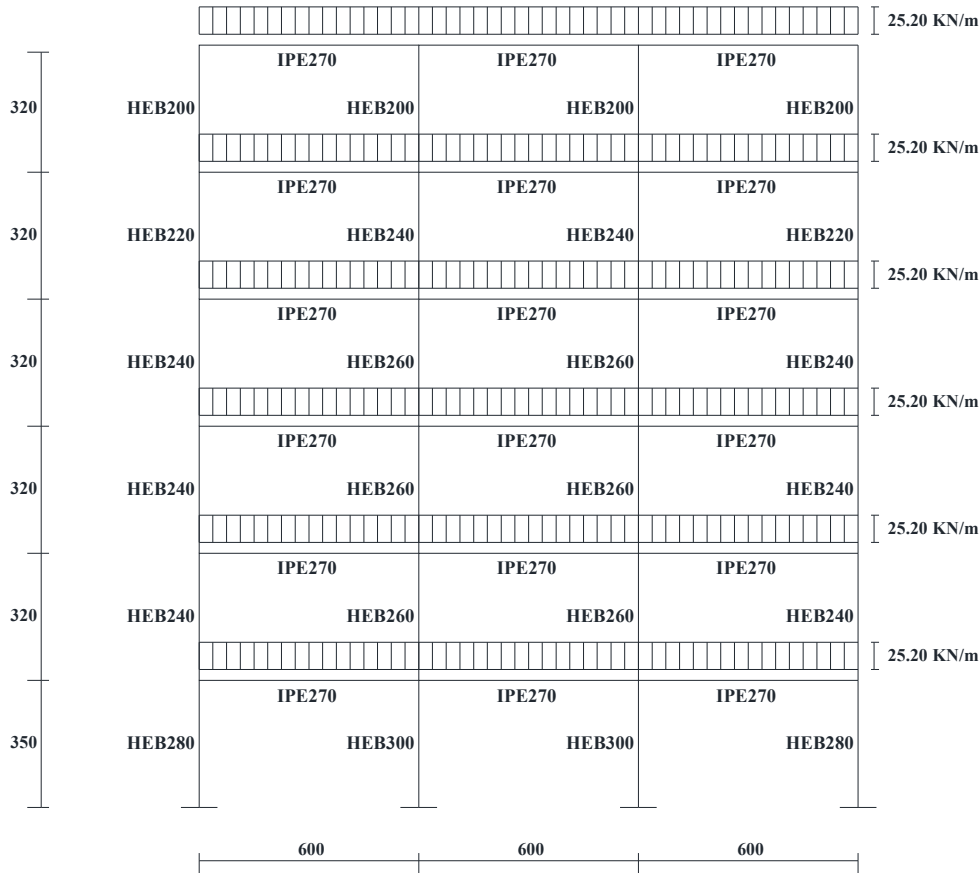
The whole design procedure has been carried out with reference to S275 steel grade. However, in order to assure a frame structural response consistent with the joint rotational behavior obtained from experimental tests and modeled as preliminarily described, the values of column and beam material mechanical properties to be adopted in non-linear dynamic analyses are assumed to be equal to those measured in testing beam-to-column joint sub-assemblages and reported in Table 1.

4. INFLUENCE OF BEAM-TO-COLUMN JOINTS ON SEISMIC RESPONSE

Regarding beam and column elements, a bilinear model characterized by a hysteretic behavior with no stiffness degradation, no ductility-based strength decay, no hysteretic energy-based decay and no slip has been considered. However, it is useful to underline that this issue is not significant, because the use of partial-strength connections leads to the concentration of yielding at connections, so that only the connection modeling is of primary importance.

The seismic performances of the examined MR-Frame with the four structural details of beam-to-column connections are investigated by means of non-linear dynamic analyses, carried out by means of SeismoStruct computer program, for increasing levels of the seismic intensity measure. Record-to-record variability is accounted for performing Incremental Dynamic Analyses considering ten earthquake records selected from PEER database. Mass and stiffness proportional damping, 3% of critical value, has been assumed.

Aiming to perform an IDA, all the records have been properly scaled to provide increasing values of the spectral acceleration $S_a(T_1)$ corresponding to the fundamental period of vibration of the structure, equal to $T_1=1.6$ sec for connections EEP-CYC 02 and EEP-DB-CYC 03 and equal to $T_1=1.7$ sec for connection TS-CYC 04 and TS-M2-460-CYC-09. In particular, the analyses have been repeated increasing the $S_a(T_1)/g$ until the target collapse value corresponding to the attainment of the experimental ultimate value of the plastic rotation supply of EEP-CYC 02, EEP-DB-CYC 03 and TS-CYC 04 connections and the target interstorey drift for TS-M2-460-CYC-09 connection (Table 2).

Table 2. *Ultimate rotation of EEP-CYC 02, EEP-DB-CYC 03, TS-CYC 04 connections and ultimate interstorey drift of TS-M2-460-CYC 09 connection*

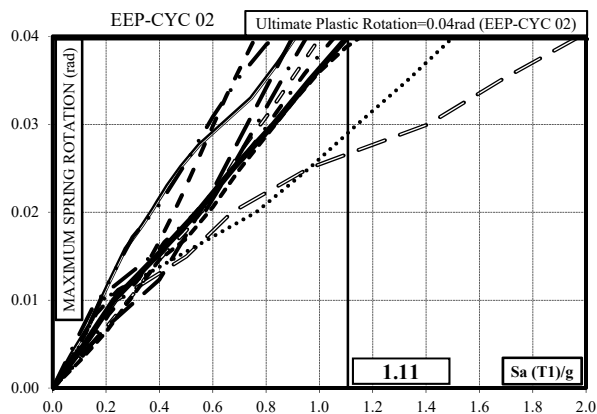|	**Ultimate Rotation (rad)**
EEP-CYC 02	0.04
EEP-DB-CYC 03	0.06
TS-CYC 04	0.07
	Ultimate interstorey drift (rad)
TS-M2-460-CYC 09	0.10

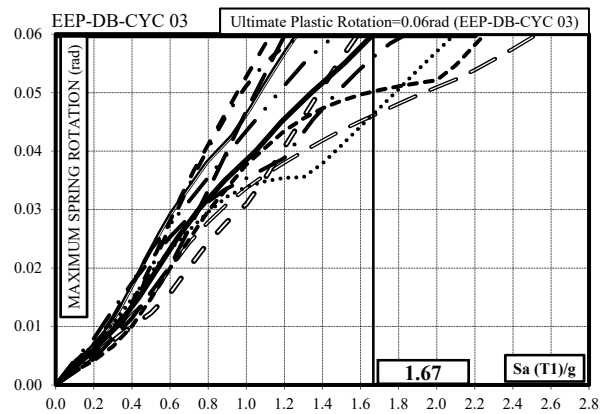Figure 11. *Maximum Spring Rotation vs Spectral Acceleration for EEP-CYC 02 connection*

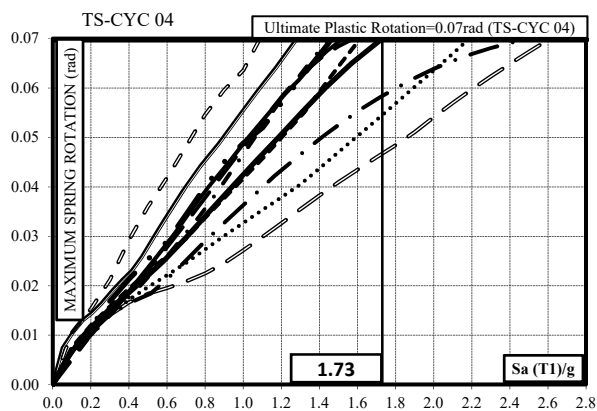Figure 12. *Maximum Spring Rotation vs Spectral Acceleration for EEP-CYC 03 connection*

Figure 13. *Maximum Spring Rotation vs Spectral Acceleration for TS-CYC 04 connection*
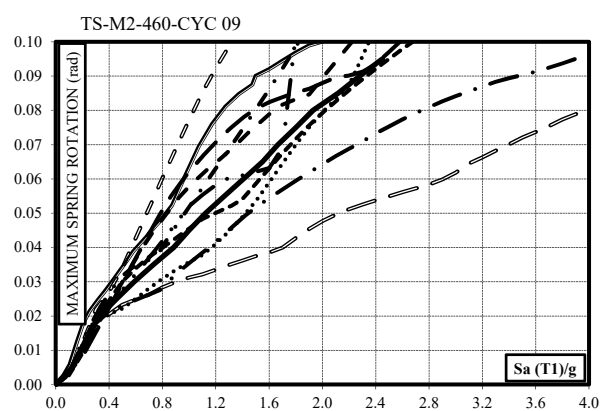

Figure 14. *Maximum Spring Rotation vs Spectral Acceleration for TS-M2-460-CYC 09 connection*

The target Maximum Interstorey Drift (MIDR) has been assumed as 0.1 according to FEMA [FEMA 351, 2000, FEMA 352, 2000] for the Near Collapse Limit State. Scaling the records at the same value of S_a gives the possibility to reduce the variability of structural seismic response. In Fig. 11 to Fig. 14, Maximum Spring Rotation for increasing values of the spectral acceleration are reported. IDA analyses have been stopped for EEP-CYC 02, EEP-DB-CYC 03 and TS-CYC 04 connections when the first dissipative element achieve the ultimate available rotation reported in Table 2. This operation cannot be performed for the TS-M2-460-CYC 09 for which the collapse condition is achieved for the target MIDR equal to 0.1. With reference to the first three connections, IDA analyses in term of maximum spring rotation show the dependence from the earthquake record and, first of all, from the available ductility supply of the connection. It can also be observed that such results are a combination of the effects due, on one hand, to the plastic rotation supply of connections and, on the other hand, to the quality and stability of the hysteresis loops. In addition in Figures 15 to 18 the maximum interstorey drift ratio (MIDR) versus spectral acceleration curves are reported for the different earthquake records. The behavior of the structures is similar. This is probably due to the design method adopted for the analyzed MR-Frame which is devoted to assure a collapse mechanism of global type. This type of collapse mechanism leads to a structural damage well distributed among the different storeys. Finally, the seismic performances of the analyzed structure in term of maximum spectral acceleration for the achievement of the available ductility of the connections are reported in Table 4 where the average value of the spectral acceleration for each connection typology are considered.

Generally speaking, TS-CYC 04 and EEP-CYC 03 connections leads to good seismic performances as testified by Fig. 19 and Fig. 20. This result is justified because TS-CYC 04 connection assured the higher ductility capacity in term of plastic rotation (Table 2) which is able to redeem the significant pinching effect. From its side EEP-DB-CYC 03 connection show a lower plastic ductility supply if compared with the TS-CYC 04 connection but more stable hysteresis loops. However, the average best behavior is assured by the connection namely TS-M2-460-CYC 09 showing the best performances both in term of maximum plastic rotation than MIDR. However, taking into account the results of each selected ground motion, it is possible to observe that the structures equipped with friction dampers show the best performances with the only exception of Santa Barbara earthquake (terms underlined in Table 4) being assumed an ultimate interstorey drift equal to 0.1 at CP limit state. In addition, it is important to observe that after the achievement of the maximum device stroke the collapse did not occur because of the activation of new resistant mechanism as the shear resistance of bolts.

Conversely, the worst seismic performances are always obtained in case of extended end plate connections (EEP-CYC02). As the motivation making EEP-CYC02 the worst, it is useful to remember that, during the experimental test, being the displacement amplitude increased, the plastic engagement of the end-plate at the welded flange-to-end plate connection zone increases, leading to the formation of a crack along the whole width of the end-plate starting from the heat affected zone which progressively propagated along the thickness up to the complete fracture of the end-plate [Iannone *et al.*, 2011]. Even though this failure mode is consistent with the design purposes of type-1 collapse mechanism for the end-plate in bending, it provides a reduction of the plastic rotation supply under cyclic loads.
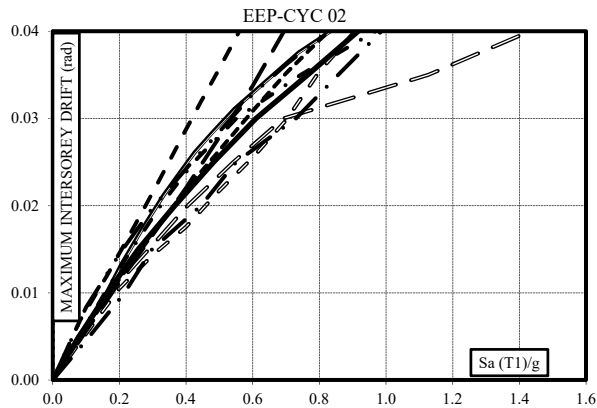
Figure 15. *Maximum Interstorey Drift Ratio vs Spectral Acceleration for TS-CYC 04 connection*
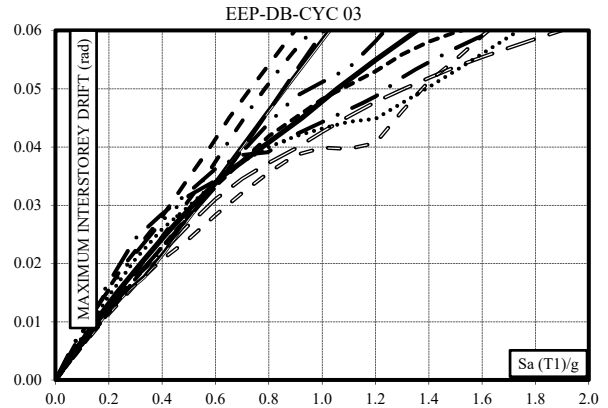

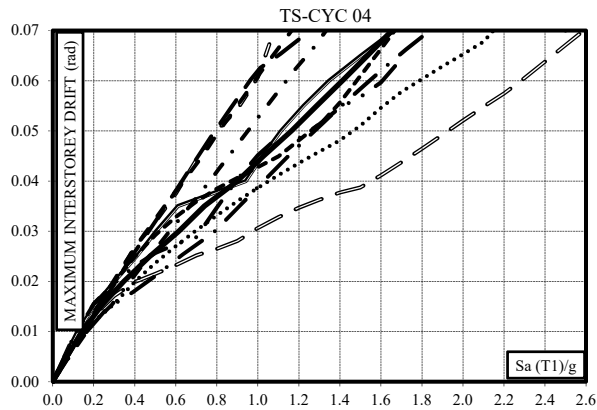Figure 16. *Maximum Interstorey Drift Ratio vs Spectral Acceleration for EEP-CYC 03 connection*

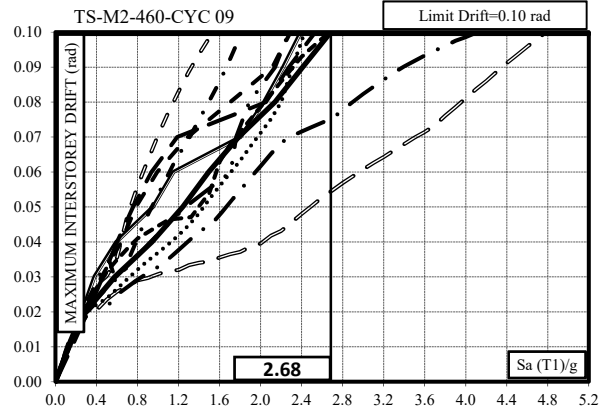Figure 17. *Maximum Interstorey Drift Ratio vs Spectral Acceleration for EEP-CYC 02 connection*

Figure 18. *Maximum Interstorey Drift Ratio vs Spectral Acceleration for TS-M2-460-CYC 09 connection*

Table 3. *Spectral acceleration corresponding to the achievement of the connections ultimate plastic rotation of each considered earthquake record*

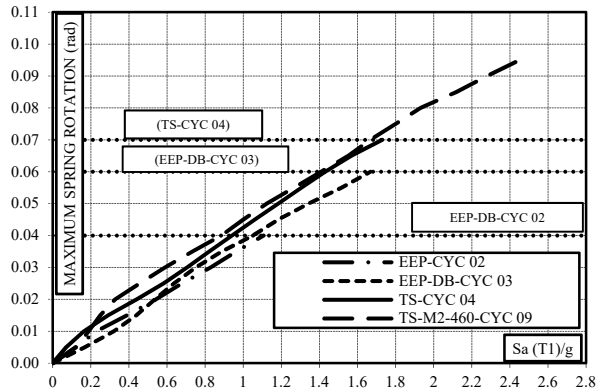| Earthquake	EEP-CYC 02	EEP-DB-CYC 03	TS-CYC 04	TS-M2-460-CYC 09
Coalinga	1.16	2.25	1.61	<u>2.67</u>
Imperial Valley	0.76	1.13	1.52	<u>2.29</u>
Northridge	0.91	1.27	1.29	<u>2.39</u>
Spitak Armenia	1.06	1.30	1.45	<u>1.82</u>
Victoria Mexico	0.90	1.20	1.58	<u>2.53</u>
Kobe	0.95	1.84	2.50	<u>4.11</u>
Friuli	1.98	2.53	2.61	<u>4.78</u>
Helena	0.84	1.48	1.47	<u>2.28</u>
Santa Barbara	1.00	<u>1.59</u>	1.09	1.54
Irpinia	1.50	2.09	2.19	<u>2.43</u>
Average Sa(T_1/g)	**1.11**	**1.67**	**1.73**	**2.68**

Figure 19. *Comparison between Maximum Spring Rotation vs Spectral Acceleration for the four considered connections*
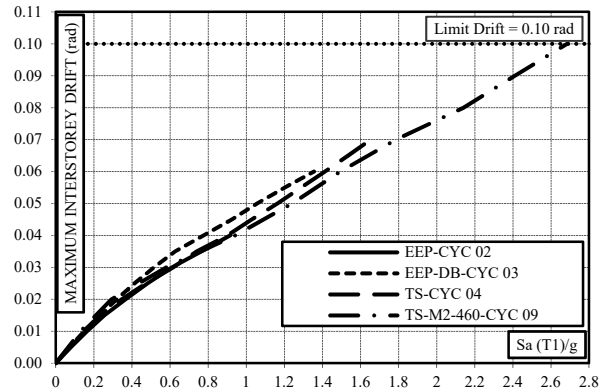
Figure 20. *Comparison between Maximum Interstorey Drift vs Spectral Acceleration for the four considered connections*

5. CONCLUSIONS

Partial-strength connections offer a number of advantages if compared with full strength connections because the yield point may be controlled in the design process leading to lighter beams and columns. From their side, semi-rigid partial-strength connections if well designed, own enough ductility and dissipation capacity in order to satisfy the seismic demand leading to hysteresis loops properly wide and stable.

In this paper the influence of partial strength beam-to-column connections on the seismic response of regular MR-Frames has been studied. Starting from the knowledge of the cyclic rotational behaviour of beam-to-column joints, four different MR-Frames have been considered. The first three are semi-rigid connections while the last one is a full rigid connection equipped with friction dampers. Each structure is characterized by a different structural detail of beam-to-column connections. The cyclic behaviour of each joint has been modelled by means of the spring element of Seismostruct computer program with the smooth hysteretic model whose parameters have been calibrated on the base of available experimental tests obtaining a good agreement between experimental and modelled behaviour. The observation of the results obtained from IDA performed by means of Seismostruct shows that the behaviour of the analysed MR-Frames equipped with TS-CYC04 connections, i.e. bolted double split tee connections, is comparable to the one of the MR-Frame equipped with EEP-DB-CYC03 connections, i.e. bolted extended end-plate connection with RBS. The worst performances are achieved by EEP-CYC02 connection while it is possible to conclude that MRF equipped with friction dampers constitute the more suitable solution for destructive earthquake exhibiting the best performances as testified by the spring rotation and MIDR results. Additional comparisons between the behavior of MR-Frames regular and with "set-backs" investigating the same connection typologies herein presented are reported in a previous work [Montuori *et al.*, 2016].

6. REFERENCES

Bouc, R. [1967], "Forced Vibration of Mechanical System with Hysteresis." Proc., 4-th Conf. on Nonlinear Oscillations.

Bruneau, M., Uang, C. M., and Whittaker, A. [1998] "Ductile Design of Steel Structures", *McGraw Hill*, New York.

Castaldo P, Palazzo B, Della Vecchia P., [2015] "Seismic reliability of base-isolated structures with friction pendulum bearings", *Engineering Structures*, Vol. 95, 80-93.

Castaldo P, Tubaldi E. [2015] "Influence of FPS bearing properties on the seismic performance of base-isolated structures", *Earthquake Engineering and Structural Dynamics* 2015; Vol. 44, 2817–2836.

Castaldo P. [2014] "Integrated Seismic Design of Structure and Control Systems", *Springer International Publishing: New York*, 2014. DOI 10.1007/978-3-319-02615-2.

Castaldo P., De Iuliis M., [2014] "Optimal integrated seismic design of structural and viscoelastic bracing-damper systems", *Earthquake Engineering and Structural Dynamics*, Vol. 43(12),1809–1827.

Castaldo, P., Amendola, G. & Palazzo, B. [2016a]. Seismic reliability-based design of structures isolated by FPS. ECCOMAS Congress2016, Crete Island, Greece, 5–10 June 2016.

Castaldo P., Palazzo B., Della Vecchia P. [2016b] "Life-cycle cost and seismic reliability analysis of 3d systems equipped with FPS for different isolation degrees," Engineering Structures, *http://dx.doi.org/10.1016/j.engstruct.2016.06.056*.

Castaldo, P., Palazzo, B., Perri, F., Marino, I., Faraco, M.M. [2016c]. Seismic retrofit of existing buildings through the dissipative columns. ECCOMAS Congress2016, Crete Island, Greece, 5–10 June 2016.

Castiglioni, C.A., Kanyilmaz, A., Calado, L [2012] Document Experimental analysis of seismic resistant composite steel frames with dissipative devices*, Journal of Constructional Steel Research* 76, pp. 1-12

CEN [2005] "EN 1998-1-1: Eurocode 8 - Design of Structures for Earthquake Resistance, Part 1: General Rules, Seismic Actions and Rules for Buildings", *CEN/TC* 250.

De Iuliis M., Castaldo P., [2012] "An energy-based approach to the seismic control of one-way asymmetrical structural systems using semi-active devices", *Ingegneria Sismica - International Journal of Earthquake Engineering 2012*; XXIX(4):31–42.

De Matteis, G., Brando, G., Mazzolani, F.M. [2011] *"*Hysteretic behaviour of bracing-type pure aluminium shear panels by experimental tests" *Earthquake Engineering and Structural Dynamics 40 (10), pp. 1143-1162*

Faella, C., Piluso, V. and Rizzano, G. [2000] "Structural Steel Semirigid Connections", *CRC Press*, Boca Raton, Florida.

Faella, C., Piluso, V., and Rizzano, G. [1997] "A new method to design extended end plate connection and semirigid braced frames", *Journal of Constructional Steel Research,* 41(1), 61-91.

FEMA 351 [2000] "Recommended seismic evaluation and upgrade criteria for existing welded steel moment-frame buildings", *Federal Emergency Management Agency*, Washington, D.C.

FEMA 352 [2000] "Recommended post earthquake evaluation and repair criteria for steel moment-frame buildings", *Federal Emergency Management Agency*, Washington, D.C.

Ferraioli*,* M., Avossa, A.M., Lavino, A., Mandara, A. [2014a] Accuracy of advanced methods for nonlinear static analysis of steel moment-resisting frames *Open Construction and Building Technology Journal 8, pp. 310-323*

Ferraioli, M., Lavino, A., Mandara, A. [2014b] Behaviour factor of code-designed steel moment-resisting frames, *International Journal of Steel Structures 14 (2), pp. 243-254*

Formisano, A., Faggiano, B., Landolfo, R., Mazzolani, F.M.[2006a]. "Ductile behavioural classes of steel members for seismic design". *Proceedings of the 5th International Conference on Behaviour of Steel Structures in Seismic Areas - Stessa 2006, pp. 225-232.*

Formisano, A., Gamardella, F., Mazzolani, F.M.[2013]. "Capacity and demand of ductility for shear connections in steel MRF structures". *Civil-Comp Proceedings, 102, .*

Formisano, A., Mazzolani, F.M., Brando, G., De Matteis, G. [2006b].*" Numerical evaluation of the hysteretic performance of pure aluminium shear panels" Proceedings of the 5th International Conference on Behaviour of Steel Structures in Seismic Areas - Stessa 2006 pp. 211-217.*

Iannone, F., Latour, M., Piluso, V. and Rizzano G. [2011] "Experimental Analysis of Bolted Steel Beam-to-Column Connections: Component Identification", *Journal of Earthquake Engineering*, Vol.15, 215-244.

Kanyilmaz, A., Castiglioni, C.A. [2015] Performance of multi-storey composite steel-concrete frames with dissipative fuse devices, *COMPDYN 2015 - 5th ECCOMAS Thematic Conference on Computational Methods in Structural Dynamics and Earthquake Engineering,* pp. 334-348.

Latour M., Piluso V., Rizzano G. [2014], "Experimental analysis on friction materials for supplemental damping devices", *Construction and Building Materials*, Volume 65, 29 August 2014, 159-176.

Latour M., Piluso V., Rizzano G. [2015], "Free from damage beam-to-column joints: Testing and design of DST connections with friction pads", *Engineering Structures*, Volume 85, February 05, 219-233.

Latour M., Rizzano G., Piluso V. [2012]: "Experimental Analysis of Innovative Dissipative Bolted Double Split Tee Beam-to-Column Connections", *Steel Construction*, 4 (2011), N.2, 53-64.

Latour M., Rizzano G., Piluso V. [2013]: "Experimental behaviour of friction T-stub beam-to-column joints under cyclic loads", *Steel Construction*, 6, No. 1, p.11-18.

Longo, A., Montuori, R., Piluso, V [2012a] Failure mode control and seismic response of dissipative truss moment frames, *Journal of Structural Engineering (United States)* 138 (11), pp. 1388-1397.

Longo, A., Montuori, R., Piluso, V [2012b] Theory of plastic mechanism control of dissipative truss moment frames *Engineering Structures* 37, pp. 63-75

Mazzolani F.M., Piluso V. 1997: "Plastic design of seismic resistant steel frames", *Earthquake Engineering and Structural Dynamics*, vol. 26, pp. 167-191.

Montuori R., [2015] "Design of "Dog-bone" connection: The role of vertical loads", COMPDYN 2015 - *5th ECCOMAS Thematic Conference on Computational Methods in Structural Dynamics and Earthquake Engineering*, 3368-3387.

Montuori, R. [2014] The influence of gravity loads on the seismic design of RBS connections*, Open Construction and Building Technology Journal ,* 8, pp. 248-261

Montuori, R., Nastri, E., Piluso, V., [2014a]: "Advances in the Theory of Plastic Mechanism Control: Closed Form Solution for MR-Frames", *Earthquake Engineering & Structural Dynamics* vol. 4, pp. 1035-1054.

Montuori, R., Nastri, E., Piluso, V., Troisi, M., [2016] "Influence of connection typology on seismic response of MR-Frames with and without 'set-backs'", Earthquake Engineering and Structural Dynamics, Article in press, 10.1002/eqe.2768.

Montuori, R., Nastri, E., Piluso, V., [2014b], "Theory of plastic mechanism control for the seismic design of braced frames equipped with friction dampers", *Mechanics Research Communications*, Volume 58, June 2014, pp. 112-123.

Moore, K.S., Malley, J. O., and Engelhardt, M. D. [1999] "Design of Reduced Beam Section (RBS)Moment Frame Connections",*AISC Structural Steel Educational Council*, Moraga, CA.

Palazzo B, Castaldo P, Della Vecchia P. [2014] "Seismic reliability analysis of base-isolated structures with friction pendulum system", *2014 IEEE Workshop on Environmental*, Energy and Structural Monitoring Systems Proceedings, Napoli September 17-18.

Palazzo B, Castaldo P, Marino I. [2015] "The Dissipative Column: A New Hysteretic Damper". *Buildings 2015*; 5(1):163-178; doi:10.3390/buildings5010163.

Piluso V., Montuori R., Troisi M. [2014], "Innovative structural details in MR-frames for free from damage structures", *Mechanics Research Communications*, Vol. 58, June 2014,146-156.

Piluso, V., Faella, C. and Rizzano, G. [2001]. Ultimate behavior of bolted T-stubs, I: theoretical model, *Journal of Structural Engineering ASCE*, 127 (6), 686-693.

Sivaselvan, M., Reinhorn, A. M., [2001]. "Hysteretic Models for Deteriorating Inelastic Structures." ASCE/Journal of Engineering Mechanics, 126(6), 633-640.

Sivaselvan, M.V., Reinhorn, A.M.; [1999]. "Hysteretic Models for Cyclic Behavior of Deteriorating Inelastic Structures." Technical Report MCEER, University at Buffalo, SUNY.

Wen, Y. K.; [1976]. "Methos for Random Vibration of Hysteretic Systems." J. Engrg. Mech. Div., ASCE, 102(2), 249-263.

INFLUENZA DEL COMPORTAMENTO CICLICO DEI COLLEGAMENTI TRAVE-COLONNA SULLA RISPOSTA SISMICA DI TELAI IN ACCIAIO REGOLARI

Rosario Montuori, Elide Nastri*, Vincenzo Piluso, Marina Troisi

Department of Civil Engineering, University of Salerno

SOMMARIO*: Il presente articolo ha lo scopo di investigare l'influenza dei collegamenti trave-colonna a parziale ripristino di resistenza inseriti all'interno di telai in acciaio regolari, progettati mediante la Teoria del Controllo del Meccanismo di Collasso (TPMC). I quattro collegamenti utilizzati sono progettati al fine di ottenere la medesima resistenza flessionale. I primi tre sono progettati sfruttando il metodo delle componenti considerando una differente disposizione dell'elemento debole che porta ad una rigidezza e ad una rotazione ultima differente. Il quarto collegamento è invece un dissipatore ad attrito opportunamente progettato per garantire la dissipazione dell'energia in ingresso.*

Le strutture investigate sono state modellate al fine di rappresentare accuratamente sia la rigidezza che la resistenza nonché le capacità deformative, specialmente con riferimento alle connessioni semi-rigide. I collegamenti trave-colonna sono modellati per mezzo di molle rotazionali collocate alle estremità delle travi per le quali i cicli di isteresi sono caratterizzati sia da un degrado di rigidezza che da fenomeni di pinching.

I parametri che caratterizzano il comportamento ciclico del nodo sono stati calibrati sulla base delle prove sperimentali. A partire da tale calibrazione, si sono condotte analisi dinamiche incrementali con lo scopo di predire il comportamento di telai regolari in acciaio equipaggiati con tali dispositivi.

---

*Corresponding author: Elide Nastri, Department of Civil Engineering, University of Salerno, Italy.
Email: enastri@unisa.it